

Abstract

Title: DESIGN AND MECHANICAL PROPERTIES
OF FOAMED ASPHALT STABILIZED BASE
MATERIAL

Sadaf Khosravifar, Master of Science, 2012

Directed By: Professor Charles W. Schwartz, Department of
Civil and Environmental Engineering

Foamed asphalt stabilized base (FASB) combines reclaimed asphalt pavement (RAP) and/or recycled concrete (RC) with a foamed asphalt binder. The pavement structural properties of FASB fall somewhere between conventional graded aggregate base (GAB) and hot mix asphalt (HMA). Therefore, the required thickness of the pavement section can be reduced, resulting in cost savings in addition to recycling benefits. Mix designs were developed for eight different combinations of RAP, RC, and GAB. Details of the mix design procedure and the effects of factors representative of design and field conditions are evaluated. Triaxial test specimens from the weakest and strongest mixtures were tested for dynamic modulus and repeated load permanent deformation resistance, which can be used as inputs to the new AASHTO mechanistic-empirical design procedure. The measured stiffness values were also used to determine an appropriate structural layer coefficient value for use in the AASHTO empirical pavement design method.

DESIGN AND MECHANICAL PROPERTIES OF FOAMED ASPHALT
STABILIZED BASE MATERIAL

Sadaf Khosravifar

Thesis submitted to the Faculty of the Graduate School of the
University of Maryland, College Park, in partial fulfillment
of the requirements for the degree of
Master of Science
2012

Advisory Committee:

Professor Charles W. Schwartz, Chair
Associate Professor Dimitrios G. Goulias
Professor M. Sherif Aggour

© Copyright by

Sadaf Khosraviar

2012

Dedication

To my parents whose love and support took me to where I am right now

Acknowledgments

I would like to take this opportunity to thank those whose help made it possible for me to complete this work.

First and foremost: Dr. Charles W. Schwartz; the most influential teacher and person in my life. The guidance he provided me as an advisor was crucial to my technical work at University of Maryland as well as a great enthusiasm for me to pursue my academic travel toward the PhD.

Funding was provided partly by Maryland State Highway Administration and the prestigious A. James Clark fellowship of School of Engineering, University of Maryland.

I am also very thankful to the faculty members in University of Maryland who guided my academic exploration: Dr. Dimitrios G. Goulias, my other thesis committee member, who provided important comments on the Laboratory aspects of my research work which undoubtedly improved this work; Dr. M. Sherif Aggour for his time to serve as my committee member, and Dr. Ahmet Aydilek. Moreover, valuable technical instructions and help from Dan Sajedi, Nathan Moore, Dr. Regis L. Carvalho, Dr. Nelson H. Gibson, Dr. XinJun Li, Frank Davis, Harold Green, Tom Norris, Rennie Shunmugam, Mike Marshall, Dr. Michael Heitzman, Dr. Brian K. Diefenderfer, Dr. Alex K. Apeagyei, Dr. Larry H. James, Dr. Ali Regimand, and Alfredo L. Bituin; and testing equipments and resources from Global Resource Recyclers (GRR) and P. Flanigan and Sons Inc. are gratefully acknowledged.

Finally, completing this important step of my academic life could have not been possible without support and love from my family and friends. I would like to thank my parents, Parivash and Asgar, for being my strong supporter in my whole life. I am also very thankful to my brother, Arash, for having my back in my personal or educational life.

I am also very thankful to my dearest friends Shahin Sefati, Sahar Nabaee, Sahar Akram, Mersedeh TariVerdi, Ehsan Aramoon, Naeem Masnadi, Endri Mustafa, Rui Li, for their great friendship. And to Giti Malek, Saena Nejadi, Negin Kananizadeh, Leila Zavareh, and many others who are not physically close but have been there for me throughout the tough times and good times. I am also thankful to Timothy Briner who assisted me during the laboratory testing required in this work.

Table of Contents

Table of Contents	iv
List of Tables	vi
List of Figures	vii
CHAPTER 1. Introduction.....	1
1.1. Motivation for the study.....	1
1.2. Key objectives of this study	4
1.2.1. Mix design procedure and implications of internal structure of FASB	4
1.2.2. Performance tests: Triaxial dynamic modulus and repeated load permanent deformation tests	4
1.3. Organization of the thesis	5
CHAPTER 2. Material and Mix Design	6
2.1. Material characteristics	6
2.1.1. Binder.....	6
2.1.2. Aggregates	8
2.1.3. Active additives	11
2.1.4. Water.....	11
2.1.5. Evaluated Mixtures	12
2.2. FASB preparation procedure	13
2.2.1. Equipment.....	13
2.2.2. Mixing and compaction process	14
2.2.3. Curing process	17
CHAPTER 3. Laboratory Evaluation of Mechanical Properties of FASB.....	19
3.1. Mix Design Test: Indirect Tensile Strength Test.....	19
3.1.1. Background.....	19
3.1.2. Specimen fabrication procedure	20
3.1.3. ITS: Test Configuration and Analysis	20
3.2. Mix Performance Tests: Dynamic Modulus and Repeated Load Permanent Deformation Tests.....	21

3.2.1. Background	21
3.2.1. Specimen fabrication procedure	30
3.2.2. Triaxial DM: Test Protocol and Analysis	33
3.2.3. Triaxial RLPD: Test Configuration and Analysis	37
CHAPTER4. Mix Design Test Results and Interpretations.....	41
4.1. Indirect tensile strength test results.....	41
4.1.1. Effect of foaming asphalt content on ITS	43
4.1.2. Effect of RAP, RC, and GAB on ITS	46
4.1.3. Effect of Soaking Process on ITS	49
4.1.4. Effect of Active Additives on ITS	50
4.1.5. Effect of Mixing Moisture Content (MMC) on ITS	52
4.1.6. Effect of Stockpiling on ITS	53
4.1.7. Conclusions and Recommendations for Mix Design.....	55
CHAPTER 5. Performance Test Results	58
5.1. Introduction.....	58
5.2.DM test results	58
5.2.DM test results	59
5.2.1. Effect of stress state, loading duration, and temperature	60
5.3. RLPD test results	70
5.4. Structural layer coefficient for AASHTO design	76
5.5. Conclusions and recommendations.....	81
CHAPTER 6. Summary and Conclusions	83
6.1. Mix Design Test Results and Interpretations.....	83
6.2. Performance Test Results and Interpretations	85
Appendix I	87
References.....	96

List of Tables

Table 2.1. Foaming Characteristics of the Studied Binders.....	8
Table 2.2. Material description	9
Table 2.3. Mix Design Groups Description and Properties	12
Table 2.4. Optimum moisture content and maximum dry density of evaluated mixtures...	16
Table 3.1. Typical indirect resilient modulus ranges for FASB, after Wirtgen (2004)	23
Table 3.2. DM Averaged Across Deviatoric Stress State and Frequency, Berthelot <i>et al.</i> (2007).....	25
Table 3.3. Test details for each specimen, Fu <i>et al.</i> (2010)	28
Table 4.1. ITS test results for the evaluated mixtures at different foaming asphalt contents	42
Table 4.2. The average ITS test results in unsoaked and soaked condition with incremental foamed asphalt content along with their coefficients of variation (CV).....	44
Table 4.3. The effect of soaking process on 40% RAP + 60% RC+ 1% cement mixture...	49
Table 4.4. Effect of cement on ITS results of Mix G with 100% RAP-2	51
Table 4.5. Effect of cement on ITS results of Mix A with 40%RAP-1+60%RAP	51
Table 4.6. Effect of MMC on Mix F with 2% foamed asphalt content	53
Table 5.1. Test specimens description	59
Table 5.2. Comparison between laboratory DM (IE^*) at 5 Hz and field core indirect tension resilient modulus (M_r) for FASB-H (I Specimens)	67
Table 5.3. Average Phase angle for FASB mixtures	68
Table 5.4. Regression coefficient for master curve and its temperature shift factors for different mixtures.....	69
Table 5.5. Test variables for RLPD test.....	70
Table 5.6. Flow number and strain at flow for I specimens (Mix FASB-H).....	71
Table 5.7. Regression constants for RLPD fitted models	75
Table 5.8. M_r at 68F and unsoaked ITS for FASB mixtures, Average value $\pm \sigma$	79
Table 5.9. Estimated layer coefficients based on average M_r and average unsoaked ITS ..	80
Table 5.10. Estimated layer coefficients based on average M_r - σ and average unsoaked ITS - σ derived from different methods.....	80

List of Figures

Figure 1.1. Schematic of FASB internal structure, after Wirtgen (2010).....	1
Figure 1.2. Schematic of foaming process, after Wirtgen (2004).....	2
Figure 2.1. A sample of foaming characteristic test performed on B-1 at 320°F (160°C).....	7
Figure 2.2. Gradation of the raw material used in this study	9
Figure 2.3. Visual properties of aggregates: (a) GAB, (b) RC, (c) RAP-1, (d) RAP-2, (e) RAP-3	10
Figure 2.4. Surface texture of (a) GAB, (b) RC, (c) RAP-1, (d) RAP-2, (e) RAP-3.....	10
Figure 2.5. Gradation of Evaluated Mixtures	13
Figure 2.6.a) Laboratory-scale foamed bitumen plant WLB 10 S, b) Laboratory-scale pugmill mixer WLM 30.....	14
Figure 2.7. Schematic of the microstructure of FASB mixture, Fu <i>et al.</i> (2010.b)	15
Figure 2.8. Curing process of foamed asphalt: (a) moist aggregate and asphalt mastic droplet; (b) after compaction; (c) evaporation of water during curing; (d) bonds developed during curing; and (e) water reintroduced into the mix after curing. Fu <i>et al.</i> (2010.b).....	17
Figure 3.1. Effects of specimen temperature on Mr for various bulk stresses, when sd=2 pc, Fu and Harvey (2007)	24
Figure 3.2. DM for seven RAP aggregates stabilized with 1%,2%, and 3% foamed asphalt content, (a) test temperature 40°F (4.4°C), (b) test temperature 70°F (21.1°C), (c) test temperature 100°F (37.8°C), Kim <i>et al.</i> (2009).....	26
Figure 3.3. Triaxial RLPD tests for different curing conditions and different cement and foamed asphalt contents.....	29
Figure 3.4.Uniaxial permanent deformation for seven RAP mixtures stabilized with 2% foamed asphalt content	30
Figure 3.5. FASB-A, core obtained from MD-295 site	32
Figure 3.6. FASB-H laboratory prepared sample, capped with sulfur capping compound.	33
Figure 3.7. Phase lag between stress and strain in dynamic loading of viscoelastic material	33
Figure 3.8.a) UTM-100, (b) MTS test machine.....	35
Figure 3.9. Construction of master curve, temperature shifting process	36
Figure 3.10. Example of DM master curve and its shift factors	37

Figure 3.11. AMPT machine, triaxial RLPD test	38
Figure 3.12. Schematic of RLPD test, three main stages, slope and intercept of secondary stage, and flow number	40
Figure 4.1. ITS in unsoaked and soaked condition versus incremental foaming asphalt content for Mix A: 40%RAP-1+60%RC, Mix A*: 40%RAP-1+60%RC+1%cement, Mix B: 60%RAP-1+40%RC, Mix C: 80%RAP-1+20%RC, Mix D: 40%RAP-1+60%GAB, Mix E: 60%RAP-1+40%GAB, Mix F: 80%RAP-1+20%GAB, Mix G: 100%RAP-2, Mix G*: 100%RAP-2+1%cement, Mix H: 100%RAP-3.....	45
Figure 4.2. ITS in unsoaked and soaked conditions for RAP-1/RC (blue) and RAP-1/GAB mixtures (red) versus percentage RAP-1 in the mixture: (a) Experimental data for Mix A to F; (b) Fictitious mixture of 100% RAP-1 obtained from extrapolating and averaging the trend lines for RAP-1/RC and RAP-1/GAB mixtures	47
Figure 4.3. FASB mixtures from different RAP sources. RAP-1 is the fictitious mixture from extrapolation of experimental data from Mixes A to F.....	48
Figure 4.4. Soaking process effect on MC and ITS values (40%RAP-2+60%RC+1%cement), after Khosravifar <i>et al.</i> (2012)	50
Figure 4.5. Effect of cement on average ITS of Mix A and Mix G in soaked and unsoaked condition	52
Figure 4.6. Unsoaked and soaked ITS versus stockpiling time for Mix C (80%RAP-2+20%RC), Mix D (40%RAP-2+60%GAB), and Mix G* (100%RAP-2+1%cement)	55
Figure 5.1. $ E^* $ versus reduced time for B cores (Baltimore-Washington Parkway Site) at 14.5 psi, 7.3 psi, and 0 psi confining pressure at 44°F, 59°F, 77°F, and 95°F temperatures	60
Figure 5.2. $ E^* $ versus reduced time for F cores (P. Flanigan and Sons Inc. demonstration strip) at 14.5 psi, 7.3 psi, and 0 psi confining pressure at 44°F, 59°F, 77°F, and 95°F temperatures	61
Figure 5.3. $ E^* $ versus reduced time for I samples (laboratory FASB-H specimens/I-81) for at 16.6 psi, 9.3 psi, and 0 psi confining pressure at 86°F temperature	61
Figure 5.4. Master curves at different confining pressures along with their temperature shift factors for sample F2	62

Figure 5.5. Master curves at different confining pressures along with their temperature shift factors for sample B1	63
Figure 5.6. Comparison of the DM measured by UTM-100 and MTS machine at zero confining pressure.....	63
Figure 5.7. Master curves along with their shift factors for all the field and laboratory specimens of FASB-A and FASB-H mixtures at zero confining pressure. Error bars show the maximum, and minimum $ E^* $ for a given temperature and loading rate.....	64
Figure 5.8. Master curves along with their shift factors for FASB-A material from three different test segments at Baltimore-Washington Highway project, at zero confining pressure. Error bars show the maximum, and minimum $ E^* $ for a given temperature and loading rate time	65
Figure 5.9. Master curves along with their shift factors for all the field and laboratory specimens of FASB-A and FASB-H mixtures and corrected FASB-H mixture.....	67
Figure 5.10. Master curves for all FASB-A specimens. For a given temperature and loading rate, error bars show the maximum and minimum $ E^* $, and the shaded area shows +/- one standard deviation	68
Figure 5.11. Comparison of phase angle of FASB and HMA.....	69
Figure 5.12. Triaxial RLPD test results for B, F, and I specimens.....	71
Figure 5.13. (a) Triaxial RLPD test results on FASB-A mixture; (b) Test results in log-log space.....	73
Figure 5.14. Effect of confining pressure on F cores (F1, F2, F3) tested at 95°F	74
Figure 5.15. Effect of test temperature on RLPD test results. F1-F3 tested at 95°F (average) and F4-F6 were tested at 104°F (average)	74
Figure 5.16. Chart for estimating the structural layer coefficient a_1 of dense-graded asphalt concrete based on resilient modulus (AASHTO, 1993)	77
Figure 5.17. Variation in structural layer coefficient a_2 with base strength parameters for bituminous treated bases (AASHTO, 1993)	78
Figure 5.18. Suggested structural layer coefficients for bitumen stabilized materials (Wirtgen, 2010).....	78

CHAPTER 1. Introduction

1.1. Motivation for the study

Foamed asphalt stabilized base (FASB) combines combinations of reclaimed asphalt pavement (RAP), recycled concrete (RC), and/or graded aggregate base (GAB) with a foamed asphalt binder to produce a partially stabilized base material. FASB works as a granular material with increased cohesion and stiffness from “spotweld” bonds between the foamed asphalt and aggregate (Wirtgen, 2010). A schematic of FASB internal structure including the aggregates (coarse and mineral filler), foamed asphalt “spotwelds”, moisture, and air voids is illustrated in Figure 1.1.

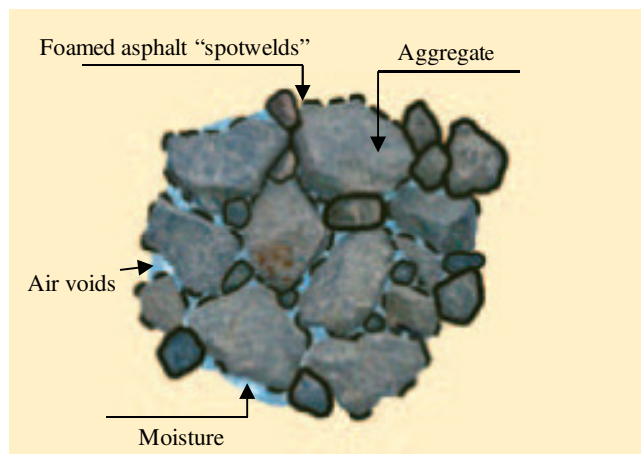


Figure 1.1. Schematic of FASB internal structure, after Wirtgen (2010)

The original foaming process developed by Csanyi (1957) for full-depth reclamation projects injected steam into hot asphalt through a specially designed nozzle. This reduced the viscosity and surface energy in the foamed asphalt to enable intimate coating when mixed with wet aggregate at its ambient temperature. In 1980s, Mobil Oil Australia made the process more practical for field applications by replacing steam with pressurized cold water. A controlled flow of cold water and pressurized air is introduced into a hot asphalt stream in a mixing chamber and then delivered through a nozzle as asphalt foam. Figure 1.2 shows the schematic of this foaming process.

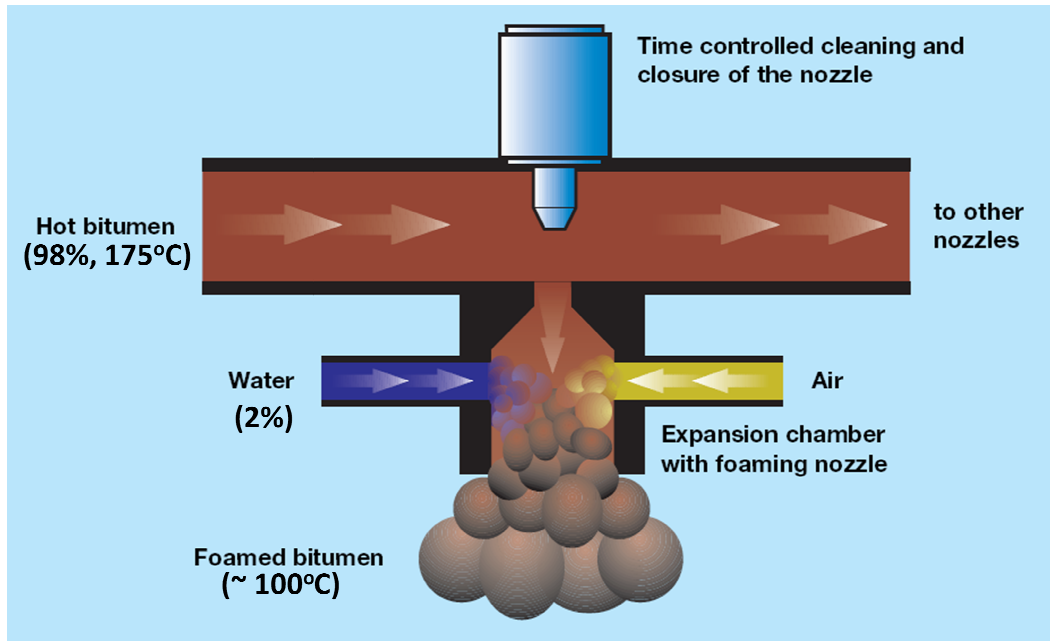


Figure 1.2. Schematic of foaming process, after Wirtgen (2004)

Foamed asphalt treatment can be used either in cold in-place recycling of HMA and existing aggregate base layers or plant recycling. FASB holds the potential to incorporate significant quantities of recycled materials into paving projects. Its structural properties are expected to fall somewhere between conventional untreated GAB and HMA. Since FASB provides more structural capacity than an equivalent thickness of GAB it replaces, it is possible to reduce the thickness of pavement sections. As an added benefit, FASB has the potential for significantly reducing the cost of conventional flexible paving. Consequently, the Maryland State Highway Administration (SHA) is interested in evaluating the suitability of FASB for Maryland paving conditions.

Foamed asphalt stabilization of recycled material (mostly RAP) with/without virgin aggregate has gained great attention worldwide. It has been implemented over the past decades in South Africa e.g., Jenkins *et al.* (2000), Asphalt Academy (2002), Long and Theyse (2004), Saleh (2004), Jenkins *et al.* (2007); Australia e.g., Ramanujam and Jones (2007); and Europe e.g., Schimmoller *et al.* (2000), Nunn and Thom (2002), Loizos *et al.* (2004), Loizos (2007), Khweir (2007) with only a recent resurgence of interest—and to a much lesser extent—in the U.S. (e.g., Marquis *et al.* (2003), Mohammad *et al.* (2003,

2006), Romanaschi *et al.*(2004), Kim and Lee (2006), Kim *et al.* (2007) and Fu *et al.* (2008).

As compared to other recycled road base materials treatment methods, e.g., asphalt emulsion, Portland cement stabilization, etc., foamed asphalt treatment has shown significantly better performance as reported by researchers. Ramanujam and Jones (2007) reported a direct comparison between foamed asphalt (with lime) treatment and emulsion treatment (with Portland cement) in which the foamed asphalt section showed significantly better performance in terms of handling early traffic and also superior rain resistance before applying the wearing course. Compared to recycled road base materials treated with Portland cement or other cementitious agents, foamed asphalt mixes (which may include small amounts of cement as well) have the additional benefit of improved flexibility or reduced brittleness. Jenkins *et al.* (2000) also reported that foamed asphalt and asphalt emulsion stabilized mixes have comparable strength, stiffness, and moisture susceptibility. However, the foamed asphalt strategy is often preferred because the asphalt emulsion treatment introduces extra moisture (the continuous phase in the emulsion) into the mix and requires considerably longer curing periods before the road can be opened to traffic. Muthen (1999) demonstrated that foamed asphalt treated material exhibits higher stiffness in comparison to emulsion treated material at ambient temperature and it can resist higher strains before failure. In summary, FASB provides a potentially fast, cost-effective and environmentally friendly flexible pavement rehabilitation strategy if designed and produced effectively.

Several FASB mix design procedures already exist, e.g., ARRA (2001), Asphalt Academy (2002), Mohammad *et al.* (2003), Kim and Lee (2006), Wirtgen (2010), and others. Most of the methods are based on Marshall compaction and a combination of Marshall stability and indirect tensile strength (ITS) test under wet vs. dry conditions. It is important to note that several of these design procedures were developed in geographic regions that have quite different climate conditions than in Maryland with respect to high/low temperatures, precipitation/moisture, and freeze/thaw cycles. In addition, the native materials, design standards, and trafficking are much different in Maryland than they are in South Africa and much of Europe and even much different from U.S. locations like Louisiana and Iowa

where earlier evaluations were conducted. The suitability of existing design procedures for Maryland conditions must therefore be very carefully evaluated.

1.2. Key objectives of this study

1.2.1. Mix design procedure and implications of internal structure of FASB

The first objective of the study documented in this thesis was to employ laboratory design tests, i.e. ITS, in unsoaked and soaked conditions to understand the complex structure and behavior of FASB mixtures of interest in Maryland.

Details of FASB mix design were investigated for eight different mixtures of RAP/RC/GAB of interest in Maryland. The important factors in mix design procedure from relevant studies in the past were pulled together with the experience gained during this phase of study. These include the role and characteristic of each component, e.g., aggregate, active additives, binder, and water in the foamed asphalt stabilization process, and the complexities and considerations with respect to mixing, compaction, curing, soaking, and stockpiling in order to attain a proper FASB mixture.

1.2.2. Performance tests: Triaxial dynamic modulus and repeated load permanent deformation tests

The second objective of this study was to address the most important performance related parameters of FASB material: stiffness and permanent deformation resistance, which can potentially be used in the new mechanistic-empirical pavement design guide (MEPDG) to compute stresses and distresses in the pavement layers.

Triaxial dynamic modulus (DM) tests were performed on laboratory prepared specimens and field cores of various FASB mixtures to assess the distinct behavior of FASB under a triaxial dynamic loading. These include the influence of stress dependency and viscoelasticity.

Triaxial repeated load permanent deformation (RLPD) tests were also performed to assess the resistance of FASB material to rutting. This is an important distress in flexible pavement structures under the cyclic loading.

The last objective was to estimate an appropriate structural layer coefficient for use in the older AASHTO empirical pavement design method based on the stiffness and strength of FASB mixtures of interest in Maryland.

1.3. Organization of the thesis

Chapter 2 introduces the materials used in the study and the FASB preparation procedure. When appropriate, relevant findings from previous studies in the literature are provided.

Chapter 3 presents the laboratory testing procedures for evaluating the mechanical properties of FASB material. These include:

- (1) Strength: Soaked and unsoaked ITS test;
- (2) Stiffness: Triaxial DM test and;
- (3) Permanent deformation: Triaxial RLPD tests.

For each test, a review of past procedures from the literature is presented followed by the specimen fabrication and testing procedures used in the present study for each of the mentioned tests.

Chapter 4 investigates the role and effect of different components in the FASB structure, e.g. aggregate, foamed binder, active additives, and moisture on the mixture ITS test results and the potential reasons on how these components incorporate and influence the strength of FASB mixtures in soaked and unsoaked conditions.

Chapter 5 evaluates the DM and RLPD performance test results followed by analyses to estimate an appropriate structural layer coefficient value for FASB mixtures of interest of Maryland.

Chapter 6 summarizes the findings regarding the mix design and performance tests.

CHAPTER 2. Material and Mix Design

2.1. Material characteristics

In this chapter, the materials used in this study along with their characteristics and specific roles in foamed asphalt stabilization process are explained. When appropriate, relevant findings from previous studies are also provided.

2.1.1. Binder

The binder used in foamed asphalt stabilized base (FASB) mixtures must have adequate foaming characteristics to insure proper foamed asphalt dispersion in the mixture. The best binder for foaming purposes is the one that expands the most and stays foamed as long as possible. These characteristics are quantified in terms of the expansion ratio (ER) and half-life ($t_{1/2}$).

- ER is a measure of viscosity of the binder and is defined as the ratio of maximum foamed volume to original liquid asphalt volume. Values for ERs typically range between 10 to 20.
- $t_{1/2}$ is a measure of stability of the binder and is defined as the time in seconds for the foam volume to dissipate to half of its initial maximum value. Typical values for $t_{1/2}$ range from 6 to 15 seconds.

Because of the rapid foaming and settling and the manual timing measurements, the $t_{1/2}$ test is highly dependent on the technician's estimation and judgment. A minimum ER of 8 and a minimum $t_{1/2}$ of 6 seconds are typical foaming requirements provided in literature (Wirtgen, 2010). The usual foaming temperature ranges from 300°F to 360°F and the usual foaming water content ranges from 2 to 3%.

For a given binder, increasing the asphalt temperature and foaming water content generally increases the ER but decreases the $t_{1/2}$ (Wirtgen, 2010). The objective of the binder foaming tests is to determine the temperature and foaming water content that optimizes the foamed asphalt ER and $t_{1/2}$.

Three PG 64-22 binders were used in different parts of the study. The binders included:

- B-1 provided by P. Flanigan and Sons Inc. This binder was refined by NuStar GP Holdings LLC.
- B-2 provided by Global Resource Recyclers, Inc. (GRR). This binder was also refined by NuStar GP Holdings LLC.
- B-3 provided by the Virginia Department of Transportation.

To measure the ER and $t_{1/2}$ values, three replicate tests were performed on each binder at different temperatures and foaming water contents according to the Wirtgen Cold Recycling Technology manual (Wirtgen, 2010). The optimum foaming water content was obtained as the average of the two foaming water contents met the minimum ER of 8 and $t_{1/2}$ of 6 seconds at a specific temperature. The lowest temperature that could provide acceptable foaming characteristics was desirable. Figure 2.1 shows the foaming test results for binder B-1 at 320°F (160°C).

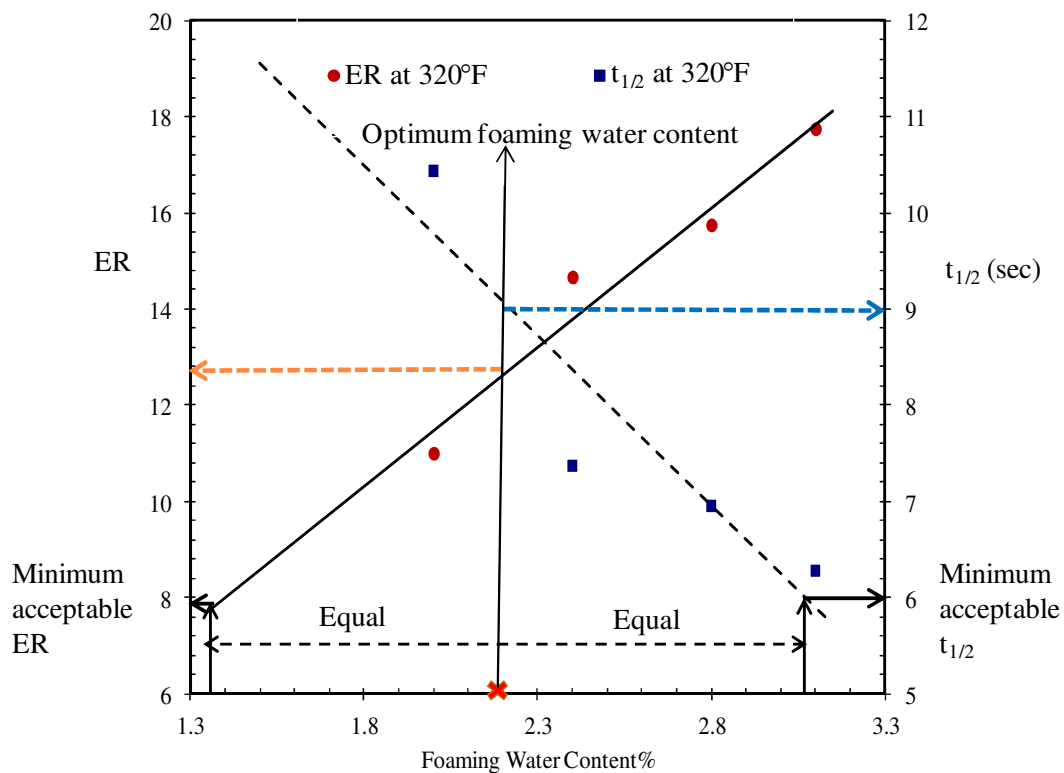


Figure 2.1. A sample of foaming characteristic test performed on B-1 at 320°F (160°C)

The foaming parameters for the three binders in this study are tabulated in Table 2.1.

Table 2.1. Foaming Characteristics of the Studied Binders

Binder	Water content (%)	Temperature- °F (°C)	ER	t _{1/2} (sec)
B-1	2.2%	320°F (160°C)	12.8	9.0
B-2	3%	320°F (160°C)	18.5	6
B-3	2%	302°F (150°C)	26	7.5

B-2-a was found to have high ERs with a relatively low t_{1/2} barely meeting the minimum criteria of 6 seconds. However the ER was high enough to compensate for the short t_{1/2}. This means that by assuming a linear trend for collapsing the foamed asphalt the retained volume after 6 seconds is still well beyond the minimum ER of 8 suggested by researchers and design procedures. Fu et al (2011) found that optimizing the foaming parameters (temperature and foaming water content) significantly affected the ER and t_{1/2}; however, the asphalt dispersion and indirect tensile strength of the FASB mixture was not significantly sensitive to small changes in temperature or foaming water content. They suggested that in design practice more effort should be devoted to sourcing a binder with the best foaming characteristics from refineries close to the project site rather than over-emphasizing identification of the “best” foaming parameters for a given asphalt binder (Fu et al., 2011).

2.1.2. Aggregates

Five different aggregates were used in this study; their general characteristics are described in Table 2.2. Graded aggregate base (GAB), recycled Portland cement concrete (RC) and recycled asphalt pavement (RAP-1) were provided by P. Flanigan and Sons Inc. RAP-2 was provided by GRR and RAP-3 was provided by the Virginia Center for Transportation Innovation and Research (VCTIR) of the Virginia Department of Transportation. RAP-2 was a processed RAP; the others were not. As shown in Table 2.2, the RC aggregate had a relatively high 4% absorption. Absorption was not a concern for the rest of the test materials.

Table 2.2. Material description

Martial	Nominal maximum size	% Fine ¹	Absorption
GAB	1"	7	-
RC	1"	5	4%
RAP-1	¾"	1	-
RAP-2	½"	8	-
RAP-3	½"	1	-

(1) Fine= Particles passing sieve #200

Figure 2.2 shows the gradation of the aggregates. The gradation was obtained according to AASHTO T-11 and was monitored during the mix design and testing process to ensure uniformity.

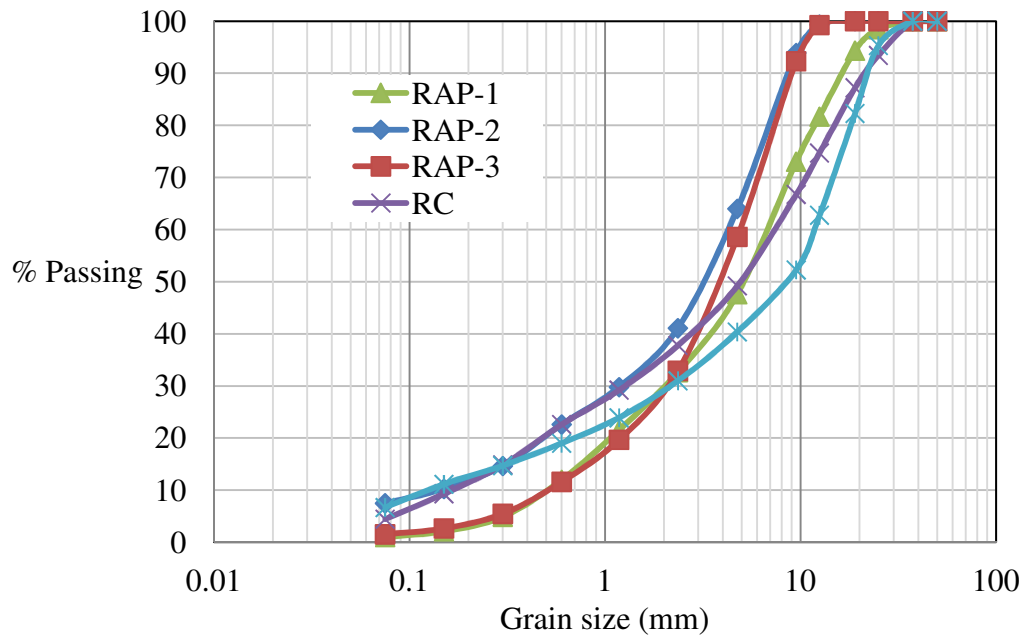


Figure 2.2. Gradation of the raw material used in this study

A visual inspection of the test material showed that the aggregate angularities of RC and GAB were similar as illustrated in Figure 2.3 and Figure 2.4, and were greater than those of

the RAP aggregates. RC and GAB had perceivably rougher surface texture than the RAP aggregates. RAP-1 aggregate particles were coated with a higher extent of oxidized asphalt binder film than RAP-2 and RAP-3. RAP-1 was also coarser than the two other RAPs.

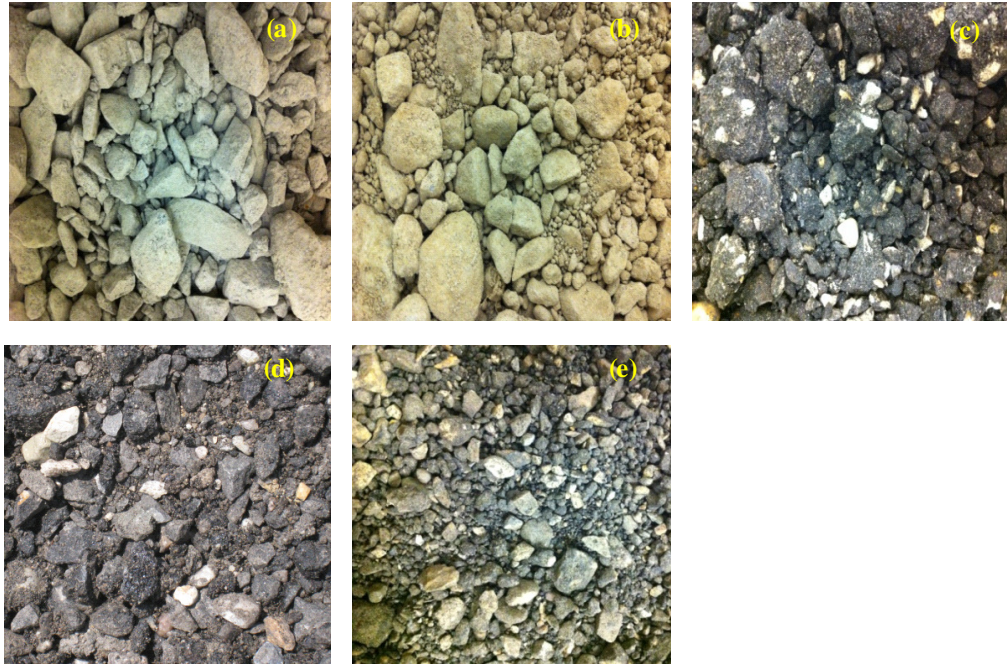


Figure 2.3. Visual properties of aggregates: (a) GAB, (b) RC, (c) RAP-1, (d) RAP-2, (e) RAP-3

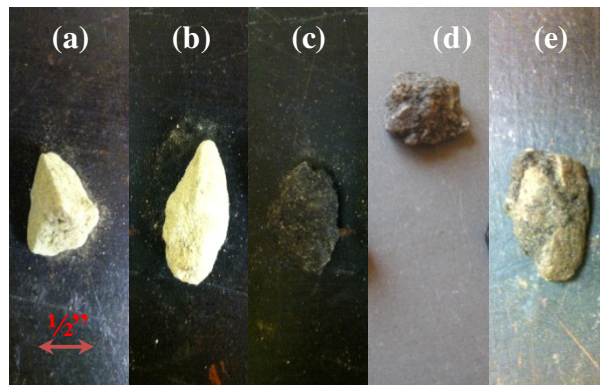


Figure 2.4. Surface texture of (a) GAB, (b) RC, (c) RAP-1, (d) RAP-2, (e) RAP-3

2.1.3. Active additives

Adding 1% of cement is a common practice in FASB design (Wirtgen, 2010).

Cement serves several important roles in FASB mixtures:

- Improved foamed asphalt dispersion in the mix. Foamed asphalt coats the fines and makes asphalt mastic. The asphalt mastic forms partial bonds with larger aggregates (Ruckel *et al.*, 1983).
- Increased adhesion of the asphalt mastic to the aggregate (Wirtgen, 2010).
- Increased initial rate of strength gain (curing) and the stiffness of the mix. Strong but brittle cementitious bonds usually form faster than the weaker but ductile bonds of foamed asphalt (Fu *et al.*, 2008).
- Reduction of moisture susceptibility of FASB (Fu *et al.*, 2008)

However, excessive use of cement should be avoided to avoid rigidity and shrinkage cracking of the brittle cementitious bonds (Fu *et al.*, 2008).

The effect of added cement is evaluated in Section 4.1.4. Whenever cement was used, it was blended together with the aggregates in the mixer just before including the foamed asphalt.

2.1.4. Water

Water has three specific roles in FASB materials.

- First, water when introduced to the hot asphalt induces foaming. Foaming water content as discussed in section 2.1.1. It is the 2-3% water needed for foaming of asphalt binder.
- Second, the mixing moisture content (MMC) is the water needed to provide lubricity during mixing. The mixing water also works as a carrier for the foamed asphalt droplets within the aggregate. Sufficient MMC is needed for adequate dispersion of foamed asphalt in the aggregate (Fu *et al.*, 2010.a).

- Third, compaction moisture content (CMC) provides workability and compactibility for the FASB mixture. Similar to any granular material, compactibility of FASB material is governed by its conventional moisture- density behavior. The maximum dry density (MDD) is achieved at optimum moisture content (OMC) (AASHTO T 180).

The second and third roles of water are explained further in the description of mix design procedures (Section 2.2.2). Tap water was used in this study with no control on its characteristics.

2.1.5. Evaluated Mixtures

Eight different combinations of RAP, RC and GAB were evaluated in this study. Their key properties are summarized in Table 2.3. All the aggregates retained on sieve $\frac{3}{4}$ " were discarded for test purposes. The blends were treated with different increments of foamed asphalt content ranging from 2% to 3.5%, which is the common range for FASB design. The target foaming asphalt contents for each mixture is stated in Table 2.3. Binder B-1 was used for Mix A to F. B-2 was used for Mix G and B-3 was used for Mix H.

Table 2.3. Mix Design Groups Description and Properties

Mix Group	Mix description	Foaming asphalt Contents (%)	Percentage passing sieve			
			$\frac{3}{4}$ "	#4	#8	#200
A	40%RAP-1+60%RC	2, 2.5, 3, 3.5 %	100	54	40	3.5
B	60%RAP-1+40%RC	2, 2.5, 3, 3.5 %	100	53	38	2.7
C	80%RAP-1+20%RC	2, 2.5, 3, 3.5 %	100	52	36	1.9
D	40%RAP-1+60%GAB	2, 2.25, 2.5, 2.75 %	100	50	36	5.3
E	60%RAP-1+40%GAB	2, 2.25, 2.5, 2.75 %	100	50	36	3.9
F	80%RAP-1+20%GAB	2, 2.25, 2.5, 2.75 %	100	50	35	2.5
G	100%RAP-2	2, 2.3, 2.6%	100	64	41	7.5
H	100%RAP-3	1.75, 2, 2.25, 2.5 %	100	59	33	1.6

Figure 2.5 shows the gradation of the eight mixtures. All of the mixtures had small percentages of fines, ranging from 1% to 7.5%. Fines are necessary for better foamed asphalt dispersion in the mixture. However, excess fines reduce the permeability and

drainage capacity, which is another important criterion for a base course. A limited study on the permeability of a selected FASB mixture (Mix A with 2.8% foamed asphalt and 3.5% passing sieve #200) showed that its coefficient of permeability of $3.2\text{E-}3$ in/sec is compatible with that of GAB ($1.1\text{E-}3$ in/sec).

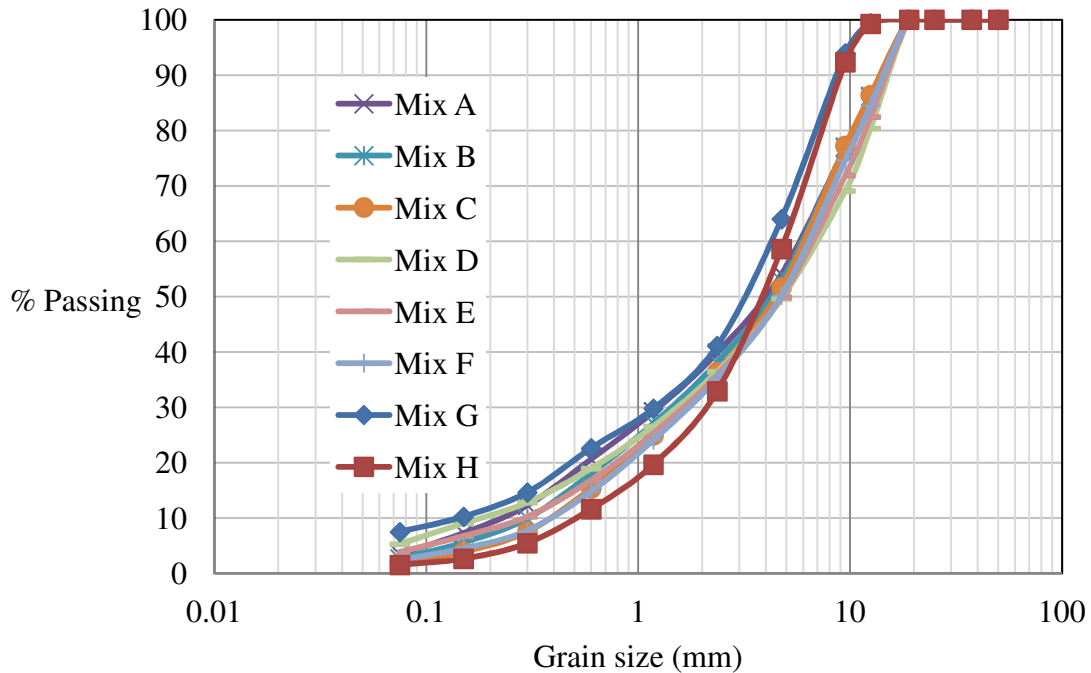


Figure 2.5. Gradation of Evaluated Mixtures

2.2. FASB preparation procedure

2.2.1. Equipment

Figure 2.6.a shows the Wirtgen laboratory-scale foamed bitumen plant WLB 10 S provided to the UMD Pavement Materials Laboratory for this research study by GRR. This mobile lab has been developed to produce small quantities of foam bitumen under laboratory conditions (Wirtgen, 2008). The foamed asphalt is mixed together with aggregates (RAP/RC/GAB) in the laboratory-scale twin-shaft pug-mill mixer WLM 30 (Figure 2.6.b). This mixer has the capacity of 50 lb.



Figure 2.6.a) Laboratory-scale foamed bitumen plant WLB 10 S, b) Laboratory-scale pugmill mixer WLM 30

2.2.2. Mixing and compaction process

The foamed asphalt is mixed together with the moist aggregate at ambient temperature in the mixer, as shown in Figure 2.6.b. During the mixing process, first the foamed asphalt droplets coat some of the fine aggregates producing an asphalt mastic phase. This asphalt mastic is dispersed in the aggregate blend and partially bonds with larger aggregates forming foamed asphalt bonds (Fu *et al.*, 2010.a). Besides the foamed asphalt bonds, there exists the mineral filler phase which are the fine particles not coated by foamed asphalt. This mineral phase can also contribute to some bonds in unsoaked condition. The

schematic of a FASB mixture and its different phases is illustrated in Figure 2.7 (Fu *et al.*, 2010.b). Moisture and air voids are not shown in this figure.

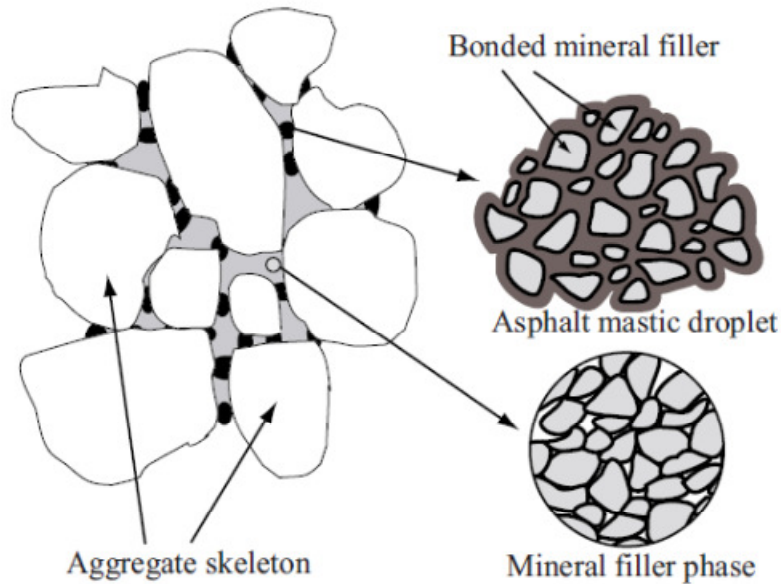


Figure 2.7. Schematic of the microstructure of FASB mixture, Fu *et al.* (2010.b)

The amount of fines is important in the mixing process. An adequate amount of fines is needed to form the asphalt mastic phase; this is usually about 4% for non-RAP aggregate (Wirtgen, 2010). For RAP aggregate, since the aggregates themselves are covered with oxidized binder, the bonds between the new foamed asphalt and RAP can form even with 1% fines (Wirtgen, 2010). During mixing, the mixing water suspends fines and makes them available to the foamed binder, acting as a carrier for better dispersion of asphalt mastic (Wirtgen, 2010). Mixing moisture content (MMC) thus has an important role in producing a homogeneous FASB mixture free from foamed asphalt globules and stringers.

After the FASB mixture is prepared it should be compacted to a density representative of field conditions. In the laboratory, the compaction procedure and molds are different depending on the test to be performed. In all cases, however, the objective of laboratory

mix preparation is to achieve adequate density. Moisture content during compaction (CMC) of the FASB mixture provides workability and compactability similar to any granular material.

Several studies in the literature have suggested mixing moisture contents on the dry side of the optimum moisture content (OMC). Lee (1981) recommended using a MMC equal to 65 to 85 percent of OMC as determined by the standard Proctor test. Wirtgen (2010) suggests mixing at 65 % – 95 % of OMC. Fu *et al.* (2010.a) suggested 75% to 90% of the modified Proctor OMC as appropriate with respect to both compactability and asphalt distribution.

In this study, all the mixtures were mixed and compacted at a target moisture content of 90% (between 84% and 96% of OMC) as determined by a modified Proctor test (AASHTO T 180), unless otherwise noted. The OMC and maximum dry density for the evaluated aggregate blends are provided in Table 2.4. Mixtures containing recycled concrete had a relatively higher OMC because of the high RC absorption (Section 2.1.2). During mix production, aggregate proportions were mixed together with the prescribed amount of water a day prior to foaming treatment to let the aggregates absorb water and reach equilibrium.

Table 2.4. Optimum moisture content and maximum dry density of evaluated mixtures

Mix Group	MDD (pcf) ¹	OMC (%) ²	MMC (%) ³	CMC (%) ⁴
A	124.8	9.1	8.2	8.2
B	125.5	8.8	7.9	7.9
C	121.5	9.3	8.4	8.4
D	126.4	7.8	7.0	7.0
E	132.2	8.8	7.9	7.9
F	137.7	6.6	5.9	5.9
G	130.9	7.6	6.8	6.8
H	113.5	8	7.2	7.2

(1) MDD= Maximum Dry Density, AASHTO T 180 (modified Proctor)

(2) OMC= Optimum Moisture Content, AASHTO T 180 (modified Proctor)

(3) MMC= 90% of OMC

(4) CMC= 90% of OMC

2.2.3. Curing process

FASB material gains stiffness and strength with time as the water in the mixture evaporates and foamed asphalt bond develop. This gain in strength forms in the mineral phase (similar to any granular material) and the asphalt mastic phase.

1. Drying process of the mineral phase: The mineral phase gets stiffer as water evaporates and matric suction increases (Fredlund and Rahardjo, 1993). This drying-induced stiffening occurs in any granular material and is mostly reversed when water is reintroduced into the material.

2. Curing process of the foamed asphalt bonds: Discrete cohesive bonds develop between the foamed asphalt mastic droplets and the larger aggregates as water evaporates and foamed asphalt bonds cures. After these bonds are formed, they are only moderately sensitive to moisture damage as compared to the drying-induced bonds in the mineral phase (Fu *et al.*, 2010.b).

Figure 2.8 illustrates how foamed asphalt bonds take form during curing process (Fu *et al.*, 2010.b). The mineral filler phase is not shown in this schematic figure.

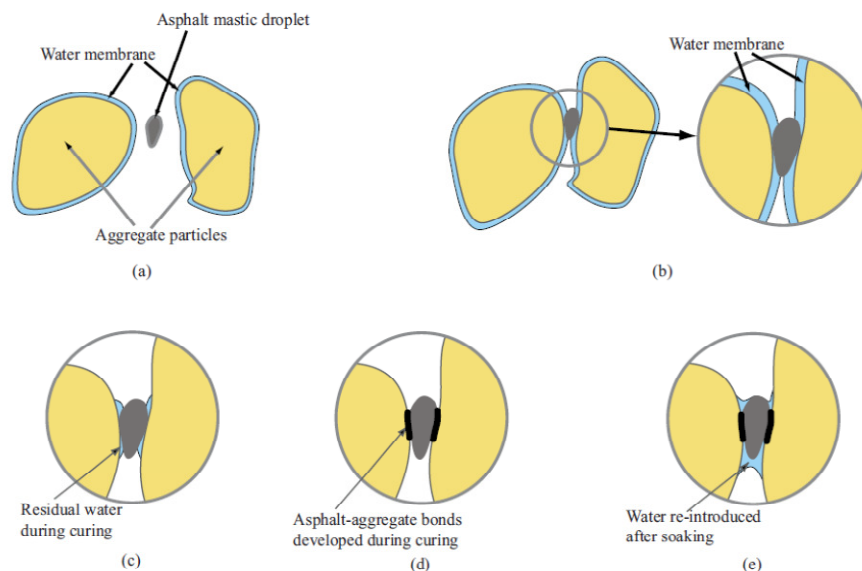


Figure 2.8. Curing process of foamed asphalt: (a) moist aggregate and asphalt mastic droplet; (b) after compaction; (c) evaporation of water during curing; (d) bonds developed during curing; and (e) water reintroduced into the mix after curing. Fu *et al.* (2010.b)

It should be mentioned that in the case of adding 1% cement, hydration of cement also contributes to the early stiffening process of FASB mixtures.

In order to simulate the curing process in the laboratory, test specimens (prepared according to 3.1.2 and 3.2.2) were kept in forced-draft oven at 104°C (40°C) for 72 hours to reach the constant mass as suggested by Wirtgen (2010). It should be noted that some older laboratory curing procedures specified 48 hours curing at 140°F. However, this temperature is beyond the softening point for bitumen and could affect the asphalt dispersion in the mixture, which is not desirable.

CHAPTER 3. Laboratory Evaluation of Mechanical Properties of FASB

3.1. Mix Design Test: Indirect Tensile Strength Test

3.1.1. Background

The indirect tensile strength (ITS), originally designed for testing the moisture susceptibility and ITS of hot mix asphalt (HMA), is an accepted method for evaluating foamed asphalt stabilized base (FASB) mixtures for mix design purposes. This test has been widely used by researchers in the past, which provides a large historical database. It is a relatively quick test to obtain strength characteristics of the FASB in soaked and unsoaked conditions. Design guides such as the South African TG2 (Collings *et al.*, 2002) and Wirtgen cold recycling manual (Wirtgen, 2004) both employ strength tests (ITS and uniaxial compressive strength (UCS)) in the dry condition for mix design optimization purposes and advise a minimum requirement for moisture susceptibility. Moisture susceptibility in terms of a tensile strength ratio (TSR) is defined as the ratio of ITS in the soaked condition to ITS in the unsoaked condition. TSR minimum criterion typically varies between 50% to 75% depending on climatic condition. Some researchers, namely Muthen (1999), Romanoschi *et al.* (2004), Marquis *et al.* (2003), Kim and Lee (2006), and Fu *et al.* (2008), proposed testing foamed asphalt specimens under soaked conditions for design optimization purposes. Mohammad *et al.* (2003) suggested maximizing the TSR value to define the optimum asphalt content for a project in Louisiana. Maryland provisional specification for FASB design (Section 50X, 2009) requires a minimum TSR of 70% along with a minimum ITS of 50.8 psi in soaked condition.

In this study, the ITS test was performed both in soaked and unsoaked conditions for all the evaluated mixtures at foaming asphalt contents ranging from 2% to 3.5%. The greatest attention was given to the soaked strength for evaluating the mixtures because of the importance of FASB performance under critical condition. For base courses in Maryland, soaked conditions can be expected during several months a year. Several case studies have reported moisture damage as the primary cause of distresses in FASB layers, e.g., Chen *et al.* (2006), Ramanujam and Jones (2007), Fu *et al.* (2008). Therefore, performance of

FASB materials in the soaked condition is critical and must be properly considered in mix design (Fu *et al.*, 2008).

3.1.2. Specimen fabrication procedure

Six indirect tension specimens were prepared for each trial mix design. In order to simulate the initial compaction after construction, Marshall compaction (AASHTO T 245-97) with 75 blows on each face was employed. Standard Marshall molds were used to construct samples 4 inches in diameter and approximately 2.5 inches high. All the specimens were prepared within 45 minutes of mixing unless otherwise noted and were kept in a forced-draft oven in order to reach constant mass condition according to Section 2.2.3.

3.1.3. ITS: Test Configuration and Analysis

The ITS test procedure for FASB material was derived from AASHTO T 283-07, 'Resistance of Compacted Hot Mix Asphalt (HMA) to Moisture-Induced Damage', with a slight deviation in the soaking process (Section 4.1.3). For the unsoaked condition, three Marshall specimens were kept in the environmental chamber at 77°F (25°C) to equilibrate to room temperature. For the soaked condition, the specimens were immersed in a water tub for 24 hours at 77°F (25°C).

In this test, the prepared specimen was positioned in the center of the ITS jig in an Instron testing machine. A compressive load was applied in strain control mode at the rate of 2inch/min until maximum load. The ITS was determined from the maximum load as follows:

$$ITS = \frac{2 \times P}{\pi \times h \times d} \quad (3.1)$$

Where P = maximum load

h = average height of test specimen after curing

d = average diameter of test specimen after curing

The ITS of the specimens usually decreased under soaked conditions, which shows the water susceptibility of the FASB material in tension. The TSR, determined as the ratio of soaked ITS to unsoaked ITS, provides a good measure of the water susceptibility of the

mixture. The dry density of the specimens was controlled and specimens with inconsistent density were disregarded.

The cured unsoaked specimens are not completely dry and generally had a moisture content (MC) value ranging from 0.5% to 2.5%. This MC should be taken into account when determining the dry density of the specimen using Equation 3.2:

$$\text{Dry Density} = \frac{\text{Bulk Density}}{1 + \text{MC}\%_{\text{cured specimen}}} \quad (3.2)$$

The bulk density of the compacted and cured specimens is determined according to the following equation:

$$\text{Bulk Density} = \frac{M}{\pi \times d^2 \times h} \quad (3.3)$$

M = mass of test specimen after curing

3.2. Mix Performance Tests: Dynamic Modulus and Repeated Load Permanent Deformation Tests

3.2.1. Background

While ITS is a useful material property test for mix design, pavement performance in the field is more directly related to other fundamental engineering properties. These properties are stiffness and permanent deformation resistance. Not much is known about the stiffness and permanent deformation resistance of FASB, so these were examined in this study. Moreover, the new mechanistic-empirical pavement design guide (MEPDG) requires a measure of stiffness and permanent deformation resistance to compute stresses and distresses in the pavement layers. The stiffness and permanent deformation resistance of FASB mixtures are dependent on the applied stress state, loading rate, temperature, moisture content, density and other variables. FASB is a partially bound material consisting of aggregate skeleton, binder, water, and air voids. It has distinct behavior different from HMA as a completely bound extreme or GAB as a complete unbound extreme.

Among various methods pursued by researchers to assess these fundamental mechanical properties of FASB material, the triaxial dynamic modulus (DM) test and the triaxial repeated load permanent deformation (RLPD) test of FASB mixtures in an unsoaked condition were selected as the most suitable performance test. The test protocols are explained in detail in 3.2.3 and 3.2.4 for DM and RLPD tests, respectively. The tests were performed on field cores of Mix A stabilized by 2.8% foamed asphalt (FASB-A) and laboratory prepared specimens of Mix H stabilized by 2.2% foamed asphalt (FASB-H). These two mixtures provided the maximum and minimum unsoaked ITS as explained in Section 4.1.2 and thus should provide brackets for the mechanical properties of FASB material expected to be used and constructed in Maryland.

The different methodologies practices by previous researchers to evaluate the stiffness and rutting susceptibility of FASB material and their limitations and advantages are described in the following paragraphs. This information provided the background for the test methods employed in this study.

3.2.1.1. Stiffness

Different researchers have employed various test methods to capture the stiffness of FASB materials. Indirect tension resilient modulus testing has been used in the past by Muthen (1999), Nataatmadja (2001), Chiu and Lewis (2003), Marquis *et al.* (2003), Collings *et al.* (2004), Ramanujam and Jones (2007), Khweir (2007), and others. Indirect tension resilient modulus tests can be performed on cores or on laboratory prepared FASB specimens. Most of the mixtures evaluated in past studies contained RAP and/or GAB with or without cement. The reported moduli ranged from 100 ksi to above 800 ksi for different mixtures. This large range of the resilient modulus values is due to the wide variety of aggregates and binders and differences in mixing, curing, and compaction procedures. Table 3.1 from the Wirtgen cold recycling manual (Wirtgen, 2004) suggests typical ranges for indirect resilient modulus at 77°F (25°C) and 10 Hz for different categories of FASB material.

Table 3.1. Typical indirect resilient modulus ranges for FASB, after Wirtgen (2004)

Material	Indirect resilient modulus, M_R (ksi)
RAP/ crushed stone (50:50 blend)	360- 580
Graded crushed stone	290- 435
Natural gravel ($PI^* < 10$, $CBR^{**} < 30$)	218- 435

*PI: Placticity Index

**CBR: California Bearing Ratio

The Wirtgen cold recycling manual (Wirtgen, 2004) also states that the resilient modulus of cured, unsoaked Marshall briquettes in indirect tensile mode often yields significantly higher values than those from dynamic triaxial and flexural beam tests as well as backcalculated moduli from falling weight deflectometer (FWD) measurements. The lack of moisture in the test specimens as well as the geometry and stress states in the indirect tension loading mode could explain the higher resilient moduli. Similar results were found by Fu *et al.* (2009).

Jenkins *et al.* (2007) performed triaxial resilient modulus tests on foamed asphalt treated RAP with and without cement and reported modulus values in the range of 40 ksi for FASB mixtures with different percentages of foamed asphalt and cement. They also found that adding cement to the FASB mixture both increased the resilient modulus and its dependency on bulk stress. Fu *et al.* (2009) performed triaxial resilient modulus tests at different loading rates, deviatoric stresses, and confining pressure. Resilient modulus was found to be a function of both stress level and load pulse duration. They concluded that foamed asphalt stabilization does not always increase the absolute values of resilient modulus as compared to the same unstabilized mixtures, under either unsoaked or soaked conditions. However, it transforms the material behavior from that of typical unbound granular materials towards that of partially asphalt-bound materials, with the resilient modulus more loading rate but less stress dependent.

Moreover, as would be expected from the rheological characteristics of the asphalt binder, the stiffness of FASB mixtures is temperature dependent. Nataatmadja (2002) reported a 30 to 44% reduction in stiffness when the test temperature increased from 50°F to 104°F. Saleh (2006) also looked into the influence of asphalt binder's temperature susceptibility

and curing conditions on temperature sensitivity of FASB stiffness values. Both studies employed indirect resilient modulus testing, which has very limited control over the stress states. Muthen (1999) investigated the temperature sensitivity of the stiffness of beam briquettes of foamed treated weathered granite and aeolian sand. He found that increasing the temperature from 41°F to 104°F caused a 20% to 45% decrease in the stiffness. Fu and Harvey (2007) looked into the temperature sensitivity of FASB mixtures of RAP/aggregate with 1.5% foamed asphalt under cyclic triaxial loading (LTPP P46). The tests were performed at different combinations of confining and deviatoric stresses at various temperatures. They found that FASB modulus was temperature sensitive and was governed more by the confining pressure than the deviatoric stress. Figure 3.1 shows the effect of temperature on resilient modulus for various bulk stresses, when deviatoric stress (s_d) is twice confining pressure (p_c). In this figure, Θ is the bulk stress = $3 p_c + s_d = 5 p_c$. The relation between resilient modulus and temperature was almost parallel for different bulk stresses suggesting that there is no interaction between bulk stress and temperature effects on resilient modulus.

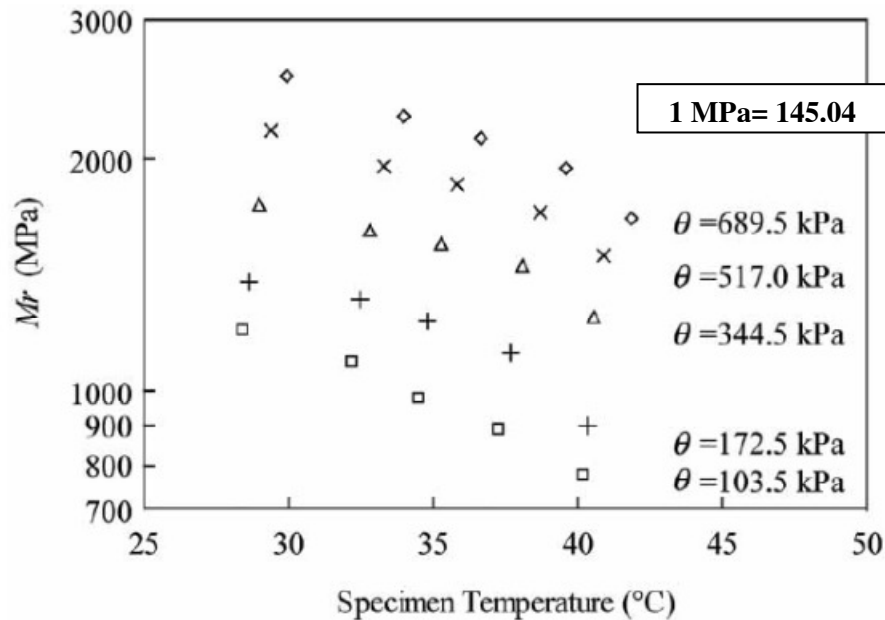


Figure 3.1. Effects of specimen temperature on Mr for various bulk stresses, when $s_d=2 p_c$, Fu and Harvey (2007)

Berthelot *et al.* (2007) used a triaxial test to investigate the stress-strain relations for different alternative stabilization methods for a recycled granular base with high fine sand fraction and high portion of intermediate plastic clay fines. The stabilization methods included foamed asphalt with and without cement. They performed tests over the full range of field stress states (i.e., bulk stress states up to 130 psi and deviatoric stresses from 7 psi to 80 psi) and loading rates (0.5 to 10 Hz). Table 3.2 shows the DM test results at different frequencies. Temperature was not controlled in this study.

Table 3.2. DM Averaged Across Deviatoric Stress State and Frequency, Berthelot *et al.* (2007)

	In Situ (MPa)	3% Cement (MPa)	5% Cement (MPa)	5% Asphalt Emulsion 5053 (MPa)	2% Cement–2% Asphalt Emulsion 5053 (MPa)	3% Foamed Asphalt (MPa)	2% Foamed Asphalt– 1.5% Cement (MPa)
Frequency							
10 Hz	665	1,106	1,588	1,357	1,873	1,618	1,954
5 Hz	668	1,132	1,576	1,280	1,806	1,483	1,743
1 Hz	667	1,141	1,558	1,064	1,755	1,230	1,746
0.5 Hz	671	1,156	1,591	993	1,748	1,142	1,694
Stress state							
250:200	835	1,447	1,956	1,430	2,229	1,620	2,133
250:400	786	1,363	1,962	1,325	2,100	1,539	1,949
50:400	508	836	1,198	963	1,378	1,143	1,459
50:600	542	888	1,198	977	1,476	1,171	1,596
Average	668	1,133	1,578	1,174	1,796	1,368	1,784

1 MPa= 145.04 psi

Loading rate and stress state dependency could be inferred from the test results (Table 3.2). The focus of their study was a comparison between different stabilization agents. They found that both foamed asphalt and asphalt emulsion with added cement yielded satisfactory mechanical properties in comparison to other stabilization methods.

Kim *et al.* (2009) performed DM tests on foam stabilized RAP from seven different sources in Iowa. The mixtures were prepared using the gyratory compactor. The reported DM was about 464-670 ksi at a 10 Hz loading frequency and a temperature of 70°F for seven RAP aggregates stabilized with 2% foamed asphalt content. At 40°F, dynamic moduli of FASB material increased slightly as the foamed asphalt content increased. However, at both 70°F and 100°F, the dynamic moduli decreased as the foamed asphalt

content increased but this effect was not significant. The results of their work is shown in Figure 3.2.

1 GPa= 145.04 ksi

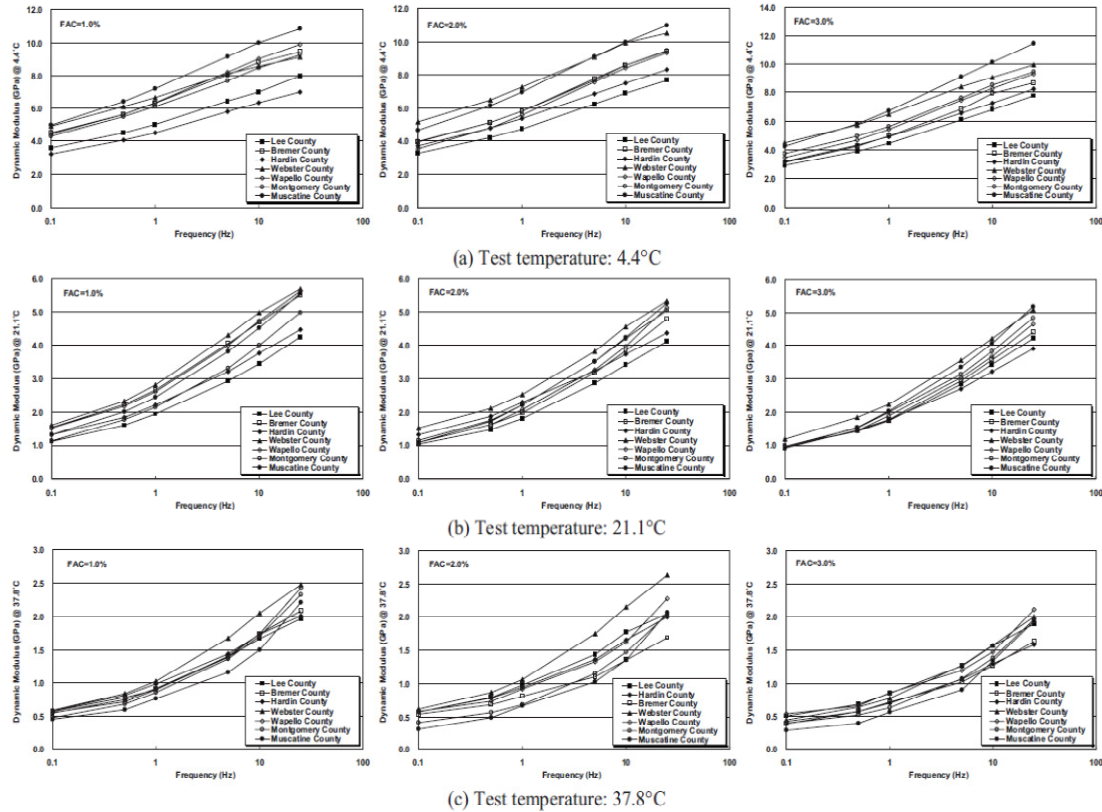


Figure 3.2. DM for seven RAP aggregates stabilized with 1%, 2%, and 3% foamed asphalt content, (a) test temperature 40°F (4.4°C), (b) test temperature 70°F (21.1°C), (c) test temperature 100°F (37.8°C), Kim *et al.* (2009)

By comparing with the typical 20 to 40 ksi range for GAB resilient modulus (Papagiannakis and Masad, 2007) and the 450 ksi to 1000 ksi range for DM of HMA at 70°F and a 10 Hz loading frequency (Huang, 1993) suggests that the stiffness of FASB relies somewhere between but closer to that of HMA. In addition, previous studies have shown that the stiffness of FASB material is loading rate, temperature, and, to a lesser extent, bulk stress dependent. Therefore, triaxial DM test at three confining pressures, six loading rates and four temperatures was adopted in this study to characterize the FASB stiffness.

3.2.1.2. Permanent deformation

Permanent deformation or rutting is one of the most important distresses occurring in pavement sections. It is the accumulated deformation from shear failure and/or densification under repeated loading. Resistance to permanent deformation of FASB mixtures can be enhanced by improving the aggregate skeleton angularity (e.g., shape, hardness, and roughness), increasing the maximum aggregate size, improving the compaction and curing process, and limiting the foamed asphalt content to a maximum of 3% (Wirtgen, 2010). Excess foamed asphalt will act as a lubricant between aggregates and decreases the friction angle, leading to an increased shear failure and consequent permanent deformation (Wirtgen, 2010).

Long and Ventura (2004) conducted triaxial dynamic RLPD tests for 50,000 cycles at 4 Hz loading frequency on a high quality granular material stabilized with 1% cement and different percentages of foamed asphalt. They performed the tests at various combinations of confinement levels, deviatoric stresses, relative densities, and saturation levels. The test temperature was not stated in their report. The writers formulated a combined model to account for all the aforementioned variables. Their principal conclusions included: (1) for stress-to-strength ratios lower than 0.6, which is typical for well-designed pavement structures, the resistance to permanent deformation is mainly governed by the characteristics of the mother aggregate and not the applied stress states; (2) permanent deformations significantly increase at stress-to-strength ratios greater than 0.6; and (3) resistance to permanent deformation decreases slightly as the foam binder content increases.

Mohammad *et al.* (2006) tested the rutting susceptibility of non-stabilized 100% RAP (RAP), a foamed asphalt stabilized blend of 50% RAP with 50% soil cement (FA-50RAP-50SC), and foamed asphalt stabilized 100% RAP (FA-100RAP). The test was conducted for 10,000 cycles with 0.1 second loading period and 0.9 second rest period. Loading consisted of a cyclic 15 psi deviatoric stress at a 5 psi confinement pressure. The testing temperature was not stated in the study. The FA-100RAP, FA-50RAP-50SC and RAP exhibited 2.1%, 0.5%, and 0.3% permanent strain at the end of the test, respectively. This showed that FA-100RAP had the highest and RAP had the lowest susceptibility to rutting.

Gonzalez *et al.* (2011) evaluated the effect of stabilizing with 1% cement and variable foamed asphalt contents for a marginal aggregate. The test procedure consisted of 50,000 load cycles at 4 Hz and a 7.2 psi confining pressure. The deviatoric stress was increased in 7 steps from 11 psi to 76 psi. The testing temperature was not stated in the study. High variability in the final plastic strains between replicates was observed. However, the results suggested that increasing foamed asphalt content significantly increases the rutting susceptibility. The final permanent strains varied between 1000 to 13000 $\mu\epsilon$ for foamed asphalt contents ranging from 0% to 4%.

Fu *et al.*, (2010.b) performed a limited set of triaxial permanent deformation tests to investigate the role of curing and cement content on the rutting resistance of foamed treated RAP aggregate. Two curing conditions were investigated.

- Curing Condition A: sealed at 20°C for 24 h
- Curing Condition B: unsealed, at 40°C for 7 days

The test sequence included 20,000 load cycles at a 43.5 psi deviator stress, followed by another 20,000 cycles at 72.5 psi, and ending with 210,000 cycles at 101.5 psi. A 10 psi confinement stress was maintained through the test. The deviator stress was applied as a haversine pulse with 0.1 seconds loading duration and 0.2 seconds resting period. The testing temperature was not stated in the study. The results showed that enhanced curing condition (curing condition B) and adding cement significantly improved FASB resistance to permanent deformation even in the soaked condition. The test conditioning for each specimen is summarized in Table 3.3 and the permanent deformation test results are shown in Figure 3.3.

Table 3.3. Test details for each specimen, Fu *et al.* (2010)

Specimen	Mix design	Test condition	Moisture content as tested (%)
TriB	0C3A	Curing Condition B, 7-day soak	5.3
TriC	2C3A	Curing Condition B, 40-day soak	4.9
TriG	1C3A	Curing Condition A	4.3
TriH	0C0A	Curing Condition A	7.1
TriI	0C3A	Curing Condition A	5.6

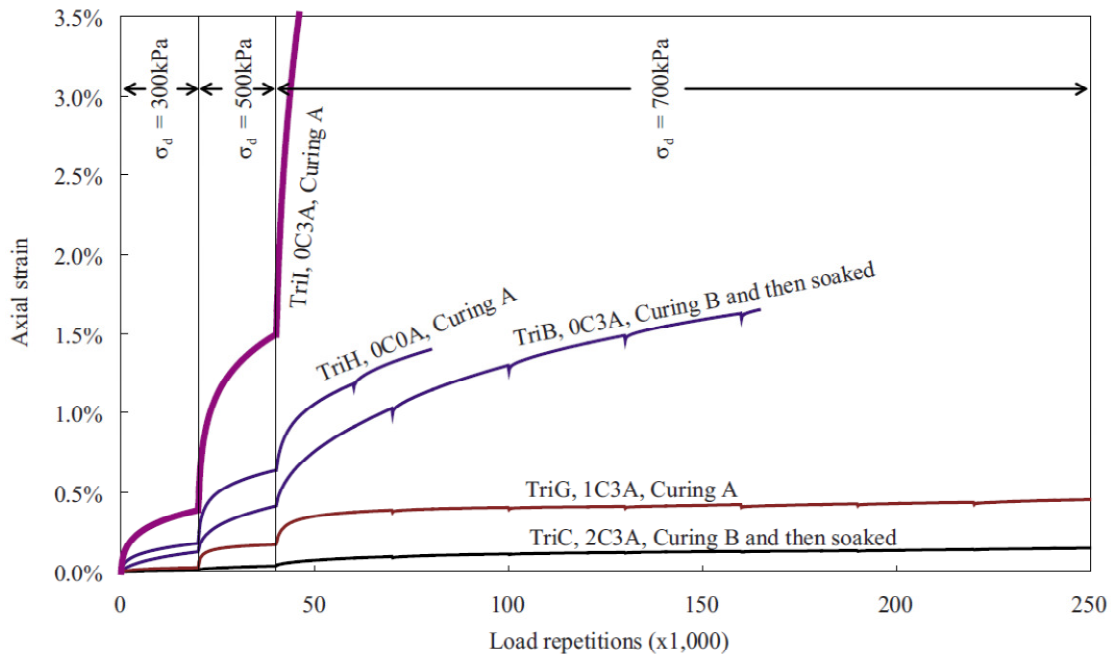


Figure 3.3. Triaxial RLPD tests for different curing conditions and different cement and foamed asphalt contents

None of these prior studies stated the testing temperature, which suggests that there was no control on the temperature during the test. However, presence of foamed asphalt and oxidized binder in RAP suggests that temperature effects should be expected. Similar to asphalt mixtures, FASB mixtures are expected to show higher permanent deformation at higher temperatures because of the lubricity effects of softened binder at high temperatures. It is important to evaluate permanent deformation resistance at high controlled temperature conditions.

Kim *et al.* (2009) performed uniaxial RLPD tests on foamed treated RAP from seven different sources in Iowa. The tests were performed at a 20 psi deviatoric stress for 10,000 cycles with 0.1 second loading and 0.9 second rest period at 104°F. In agreement with previous studies, they found that increasing the foamed asphalt content increased the susceptibility to permanent deformation. Figure 3.4 shows the cumulative strain versus loading cycles for the 14 specimens (2 replicates per mixture).

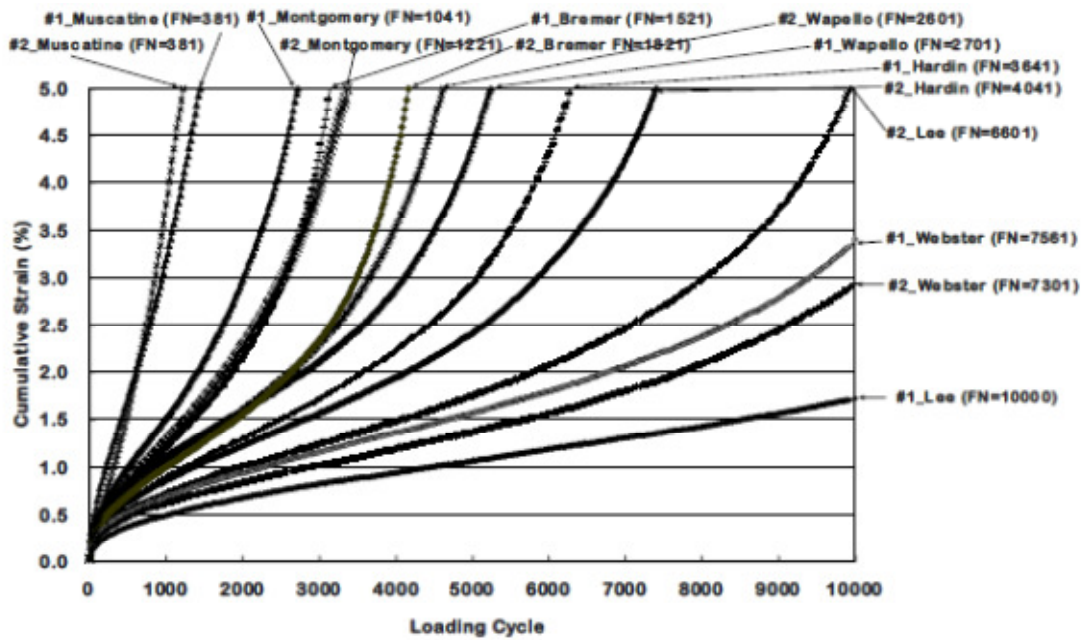


Figure 3.4. Uniaxial permanent deformation for seven RAP mixtures stabilized with 2% foamed asphalt content

Permanent deformation resistance is dominantly influenced by confining pressure. A realistic characterization methodology is triaxial testing with stress states representative of field condition. Therefore, triaxial RLPD test at field stress levels and critical temperature condition was employed for permanent deformation characterization of the FASB materials in this study.

3.2.1. Specimen fabrication procedure

For mix FASB-A, field cores with 4 inch diameter and 4.5 inch height were obtained from two distinct sites. The first site was a demonstration strip placed on May 2009 at the P. Flanigan and Sons, Inc. plant in Baltimore, MD. The demonstration strip was never covered with HMA and was directly exposed to the environment and truck traffic. Six cores (F1- F6) were transported to UMD laboratory on September 2011. The cores were air dried when transported to UMD laboratory. The linear variable differential transformers

(LVDT) studs were glued on the specimens. The specimens were kept at ambient temperature prior to test.

The second section was a lane widening on MD- 295 south of Baltimore near BWI Airport. Construction included a control strip placed in May 2011 followed by main construction (segments A and B) in July 2011. The control strip was placed in one 8 inch lift on 5/24/11. Curing conditions were ideal with clear weather, no rain, and daily average temperatures in the mid-to-upper 70°F range for the entire week after placement. The control strip was covered with 8 inch HMA layer two months after placement. The mainline construction included two segments.

Segment A: the first 4 inch layer was placed on 7/7/11 and the second 4 inch lift was placed four days later (7/11/11).

Segment B: FASB was placed in two 4 inch lifts on a same day (7/11/11).

The weather conditions for the mainline segments were mostly favorable for curing, with daily average temperatures in the low 80°F range and no rain except for a local thunderstorm on site on July 7 one night after the placement of the first layer of segment A. The mainline segments were covered by HMA seven days after placement.

Seven intact cores (example in Figure 3.5) were obtained from the three different sections. All cores were obtained just prior to opening the lane to traffic. The field cores were cut with diamond saw to 4.5 inch height and were kept uncovered in the ambient temperature for the surface to dry. The LVDT studs were glued afterward on the specimens. These cores were stored at ambient temperature in laboratory in latex membranes to maintain the near field moisture content condition prior to test.

Cores B1, B2, and B3 were obtained from segment B four months after construction. B5 the only intact core from segment A was also obtained four months after construction. Cores B4 and B6 from the same section sheared at the interface between the two FASB lifts during coring or during transport to the laboratory. Cores B7, B8, and B9 were obtained from control strip six months after construction. All the B cores were obtained before opening the construction site to traffic.

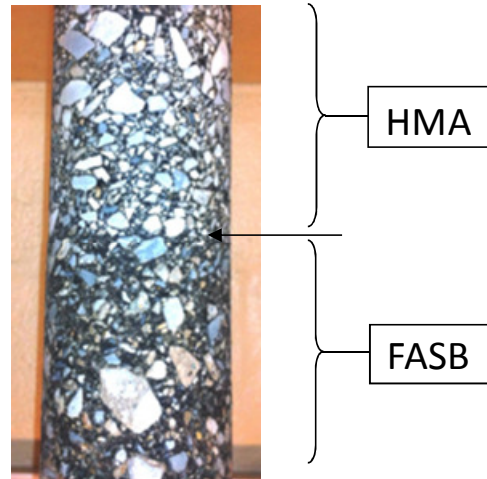


Figure 3.5. FASB-A, core obtained from MD-295 site

For mix FASB-H, 4 inch diameter and 4.5 high specimens were prepared in the laboratory. The specimens were compacted using a standard Proctor hammer with modifications in number of blows (75 blows per layer) and number of layers (5 layers) to comply with AASHTO T 180-10 modified Proctor compaction energy. This procedure was adopted because of limitations the facilities available in the laboratory of University of Maryland. After sample preparation, specimens were kept in the mold and cured in an oven at 104°F for 72 hours. The specimens were then extruded from the mold and kept at ambient temperature in the laboratory prior to test. To assure parallel ends for loading, the specimens were capped with sulfur capping compound (Figure 3.6). The LVDT studs were glued afterward on the specimens. The specimens were kept in the laboratory at ambient temperature before the test.



Figure 3.6. FASB-H laboratory prepared sample, capped with sulfur capping compound

Due to the nondestructive nature of the DM test, the same specimen was used for subsequent RLPD test unless otherwise noted.

3.2.2. Triaxial DM: Test Protocol and Analysis

The DM ($|E^*|$) test was originally developed to determine the response of asphalt mixtures at different loading rates and temperatures (AASHTO TP 62-07 Replaced by AASHTO T 342-11). The stress-strain relationship is assessed under a sinusoidal loading. DM ($|E^*|$) is defined in Equation 3.4 as the ratio of maximum dynamic stress (σ_{\max}) to the maximum recoverable axial strain (ϵ_{\max}). The peak strain lags behind the peak stress because of viscoelasticity of asphalt binder as illustrated in Figure 3.7.

$$|E^*| = \frac{\sigma_{\max}}{\epsilon_{\max}} \quad (3.4)$$

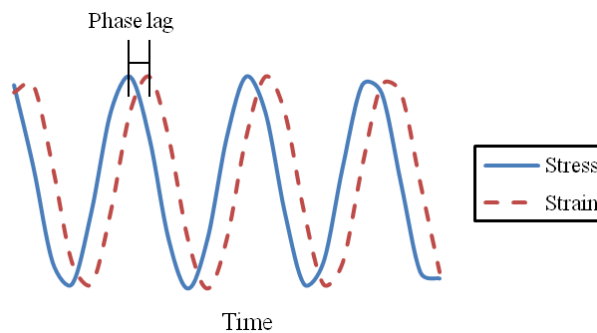


Figure 3.7. Phase lag between stress and strain in dynamic loading of viscoelastic material

AASHTO TP 62-07, 'Standard Method of Test for Determining DM of Hot Mix Asphalt (HMA)' was employed with some modifications in terms of temperature and loading rates and confining pressures to reflect the conditions that FASB materials will experience in field. The test was performed at 20, 10, 5, 1, 0.5, and 0.1 Hz loading rate frequencies. The test temperatures were 41°F (5°C), 59°F (15°C), 77°F (25°C), 95°F (35°C). The confining pressures included 0 psi, 7.3 psi, and 14.5 psi and the deviatoric stresses were adjusted at each frequency, confinement level and temperature to assure linear viscoelastic conditions corresponding to an axial strain level less than about 100 $\mu\epsilon$. The test was conducted from lowest temperature toward the highest; at each temperature, from the highest confinement level toward the lowest level; and at each confinement level, from highest frequency to the lowest frequency to reduce any potential damage during loading the specimen. Two axial linear variable differential transformers (LVDT) were used to measure the axial deflection on the specimen.

A universal test machine (UTM-100) was initially used for the tests (Figure 3.8.a). Due to some electronic problems in the data acquisition system of the machine, testing was transferred to an MTS test machine (Figure 3.8.b) provided by the Federal Highway Administration's Turner-Fairbank Highway Research Center. The test on four of the samples were repeated to assess any potential machine-to-machine differences in measured $|E^*|$ values.



Figure 3.8.a) UTM-100, (b) MTS test machine

At each confinement level, the measured dynamic moduli at different temperatures were shifted with respect to a reference temperature of 77°F to construct a master curve using standard time-temperature superposition techniques. Equation 3.5 defines the sigmoidal function (AASHTO PP 62-10) used to describe the loading rate dependency of the modulus.

$$\text{Log } |E^*| = \lambda + \frac{\alpha}{1 + e^{\beta + \gamma \log t_R}} \quad (3.5)$$

where t_R reduced time at reference temperature (77°F);

λ : minimum value of $|E^*|$;

$\lambda + \alpha$: maximum value of $|E^*|$; and

β and γ : shape parameters.

The temperature dependency of the modulus is incorporated in the reduced time parameter (t_R) in Equation 3.5. Equation 3.6 defines the reduced time as the actual loading time divided by the time-temperature shift factor, $a(T)$. The shift process is illustrated in Figure 3.9.

$$t_R = \frac{t}{a(T)} \quad (3.6)$$

where t : loading time (sec);
 $a(T)$: shift factor as a function of temperature; and
 T : temperature.

Figure 3.10 shows the final master curve along with its shift factors. To assess the shift factors over the range of different temperatures, a quadratic polynomial is fitted to the $\log a(T)$ versus temperature (T (°F)) data points (Equation 3.7)

$$\log a(T) = aT^2 + bT + c \quad (3.7)$$

where a , b , and c : polynomial fit constants.

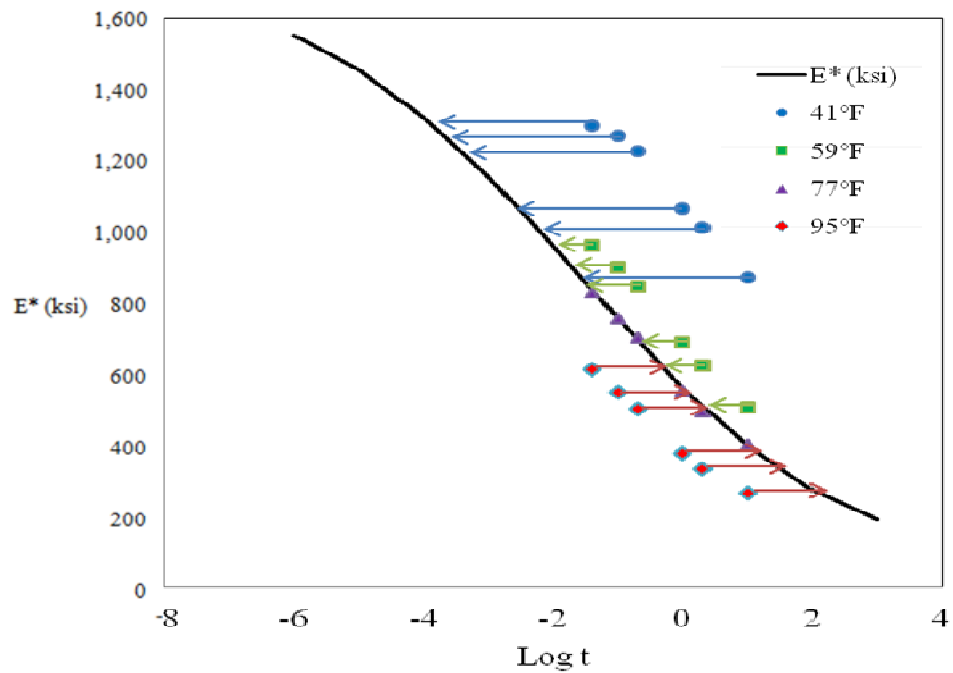


Figure 3.9. Construction of master curve, temperature shifting process

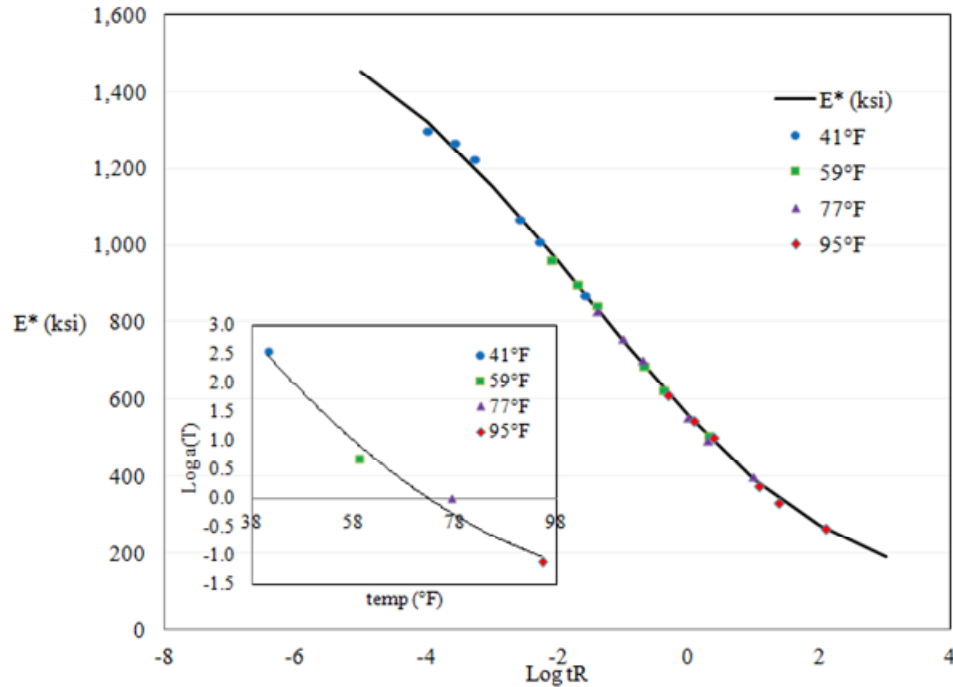


Figure 3.10. Example of DM master curve and its shift factors

3.2.3. Triaxial RLPD: Test Configuration and Analysis

The triaxial RLPD test was originally developed to identify the rutting susceptibility of asphalt mixtures and has been adopted for FASB mixtures. As explained briefly in the literature review in Section 3.2.1, the cumulative permanent strain under repeated load cycles measured and plotted versus the number of cycles.

The behavior of asphalt mixture with respect to permanent deformation is influenced by loading rate, stress levels, and test temperature as expected from the viscoelasticity of the asphalt binder. In this study, Asphalt Mixture Performance Tester (AMPT) shown in Figure 3.11 was utilized and the recommendations from NCHRP 9-30A for HMA were adopted for test stress levels and temperature.

A 0.1 second load time followed by 0.9 seconds rest period was utilized. This loading rate is incorporated in the AMPT software. A 10 psi confining pressure and a 70 psi repeated deviator stress were applied according to NCHRP 9-30A recommendationa for HMA. These stress states are expected to be high for a FASB layer below a thick HMA layer and

thus can be considered conservative for assessing its permanent deformation susceptibility in this case. However, there are other cases in which FASB may be used beneath a thin layer of HMA, and for this condition the stress states were considered reasonable. An added benefit of using the NCHRP 9-30A recommended stress states and temperatures is that the rutting susceptibility of FASB can be compared directly to that of HMA.



Figure 3.11. AMPT machine, triaxial RLPD test

The test temperature was selected based on the NCHRP 9-30A intermediate test condition defined as the average of 68°F and performance graded (PG) high temperature at 50% reliability. PG high temperature at 50% reliability was obtained as 136.4°F (58°C) for Baltimore area from LTPP Bind software. Accordingly, 102.2°F (39°C) was selected as test temperature. The test termination points were selected as 10,000 cycles or 80,000 $\mu\epsilon$ cumulative permanent strain, whichever occurred first.

The accumulated plastic strain curve can include up to three stages generally defined as (1) primary, (2) secondary, and (3) tertiary. The primary stage is defined as the initial rapid permanent deformation with a high but decreasing strain rate per cycle due mainly to densification and rearrangement of the aggregate structure.

In secondary stage, the plastic strain increases with a decreasing rate per cycle. A power law is typically used to represent the secondary stage of permanent deformation. (Equation 3.8). A power law plots as a straight line on log-log axes. The higher the slope and intercept of secondary stage, the higher is the potential for rutting. The regression constant “B” represents the secondary creep slope on a log scale. Figure 3.12 shows the intercept and slope of the secondary stage on a log-log plot.

$$\varepsilon_p = AN^B \quad (3.8)$$

where ε_p : permanent strain;
N: number of loading cycles; and
A and B: regression constants.

The tertiary stage, if present, develops when the rate of permanent deformation increases constantly leading to a shear failure or flow in the material. Flow number is defined as the number of loading cycles at the beginning of the tertiary stage and is a measure of rutting susceptibility of the mixture.

The flow number was determined using the Franken Model. The Franken Model is a composite mathematical model which captures the primary, secondary, and tertiary stages. The Franken Model is represented by the following equation:

$$\varepsilon_p = AN^B + C(e^{DN} - 1) \quad (3.9)$$

where A, B, C, and D: regression constants.

The regression constants were determined by a non-linear regression, least-squares procedure using Microsoft Excel Solver. The Franken Model is twice differentiated with respect to N to determine the gradient of the strain slope. The flow number is defined as the point where the gradient of the strain slope changes from a negative to a positive value. The regression constant “B” represents the secondary creep slope on a log scale.

A schematic of a RLPD test with all the three stages is illustrated in Figure 3.12. It should be mentioned that the behavior of material with respect to permanent deformation is highly

dependent on stress levels, temperature, density, moisture content, angularity of aggregates, binder characteristics, and other factors.

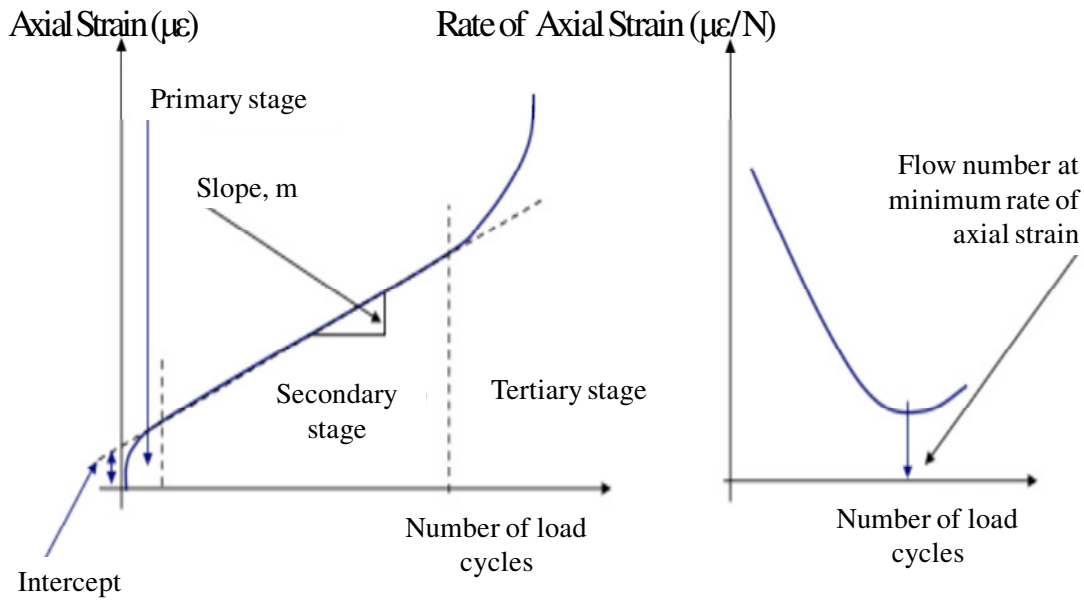


Figure 3.12. Schematic of RLPD test, three main stages, slope and intercept of secondary stage, and flow number

CHAPTER 4. Mix Design Test Results and Interpretations

4.1. Indirect tensile strength test results

The indirect tensile strength (ITS) of FASB material in the unsoaked condition is due not only to the foamed asphalt bonds but also to the following factors: the matric suction from residual water as explained in Section 2.2.3, the cohesive bonds from partially oxidized residual binder in recycled asphalt pavement (RAP) (Fu *et al.*, 2008), the cementitious bonds from residual non-hydrated cement in recycled concrete (RC) or newly introduced cement, the weak chemical bonds in the mineral phase of the aggregate (Fu *et al.*, 2008), and contacts within the aggregate skeleton, their orientations and mechanical properties. The effect of foamed asphalt stabilization is largely masked in unsoaked condition because of the combined effects of the various bonding elements in the mixture.

When the specimens are soaked, many of these bonds are negatively affected by the induced moisture to various extents. Matric suction from residual water, weak chemical bonds in mineral phase, and adhesion from partially oxidized residual binder in RAP are vulnerable to induced moisture. On the other hand, cementitious bonds and interlocking in aggregate skeleton are only slightly affected by the induced moisture. Foamed asphalt bonds are in the middle of the range and are moderately sensitive to moisture content (Fu *et al.*, 2008). Under soaked condition, most of the moisture susceptible bonds go away. Therefore, the effect of foamed asphalt bonds can be better captured in the soaked rather than in the unsoaked condition.

The mix design test results for the all mixtures in this study are provided in Appendix I and are summarized in Table 4.1. In this section, the effects of different components of mix design on the ITS of FASB material are evaluated and potential factors that affect it are discussed.

Table 4.1. ITS test results for the evaluated mixtures at different foaming asphalt contents

	Foamed asphalt (%)	ITS Unsoaked (psi)	ITS soaked (psi)	TSR ¹ (%)	Dry Density (pcf)
Mix A	2.13	86	64	74	126
	2.58	66	59	88	125
	3.04	75	64	85	127
	3.62	75	70	92	126
Mix A* ²	2.37	86	64	74	127
	2.54	97	66	68	127
	3.04	89	79	90	126
	3.59	90	76	84	124
Mix B	2.15	66	56	84	124
	2.51	69	66	95	129
	3.16	69	69	100	127
	3.00	62	60	97	126
Mix C	2.17	57	55	96	126
	2.48	52	56	108	125
	3.11	54	58	109	125
	3.49	61	58	96	125
Mix D	2.05	69	31	45	140
	2.30	69	27	39	138
	2.54	68	25	37	140
	2.83	77	29	38	140
Mix E	1.87	51	26	51	134
	2.27	59	34	57	136
	2.55	64	32	50	133
	2.80	54	31	58	132
Mix F	2.00	69	41	59	132
	2.27	61	35	57	132
	2.50	64	48	76	131
	2.81	63	39	62	132
Mix G	2.30	44	15	34	134
Mix G*	2.00	67	48	71	133
	2.30	62	61	98	133
	2.60	65	50	77	132
Mix H	1.90	53	33	62	120
	1.92	56	37	65	120
	2.21	53	41	78	120
	2.49	49	38	78	119

1: TSR: tensile strength ratio= soaked ITS/ unsoaked ITS.

2: * denotes the same mix with 1% added Portland cement.

4.1.1. Effect of foaming asphalt content on ITS

Mixtures A to H were evaluated at four different foaming asphalt contents as stated in Table 4.1 except for Mix G. Mix G had a very low soaked ITS. Therefore, the test was discontinued for this mixture and 1% cement was added to improve its soaked ITS (Mix G*). The effect of adding cement will be separately evaluated in Section 4.1.4.

Figure 4.1 shows the unsoaked (green lines) and soaked (orange lines) ITS of different mixtures of FASB material. The three columns in the figure correspond to the three groups of material types:

- (a) RAP-1/RC mixtures (A, B, C);
- (b) RAP-1/GAB mixtures (D, E, F) and;
- (c) pure RAP mixtures of RAP-2 and RAP-3 (Mix G and Mix H).

Rows within the first two columns of Figure 4.1 correspond to different proportion of RAP-1 starting from 40% RAP-1 in the first row and continuing with 60%, and 80% RAP-1 on the following rows. Mixtures noted with “*” indicate the same mixture with one percent added cement. Figure 4.1 illustrates how ITS in soaked and unsoaked conditions varies with different foamed asphalt content for each mixture. No significant upward or downward trends in ITS with foamed moisture content were observed consistently across all mixtures. Similarly, it was difficult to define the “optimum” foamed asphalt content for the mixtures. This observation suggests a low sensitivity of ITS to foamed asphalt content. This could be explained by the combined influence of different bonding mechanisms on ITS as explained earlier in this chapter. In other words, the effect of the foamed asphalt content was masked by other bonding elements. However, this should not be interpreted as ineffectiveness of foamed asphalt bonds. Foamed asphalt bonds provide ductile dispersed bonds through the mixture improving the flexibility of FASB mixtures Wirtgen (2010).

Table 4.2 summarizes the average ITS in the soaked and unsoaked conditions, the coefficients of variation (CV), and the tensile strength ratio (TSR) for each mixture. The coefficient of variation (CV) of ITS with respect to foaming asphalt content across all mixtures was less than 14% in the soaked condition with an average of 9% and less than

11% in the unsoaked condition with an average of 6%. The Kolmogorov–Smirnov statistical test on the CV of ITS values in the soaked and unsoaked conditions or different groups of mixtures (RAP-1/RC, RAP-1/GAB, and pure RAP) does not show a significant difference between the CV of different mixture groups or testing conditions (soaked and unsoaked).

Table 4.2. The average ITS test results in unsoaked and soaked condition with incremental foamed asphalt content along with their coefficients of variation (CV)

Mixture	Unsoaked ITS		Soaked ITS		TSR (%)
	Average (psi)	CV (%)	Average (psi)	CV (%)	
A	75.8	11%	63.9	7%	84.3%
A*	90.6	5%	71.2	11%	78.6%
B	66.6	5%	62.6	9%	94.0%
C	56.1	7%	57.0	3%	101.6%
D	70.9	6%	28.1	9%	39.6%
E	57.0	10%	30.9	10%	54.2%
F	64.1	5%	40.7	14%	63.5%
G	44.0	-	15.0	-	34.1%
G*	64.7	4%	53.0	13%	81.9%
H	53.0	5%	37.4	9%	70.6%

Maryland provisional specification for FASB courses (Section 50x) requires a minimum TSR of 70% for mix design optimization purposes. Based on this, Mix D, E, F, and G with TSR values below 70% cannot pass the criteria. This suggests a need for active filler for these mixtures. Adding 1% cement improved the soaked ITS of these mixtures; the effects of adding cement will be explained in more detail in Section 4.1.4.

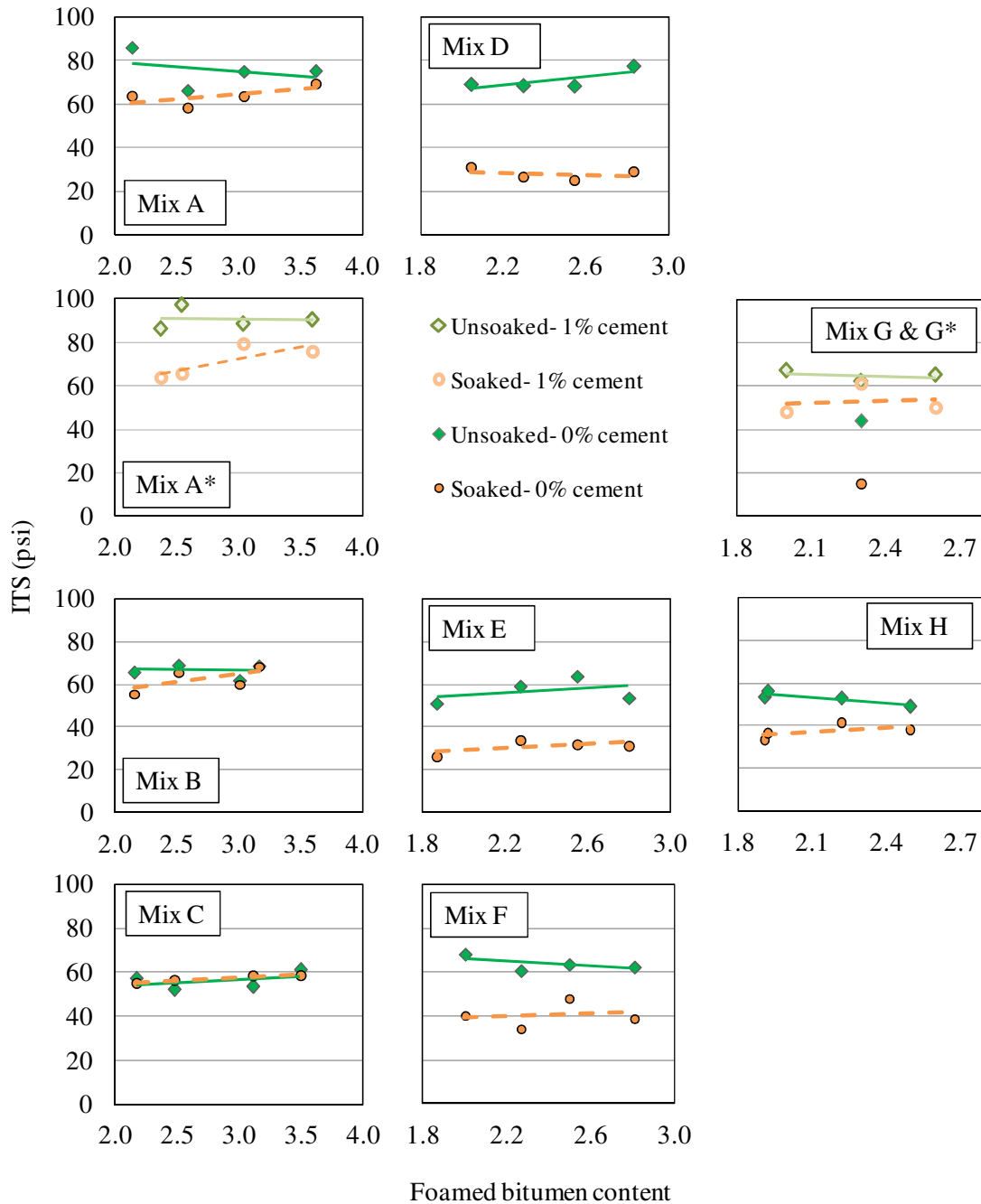


Figure 4.1. ITS in unsoaked and soaked condition versus incremental foaming asphalt content for Mix A: 40% RAP-1+60% RC, Mix A*: 40% RAP-1+60% RC+1% cement, Mix B: 60% RAP-1+40% RC, Mix C: 80% RAP-1+20% RC, Mix D: 40% RAP-1+60% GAB, Mix E: 60% RAP-1+40% GAB, Mix F: 80% RAP-1+20% GAB, Mix G: 100% RAP-2, Mix G*: 100% RAP-2+1% cement, Mix H: 100% RAP-3

4.1.2. Effect of RAP, RC, and GAB on ITS

Figure 4.2 shows the effects of RAP-1, RC, and GAB on ITS in soaked and unsoaked conditions for Mix A to F. The soaked ITS of the RAP-1/GAB mixtures was significantly lower than for the RAP-1/RC. Increasing the RAP percentage generally decreased unsoaked ITS. However, it had mixed effects on soaked ITS, i.e. it improved soaked ITS for mixtures containing GAB while decreasing ITS for mixtures containing RC. In order to explain these inconsistent effects, it is important to look precisely into the characteristics of each element in the mixture.

RAP-1 was generally coated by oxidized asphalt as illustrated in Figure 2.4.c. When the new foamed asphalt is induced, it sticks better to RAP because of the adhesion between the partially oxidized residual binder in the RAP and the foamed asphalt. Therefore, increasing the percentage of RAP can improve the foamed asphalt bonds. On the other hand, RC and GAB had stiffer and stronger skeletons with more angular aggregates (Figure 2.4.a and Figure 2.4.b) providing a better aggregate interlock. Decreasing the percentage of the stiffer material can, therefore, reduce the ITS. As an added benefit, RC has the potential to provide stronger and brittle cementitious bonds owing to its residual cement particles. In unsoaked conditions, matric suction is also added to all the aforementioned components. The effect of each component on ITS can be masked by the more dominant element in soaked and unsoaked conditions.

In RAP-1/RC mixtures, RC governs the ITS in both the soaked and unsoaked conditions and thus ITS decreases as the percentage of RC decreases. However, the slope of the strength reduction is lower in the soaked condition because of the reverse effect of RAP in improving foamed asphalt bonds, which are the more dominant component in the soaked condition. These trends can be seen in Figure 4.2.a. Blends with higher percentages of RC generally tend to absorb more water when soaked because of the relatively high absorption of RC (4%, Table 2.2), but this did not affect the strength under soaked condition

Replacing RC with GAB produced a significant reduction in soaked ITS, which again shows the dominant role of cementitious bonds in RC. This replacement had caused less of a change in unsoaked ITS, showing that other factors such as matric suction and aggregate

interlock was more dominant in the unsoaked condition. Replacing RC with GAB also increases the dry density significantly (Table 4.1) because of the higher specific gravity of GAB. However, this higher density had little effect on ITS.

In the RAP-1/GAB mixtures, there is a tradeoff between RAP and GAB leading to a slight decrease in unsoaked ITS. Under soaked condition, the role of the foamed asphalt bonds is more pronounced, causing a significant increase in soaked ITS with increasing RAP-1 percentage. This shows higher sensitivity of soaked ITS to foamed asphalt bonds.

The linear trend lines for the ITS test results from the RC/RAP mixtures and GAB/RAP mixtures were extrapolated to predict ITS for a fictitious 100% RAP-1 mixture. The predicted values were averaged to find the potential ITS of the fictitious mixture in the soaked and unsoaked conditions; this extra data point was used to fit new linear trend lines as illustrated in Figure 4.2.b.

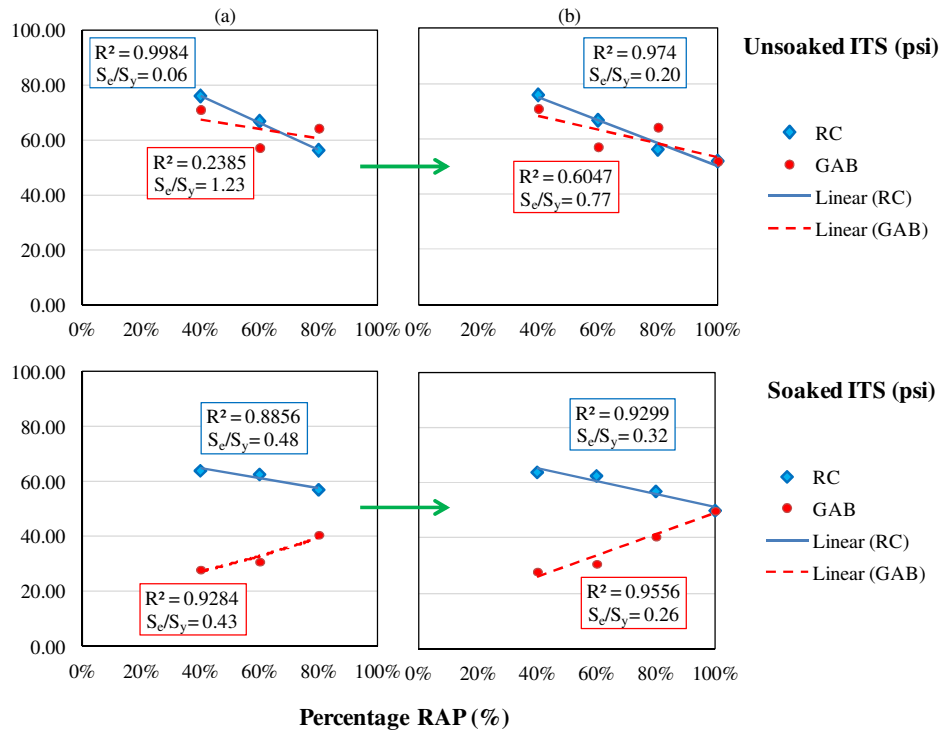


Figure 4.2. ITS in unsoaked and soaked conditions for RAP-1/RC (blue) and RAP-1/GAB mixtures (red) versus percentage RAP-1 in the mixture: (a) Experimental data for Mix A to F; (b) Fictitious mixture of 100% RAP-1 obtained from extrapolating and averaging the trend lines for RAP-1/RC and RAP-1/GAB mixtures

The ITS of the fictitious FASB mixture of 100% RAP-1 was then compared to the other two 100% RAP FASB mixtures (RAP-2 and RAP-3). The dry density of RAP-1 mixture was also found following the same extrapolation method as for ITS. Figure 4.3 shows the comparison between the average ITS, TSR, and dry density of RAP-1, RAP-2, and RAP-3. This comparison shows that ITS can be significantly different for different mixtures from different RAP sources, gradations, and foaming binders as explained in Section 2.1. This observation is also in agreement with the variability observed in the studies in literature. Moreover, it reveals that higher dry density or processing of the RAP (as was the case in RAP-2) cannot guarantee a high quality FASB mixture. Mix design tests should be performed to evaluate each individual mixture. A potential reason for the poor behavior of RAP-2 mixture could be its relatively finer gradation and higher percentage passing No. 200 sieve (7.5%, Table 2.2), which makes it more susceptible to moisture. However, this speculation is complicated by the other uncontrolled variables explained earlier.

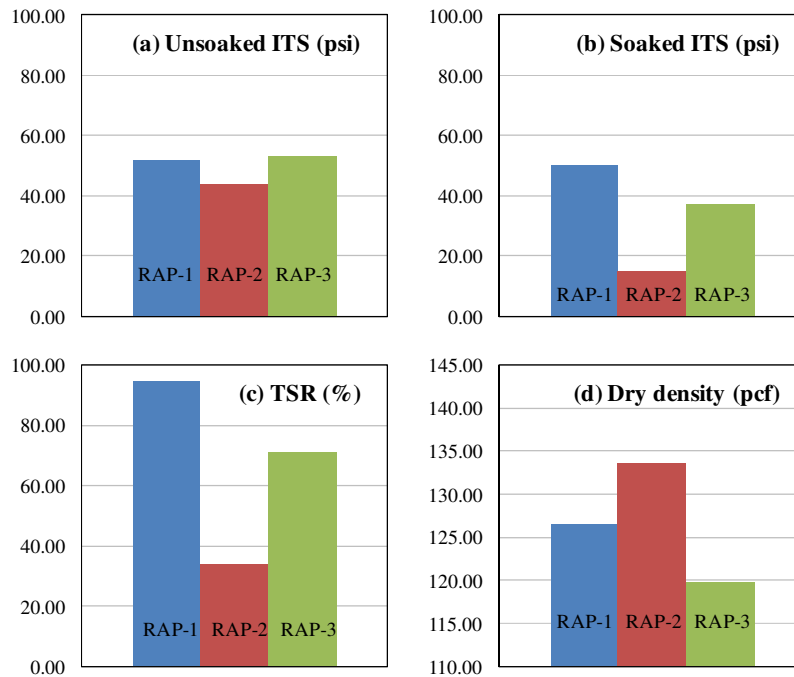


Figure 4.3. FASB mixtures from different RAP sources. RAP-1 is the fictitious mixture from extrapolation of experimental data from Mixes A to F

4.1.3. Effect of Soaking Process on ITS

The influence of the details soaking procedure were examined to find the most appropriate soaking process. Specifically, 72 hour soaking, 24 hour soaking, and low vacuum saturation were applied to an FASB blend of 40% RAP-2 and 60% RC+1% cement at two binder contents of 3% and 3.5%. The low vacuum saturation procedure consisted of soaking in a water bath for 20 minutes followed by 50 minutes of saturation under a 2" vacuum followed by a 10 minute rest period in the water bath.

The results from tests on 3 replicates for each condition are summarized in Table 4.3 and Figure 4.4. As expected, 72 hour soaking period induced more moisture into the specimens and reduced the strength the most. However, it also generally produced a higher coefficient of variation in the soaked ITS values. Low vacuum saturation was not found to be as effective as 24 hour soaking and it requires vacuum saturation facilities in the lab. The 24 hour soaking period showed more consistent ITS values with lower variability and is convenient for producers to perform for mix design testing.

High vacuum saturation was also applied to the same blend at a 2.3% binder content according to AASHTO T283. This method of saturation induced an average of 7.5% moisture content in the specimen. However, some deterioration was found on the structure of specimens due to the high vacuum level. Therefore, 24 hour soaking was adopted as the best compromise between modeling field conditions and streamlining mix design testing.

Table 4.3. The effect of soaking process on 40% RAP + 60% RC+ 1% cement mixture

	3% binder				3.5% binder			
	Dry	Vacuum*	24 hr	72 hr	Dry	Vacuum	24 hr	72 hr
MC at break (%)	1.4	5.0	6.5	6.9	1.7	5.1	5.6	5.9
ITS (psi)	63	59	52	45	87	88	77	66
TSR (%)	NA	95	83	71	NA	102	88	76
CV in ITS (%)	8%	11%	11%	26%	13%	17%	3%	16%

* 20 min bath+50 min vacuum at 2" height+10min rest

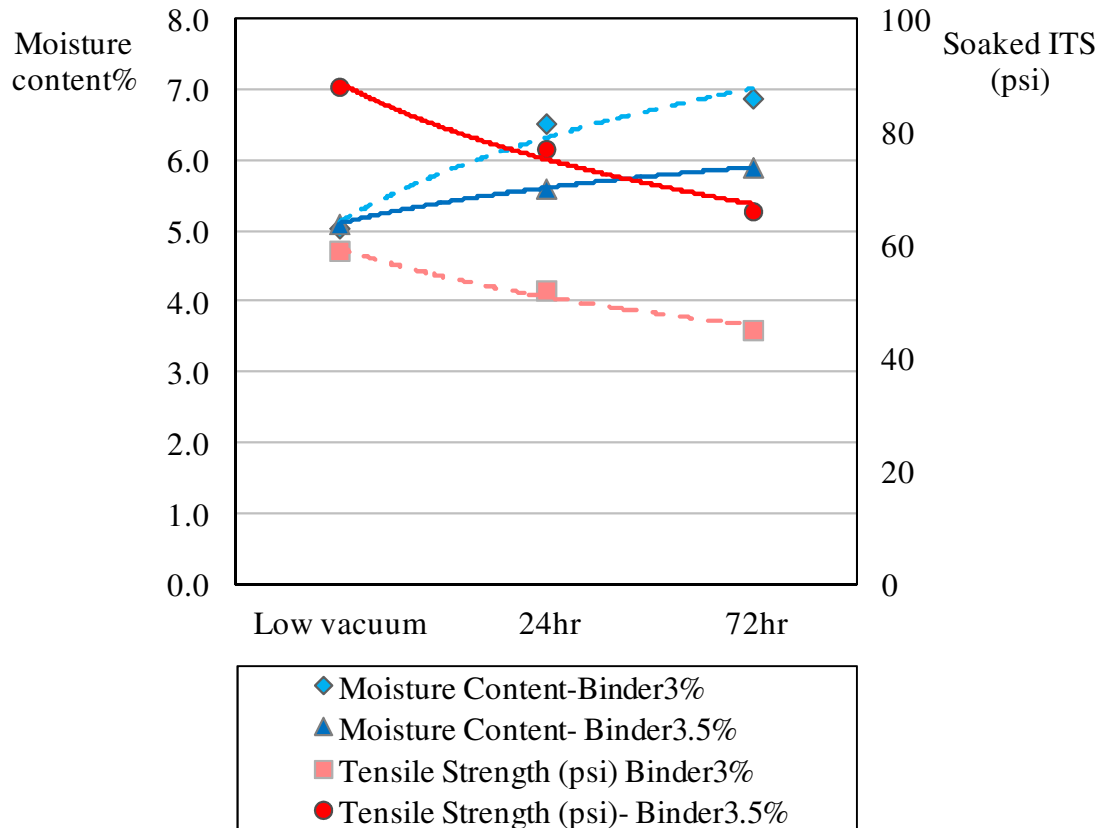


Figure 4.4. Soaking process effect on MC and ITS values (40%RAP-2+60%RC+1%cement), after Khosravifar *et al.* (2012)

4.1.4. Effect of Active Additives on ITS

Adding cement will enhance the unsoaked and soaked ITS of FASB mixtures by providing stiff, brittle cementitious bonds. The effect of added cement on tensile strength was evaluated both for Mix A (40% RAP-1 plus 60% RC) and Mix G (100% RAP-2) as they had the highest and lowest unsoaked ITS, respectively. The results are tabulated in Table 4.4 and Table 4.5. The test results for Mix G (Table 4.4) showed a 40% increase in unsoaked ITS and an over 300% increase in soaked ITS. TSR has significantly improved, too.

Table 4.4. Effect of cement on ITS results of Mix G with 100% RAP-2

Mix G	0% cement	1% cement
Foamed asphalt (%)	2.3	2.3
Unsoaked ITS (psi)	44	62
Soaked ITS (psi)	15	61
TSR (%)	34	98

Test results for Mix A at four different foamed asphalt contents (Table 4.5) showed less pronounced benefits than for Mix G, with a 20% average increase in unsoaked ITS and a 10% average increase in soaked ITS. TSR did not improve by adding cement and decreased slightly on average. Mix A had comparatively good performance in the soaked condition due to hydration of the residual cement in the RC, which contributed to a number of cementitious bonds in the mixture even in the absence of added cement.

Table 4.5. Effect of cement on ITS results of Mix A with 40%RAP-1+60%RAP

Mix A	0% cement				1% cement			
Foamed asphalt %	2.13	2.58	3.04	3.62	2.37	2.54	3.04	3.59
Unsoaked ITS (psi)	86	66	75	75	86	97	89	90
Soaked ITS (psi)	64	59	64	70	64	66	79	76
TSR (%)	74%	89%	85%	93%	74%	68%	89%	84%

Figure 4.5 illustrates the average improvements in ITS results of Mix A and Mix G after adding 1% cement. For mix design purposes, a minimum TSR criterion should be used to identify if an active additive, e.g., cement, is needed. Its use should be limited to 1% not to jeopardize the flexibility of FASB mixtures (Wirtgen, 2010).

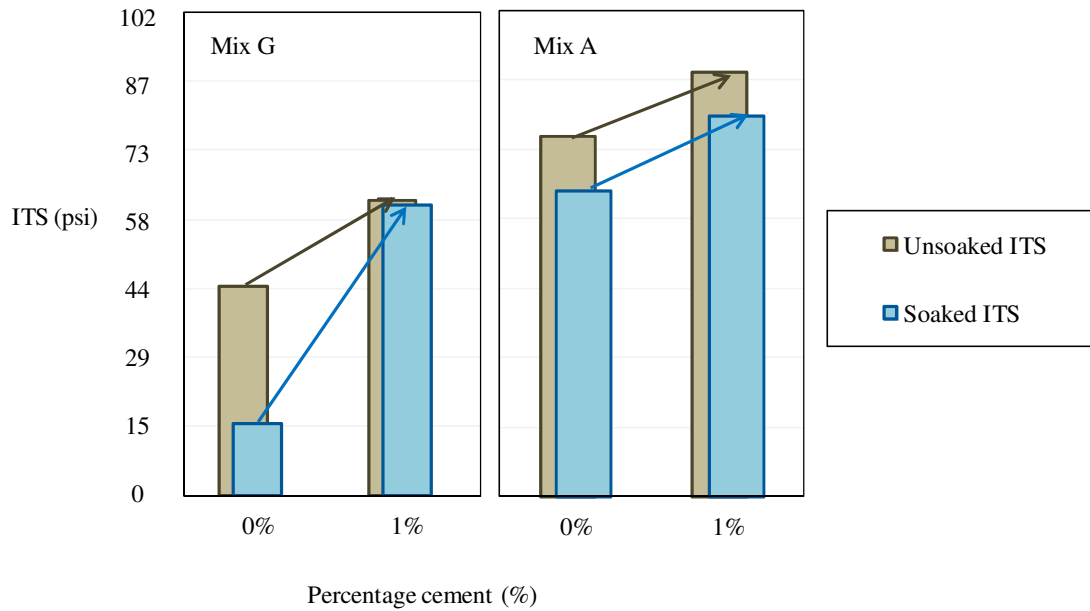


Figure 4.5. Effect of cement on average ITS of Mix A and Mix G in soaked and unsoaked condition

4.1.5. Effect of Mixing Moisture Content (MMC) on ITS

The effect of MMC was studied for Mix F (80% RAP-1 + 20% GAB) at a 2% foaming asphalt content. This mixture was selected because it was already found that its soaked ITS was moderately sensitive to changes in FA% (CV=14%, Table 4.2) and it had a low percentage of fines. Fu *et al.* (2010.a) found previously that foamed asphalt dispersion and correspondingly ITS in mixes with high fines contents (e.g. higher than 12% passing No. 200 sieve) are sensitive to MMC and it was important to evaluate the sensitivity of MMC on blends with low fines content.

The aggregate blend was mixed with the same foamed asphalt percentage (2%) at two different MMC targets: 90% of modified Proctor optimum moisture content (OMC) and 104% of OMC, which equated to 7.0% and 8.1%, respectively. Marshall specimens were made for each of two blends at different compaction moisture contents (CMC). The first blend (7% MMC, 104% of OMC) was compacted at target CMC values of 7% (90% OMC) and 5.7% (73% OMC) while the second blend was compacted at 8.1% (104% OMC) and 5.7% (73% OMC) moisture content. The measured unsoaked and soaked ITS values for

these combinations are summarized in Table 4.6. The mixture mixed and compacted at the higher moisture content (104% OMC) was 29% less strong in the unsoaked condition and 9% less strong in the soaked condition than the blend mixed and compacted at 90% of OMC. The specimens compacted at 73% of OMC showed very similar ITS values both in the soaked and unsoaked conditions regardless of the MMC at which the blend was mixed with foamed asphalt. This shows that MMC does not have a significant impact on the asphalt dispersion of this mixture and the tensile strength is mainly affected by the conventional moisture-density behavior of the granular material (Khosravifar *et al.*, 2012).

Table 4.6. Effect of MMC on Mix F with 2% foamed asphalt content

Target MMC (%)	7.0 _(90% of OMC)	8.1 _(104% of OMC)	7.0 _(90% of OMC)	8.1 _(104% of OMC)
Target CMC (%)	7.0 _(90% of OMC)	8.1 _(104% of OMC)	5.7 _(73% of OMC)	5.7 _(73% of OMC)
Unsoaked ITS (psi)	69.0	49.0	65.0	70.0
Soaked ITS (psi)	41.0	37.0	30.0	32.0
Dry Density (pcf)	131.8	129.8	131.8	133.8

Comparing these results to the earlier work by Fu *et al.* (2010.a) reveals another important role of fine particles in FASB mixtures. Excess fines such as those in the mixtures considered by Fu make the dispersion of foamed asphalt more sensitive to MMC.

4.1.6. Effect of Stockpiling on ITS

The ability to stockpile FASB is an important practical consideration for production. Jenkins *et al.* (2000) reported that FASB mixtures can be stockpiled for several months. In the other hand, Khweir (2007) found that curing of FASB mixtures can start right after mixing and during the stockpiling period before the material is placed and compacted in the field. In order to evaluate this effect in the laboratory, FASB mixtures from Mix C (80%RAP-1+20%RC), Mix D (40%RAP-1+60%GAB) and Mix G* (100%RAP-2+1%cement) were kept in sealed buckets for 15 days to investigate the effect of stockpiling. The foamed asphalt contents for Mix C and Mix D were tabulated in Table 4.1 and Mix G* was mixed with 2.5% foamed asphalt content. These three mixtures were

selected as representative of RAP/RC, RAP/GAB and RAP/cement mixtures. In order to eliminate any moisture content influence on ITS, only mixtures having the smallest CMC variations (less than 6% variation) were kept in the study. After 14 days of stockpiling, mix C (80%RAP+20%RC) showed 9% and 27% average decreases in unsoaked and soaked ITS, respectively, as compared to values immediately after mixing. Mix D (40%RAP+60%GAB) showed 14% and 29% decreases in unsoaked and soaked ITS after 14 days of stockpiling. The third mixture (100%RAP+1% cement) showed 26% and 24% decrease in unsoaked and soaked ITS after 15 days of stockpiling.

Figure 4.6 depicts the unsoaked and soaked ITS variations versus time. The results show that stockpiling the FASB significantly reduces both the unsoaked and soaked strength of all of the materials. One possible explanation is that the foamed asphalt droplets lose their adhesion after a short period of time, which could be due to oxidization of foamed asphalt. Also, although the moisture content was kept constant in the sealed buckets, any moisture redistribution in the mixture can lead to the formation of foamed asphalt bonds. Subsequent compaction can break these partially formed bonds by rearranging the FASB skeleton and aggregate contact orientation, leading to a reduction in strength. The third mixture (Mix G*) that contained cement showed a particularly higher vulnerability to stockpiling, which could be the result of breakage of the early cementitious bonds from the hydration of the cement during stockpiling.

The results showed a high variability between the behavior of each mixture in the unsoaked condition, which is due to the combined effects of different components on ITS as explained in detail in the beginning of this chapter. However, all of the mixtures regardless of aggregate types showed a very similar trend of an average 27% decrease in soaked ITS after 3 days of stockpiling. In order to extrapolate an estimate of the eventual reduced soaked ITS of the FASB due to stockpiling, a hyperbolic tangent equation was fit to the data (Equation 4.1). The eventual asymptotic strength reduction will be 27% of the initial soaked ITS. If producer intends to stockpile the material, then it is the reduced stockpiled values of ITS and TSR that should be used to determine whether the mix design is satisfactory.

$$ITS_{\text{soaked}} = ITS_{\text{initial soaked}} + 27\% \times ITS_{\text{initial soaked}} \tanh(t) \quad (4.1)$$

in which t is the stockpiling time in days.

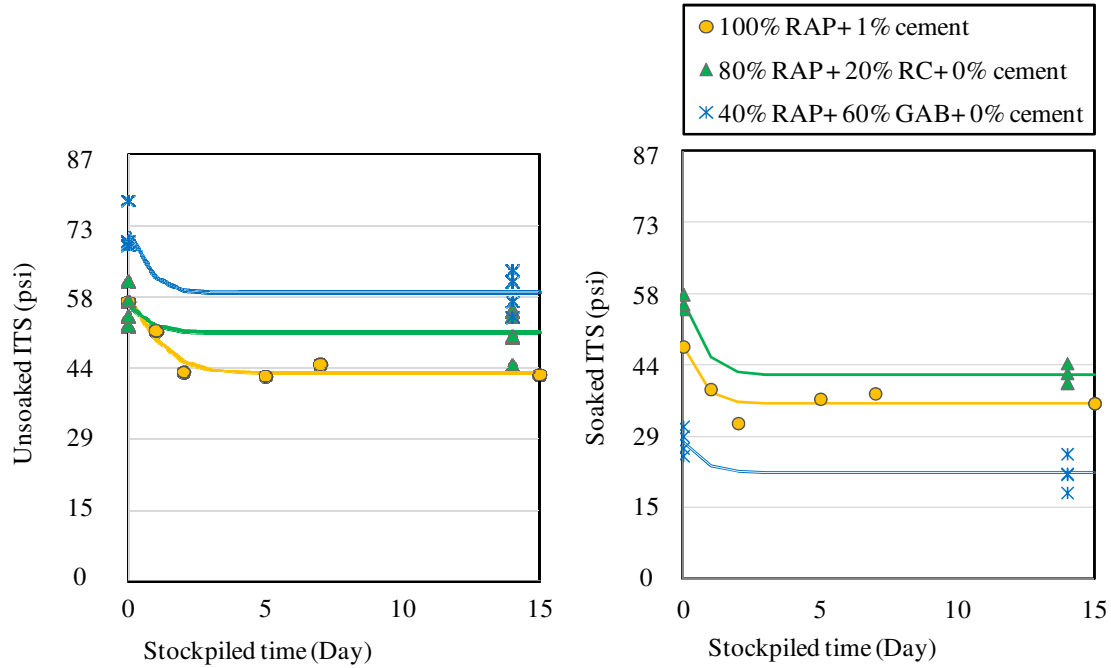


Figure 4.6. Unsoaked and soaked ITS versus stockpiling time for Mix C (80% RAP-2+20% RC), Mix D (40% RAP-2+60% GAB), and Mix G* (100% RAP-2+1% cement)

4.1.7. Conclusions and Recommendations for Mix Design

The ITS of FASB material in the unsoaked condition is not only from the foamed asphalt bonds but also from other factors such as matric suction from residual water, cohesive bonds from partially oxidized residual binder in recycled asphalt pavement (RAP) (Fu *et al.*, 2008), cementitious bonds from residual non-hydrated cement in recycled concrete (RC) or newly introduced cement, the weak chemical bonds in the mineral phase of the aggregate (Fu *et al.*, 2008), and the orientations, mechanical properties, and other characteristics of the contacts within the aggregate skeleton. Therefore, the effect of foamed asphalt stabilization is largely masked in the unsoaked condition because of the combined effects of the various bonding elements in the mixture.

When the specimens are soaked, many of these bonds are negatively affected by the induced moisture to various extents. Matric suction from residual water, weak chemical bonds in mineral phase, and adhesion from partially oxidized residual binder in RAP are vulnerable to induced moisture. On the other hand, cementitious bonds and interlocking in aggregate skeleton are only slightly affected by the induced moisture. Foamed asphalt bonds are in the middle of the range and are moderately sensitive to moisture content (Fu *et al.*, 2008). Under soaked condition, effect of foamed asphalt bonds are better observed.

Eight different FASB mixtures having different proportions of RAP, RC, and GAB aggregates were designed and evaluated. Unsoaked and soaked ITS tests on Marshall compacted specimens were performed to examine the effects of different design factors. Key conclusions drawn from the results of this study include the following:

1. There is a low to moderate sensitivity of to foamed asphalt content on unsoaked and soaked ITS, being slightly higher for soaked ITS.
2. Increasing the ratio of RAP/RC tends to decrease unsoaked and soaked ITS.
3. Increasing the ratio of RAP/GAB tends to decrease unsoaked ITS while increasing the soaked ITS.
4. Replacing RC with GAB dramatically decreases the soaked ITS.
5. Blends with a higher percentage of RC absorb more water when soaked because of the relatively high absorption of RC , but this does not affect the soaked strength; blends with higher RC/RAP ratio show higher soaked strength.
6. The ITS of FASB mixtures significantly depends on the mother aggregate characteristics and therefore design tests are required for each individual mixture.
7. Adding cement as an active filler increases the unsoaked and soaked ITS. Its effect is more significant on mixtures with TSR lower than 70%. For mix G with TSR of 34.1%, adding 1% cement increases expressed a 40% increase in unsoaked ITS and an over 300% increase in soaked ITS
8. MMC does not have a significant impact on the ITS of the mixes with low percentages of fines; the tensile strength is mainly affected by the conventional moisture-density behavior of the granular material.

9. Stockpiling FASB significantly reduced the soaked and unsoaked strength by an average of 27% and 16%, respectively. It also significantly reduced the unsoaked ITS of the mixtures containing cement.

An appropriate mixture requires a binder with good foaming parameters, an aggregate with appropriate gradation with 4% passing sieve number 200 for non-RAP aggregates and about 1% for RAP aggregates.

Mixing and compacting at 90% optimum moisture content of mother aggregate blend and curing at 104°F for 72 hours is suggested for FASB production design procedure. Soaking in bath tub at 77°F for 24 hours is advised for soaked ITS test conditioning.

Since soaked ITS is more sensitive to foamed asphalt bonds, it is suggested to select the optimum foamed asphalt content on this basis, with an additional requirement of a minimum TSR to screen for excessive moisture susceptibility. In cases where there is a well defined optimum ITS, the corresponding foamed asphalt content should be used for design, assuming that the design meets the minimum soaked ITS and TSR requirements. In cases where there is not a clear optimum soaked ITS value, the lowest foamed asphalt content at which the soaked ITS requirement and TSR requirements are met should be selected for design. If producer intends to stockpile the material, then it is the reduced stockpiled values of ITS and TSR that should be used to determine whether the mix design is satisfactory.

CHAPTER 5. Performance Test Results

5.1. Introduction

Dynamic modulus (DM) and repeated load permanent deformation (RLPD) tests were performed on field cores from FASB-A and laboratory prepared samples from FASB-H. Detailed information on sample source, construction method, curing time, and etc. is provided in Chapters 2 and 3. A universal test machine (UTM-100) was initially used for triaxial DM tests. Due to some electronic problems in the data acquisition system of the machine, testing was transferred to a uniaxial MTS test machine provided by the Federal Highway Administration's (FHWA) Turner-Fairbank Highway Research Center (TFHRC). The Asphalt Mixture Performance Tester (AMPT) at the TFHRC was utilized for RLPD test. Table 5.1 describes the test specimens, type of tests performed, and the testing equipment.

5.2. DM test results

DM tests were performed on 10 cores and 3 laboratory specimens (Table 5.1) to assess the range of stiffness for the material and its dependence on stress state, temperature and loading rate dependency. Master curves were produced according to the procedures described in Chapter 3; these which can be used as inputs to the new AASHTO mechanistic-empirical design procedure. Detailed descriptions on laboratory and field sample preparation are also provided in Chapter 3.

Master curves are provided for B, F, and I specimen types. Preliminary studies on the effects of stress states (confining pressure, and deviator stress), loading rate, and temperature on DM found that loading rate and temperature were the most significant factors influencing FASB stiffness. The influences of field construction procedures and curing conditions on stiffness are evaluated for FASB-A.

Table 5.1. Test specimens description

Specimen Name	Mixture Description	Sample Source	UTM-100 (triaxial DM)	MTS (uniaxial DM)	AMPT (RLPD)
B1	FASB-A	BW ¹ – Segment B	X		X
B2	FASB-A	BW – Segment B	X	X	X
B3	FASB-A	BW – Segment B	X	X	X
B4	FASB-A	BW – Segment A	Intact core could not obtained		
B5	FASB-A	BW – Segment A		X	X
B6	FASB-A	BW – Segment A	Intact core could not obtained		
B7	FASB-A	BW – Control Strip		X	X
B8	FASB-A	BW – Control Strip	X		X
B9	FASB-A	BW – Control Strip	X		X
F1	FASB-A	F ²		X	X
F2	FASB-A	F	X	X	X
F3	FASB-A	F	X	X	X
F4	FASB-A	F			X
F5	FASB-A	F			X
F6	FASB-A	F			X
I1	FASB-H	L ³		X	X
I2	FASB-H	L	X		
I3	FASB-H	L		X	X
I4	FASB-H	L			X

1. BW = Baltimore-Washington Parkway (MD-295)

2. F = P. Flanigan and Sons Inc. demonstration strip

3. L = UMD Laboratory made sample for FASB-H. This mix design was used in I-81(VA) highway reconstruction project.

5.2.DM test results

DM tests were performed on 10 cores and 3 laboratory specimens (Table 5.1) to assess the range of stiffness for the material and its dependence on stress state, temperature and loading rate dependency. Master curves were produced according to the procedures described in Chapter 3; these which can be used as inputs to the new AASHTO mechanistic-empirical design procedure. Detailed descriptions on laboratory and field sample preparation are also provided in Chapter 3.

Master curves are provided for B, F, and I specimen types. Preliminary studies on the effects of stress states (confining pressure, and deviator stress), loading rate, and temperature on DM found that loading rate and temperature were the most significant

factors influencing FASB stiffness. The influences of field construction procedures and curing conditions on stiffness are evaluated for FASB-A.

5.2.1. Effect of stress state, loading duration, and temperature

Triaxial tests at 3 confining pressures using UTM-100 machine were performed on B1, B2, B3, B8, B9, F2, F3, and I2 to assess the effects of confining pressure on DM ($|E^*|$). Figures 5.1 to 5.3 show the DM versus reduced loading time ($\log t_R$) for the B, F, and I specimens, respectively. The different curves correspond to different temperatures and confining pressures. Overall, the results suggested that the DM is more dependent on loading rate and temperature rather than the confining pressure.

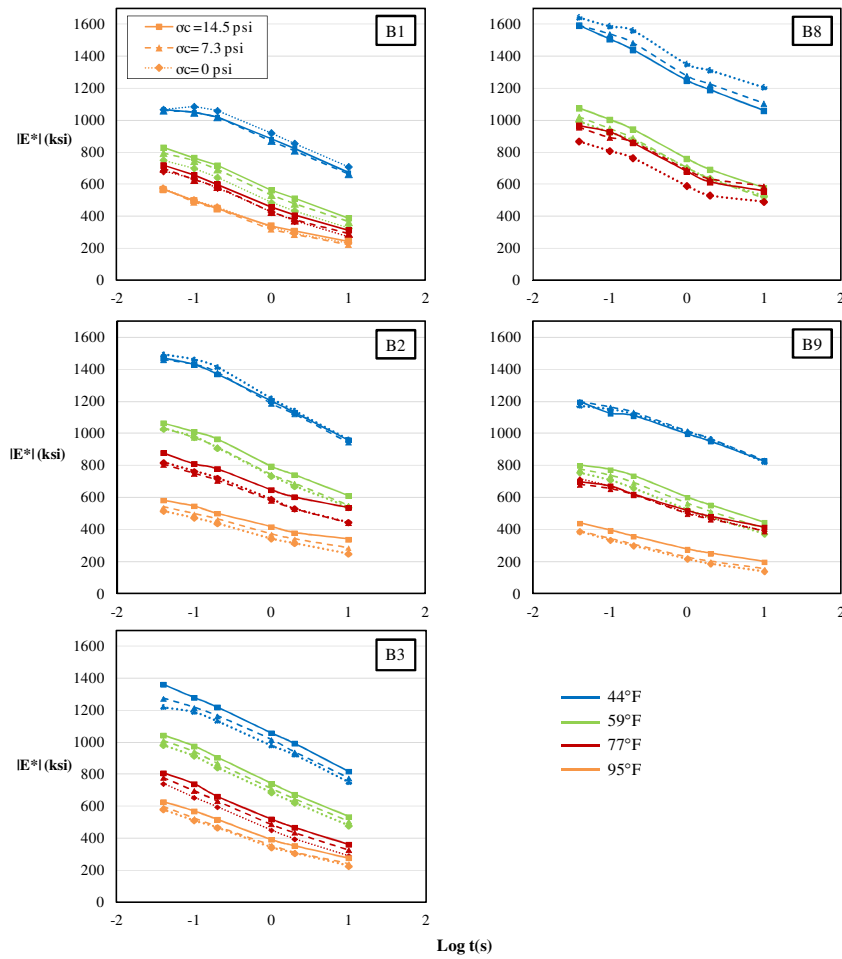


Figure 5.1. $|E^*|$ versus reduced time for B cores (Baltimore-Washington Parkway Site) at 14.5 psi, 7.3 psi, and 0 psi confining pressure at 44°F, 59°F, 77°F, and 95°F temperatures

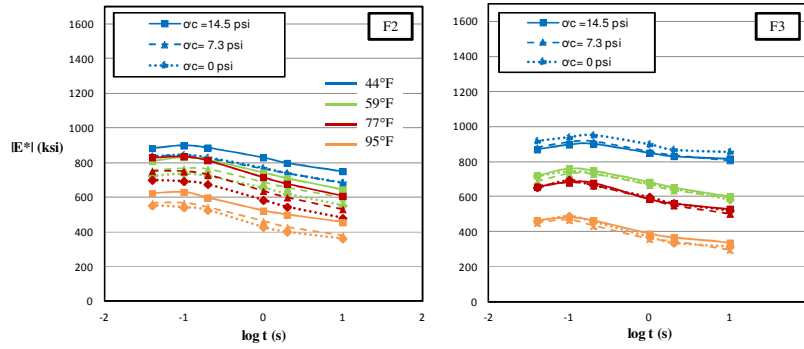


Figure 5.2. $|E^*|$ versus reduced time for F cores (P. Flanigan and Sons Inc. demonstration strip) at 14.5 psi, 7.3 psi, and 0 psi confining pressure at 44°F, 59°F, 77°F, and 95°F temperatures

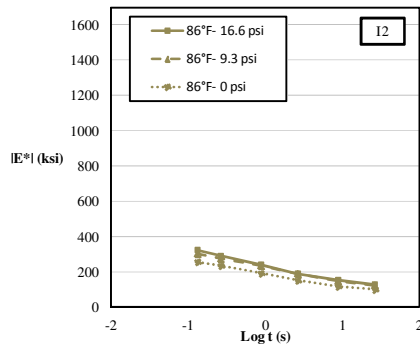


Figure 5.3. $|E^*|$ versus reduced time for I samples (laboratory FASB-H specimens/I-81) for at 16.6 psi, 9.3 psi, and 0 psi confining pressure at 86°F temperature

The extent of loading rate, temperature and confining pressure dependency varied for the different types of specimens. Sample F2 showed the highest dependency on confining stress. Master curves for F2 at the different confining stresses are shown in Figure 5.4. The results suggest a low to moderate sensitivity to confining pressure. A higher confining pressure dependency was observed in the lower part of the sigmoidal function, which is representative of higher temperatures or longer loading durations. At higher temperatures, the foamed asphalt bonds become softer and stress is primarily carried by aggregate skeleton. Therefore, FASB stiffness becomes more like granular-type behavior (i.e. confining stress dependent). Other samples showed negligible effect of confining pressure

on stiffness. An example of this is the master curves for B1 shown in Figure 5.5. Overall, these results show that the effect of confining pressure is of secondary importance.

Some deviatoric stress softening effect on measured DM was also observed during the calibration stage of the experiment while the axial load was varied to achieve the target strain of 100 $\mu\epsilon$. However, this effect was even less significant than the confining stress effects.

Since the effect of confining pressure was not found as significant as the effects of loading rate and temperature on measured DM, uniaxial DM tests were performed thereafter using the MTS test machine. Since the test equipment was changed, the tests on four of the samples were repeated to assess any potential machine-to-machine differences in measured $|E^*|$ values. The results of this assessment are illustrated in Figure 5.6, which compares the measured $|E^*|$ values from the UTM-100 to MTS test machine. In most cases, the agreement between the test results was quite close. Therefore, the test results from the two test machines were treated equally.

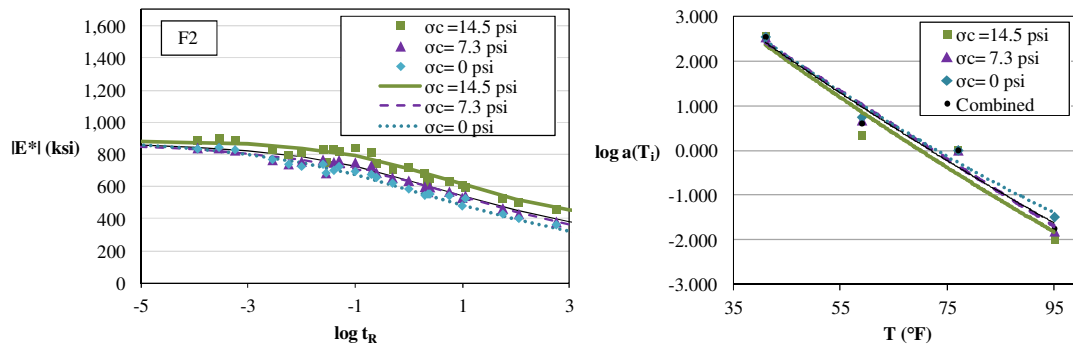


Figure 5.4. Master curves at different confining pressures along with their temperature shift factors for sample F2

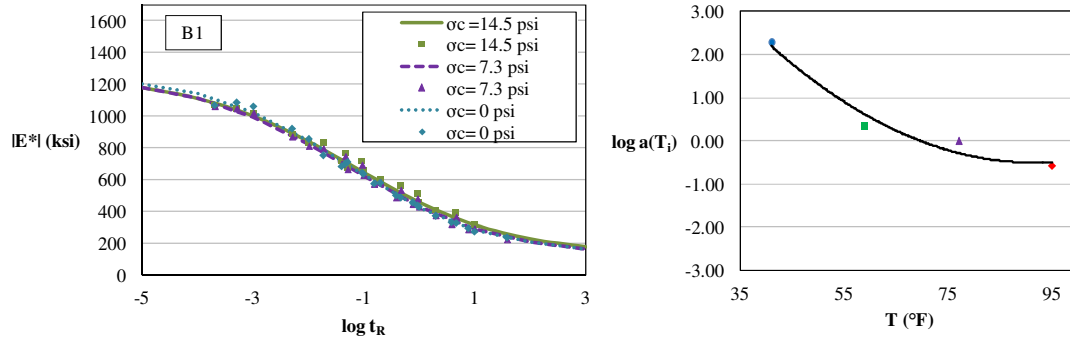


Figure 5.5. Master curves at different confining pressures along with their temperature shift factors for sample B1

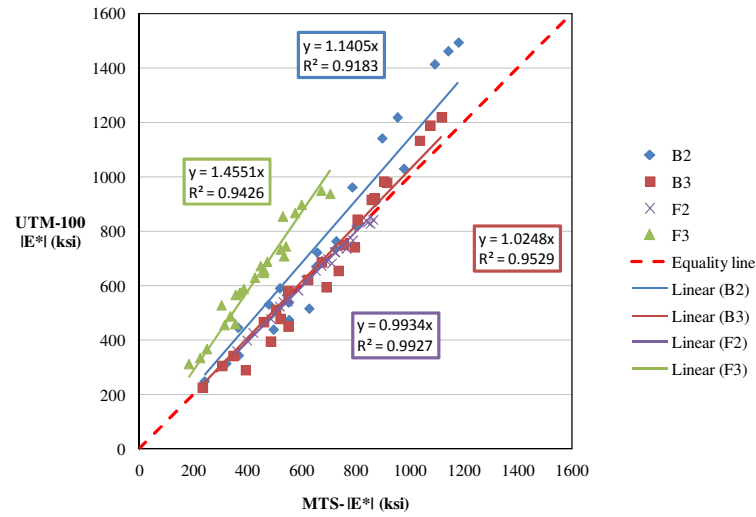


Figure 5.6. Comparison of the DM measured by UTM-100 and MTS machine at zero confining pressure

Figure 5.7 depicts master curves along with their shift factors for B, F, and I specimens. The specimens were described in Table 5.1. The error bars show the maximum and minimum DM ($|E^*|$) within the test replicates at a given temperature and loading rate. The error bars for the I specimens plot very small in this figure, showing the low variability in the laboratory made specimens.

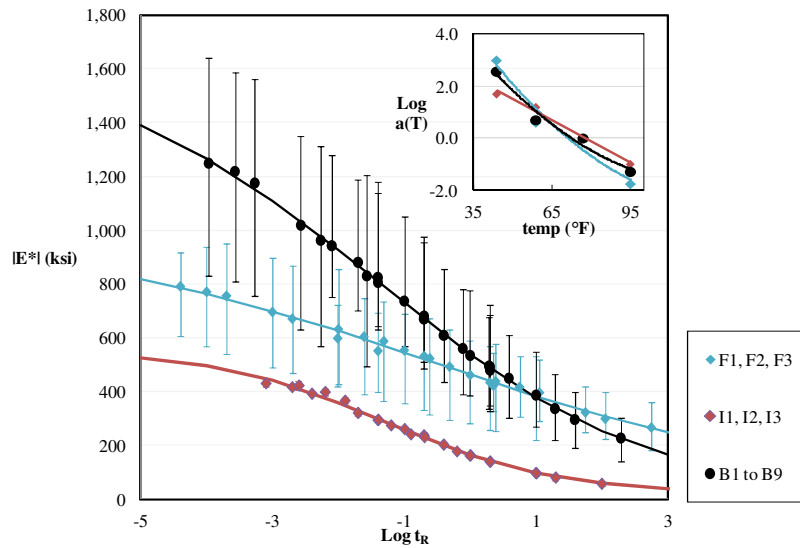


Figure 5.7. Master curves along with their shift factors for all the field and laboratory specimens of FASB-A and FASB-H mixtures at zero confining pressure. Error bars show the maximum, and minimum $|E^*|$ for a given temperature and loading rate

Based on Figure 5.7, at 77 °F temperature and 10 Hz loading rate ($\log t_R = -1$) typical for base layer conditions in highway pavements, the mean value of DM for the evaluated mixtures varies between 250 ksi and 750 ksi. This range is substantially greater than the typical 25 ksi design modulus for graded aggregate based (GAB) material. The upper bound of the FASB DM is nearly as high as the typical lower bound hot mix asphalt (HMA) at this temperature and loading rate.

Two of the master curves in Figure 5.7 are for the same FASB-A mixture but from two different sites, the P. Flanigan and Sons Inc. demonstration strip (F cores) and the Baltimore-Washington Parkway project (B cores). Although the mix designs were the same, the F cores were less stiff and expressed less viscoelasticity (i.e., loading rate/temperature dependency) than the B cores. The lower stiffness could be due to the fact that the former site was more distressed as it was trafficked by trucks at the Flanigan plant for more than two years by the time the cores were obtained. In addition, it was never covered with an HMA layer. This could have caused some foamed asphalt oxidization and therefore less loading rate dependency. On the other hand, the B cores were obtained after paving the overlying HMA layer but before trafficking. Placement of the HMA layer may

improve curing of the underlying FASB by applying additional heat and enhancing moisture evaporation.

Figure 5.8 shows the variability in the master curves for FASB-A for three different test segments at the Baltimore-Washington Parkway site. Details on the characteristics of each test segment are provided in Section 3.2.1. All samples were tested at zero confining pressure and the master curves are constructed based on the average DM test results from each segment. The lowest DM master curve corresponded to Segment A (only B5 could be tested) and the highest one corresponded to the samples from the Control Strip (B7, B8, and B9). Segment A, which had the lowest stiffness, was placed in two 4-inch lifts at two different times (4 days apart). In addition, rains the night after placing the first lift may have adversely affected its curing. In addition to the lower DM for Segment A, this segment had more problems extracting cores from this segment, as the cores would often split on the lift interface. Segments A and B were covered by HMA approximately one week after FASB placement. The Control Strip, which had the highest stiffness, was placed in one 8-inch lift under ideal weather conditions and was covered by HMA two months later, allowing ample time for curing.

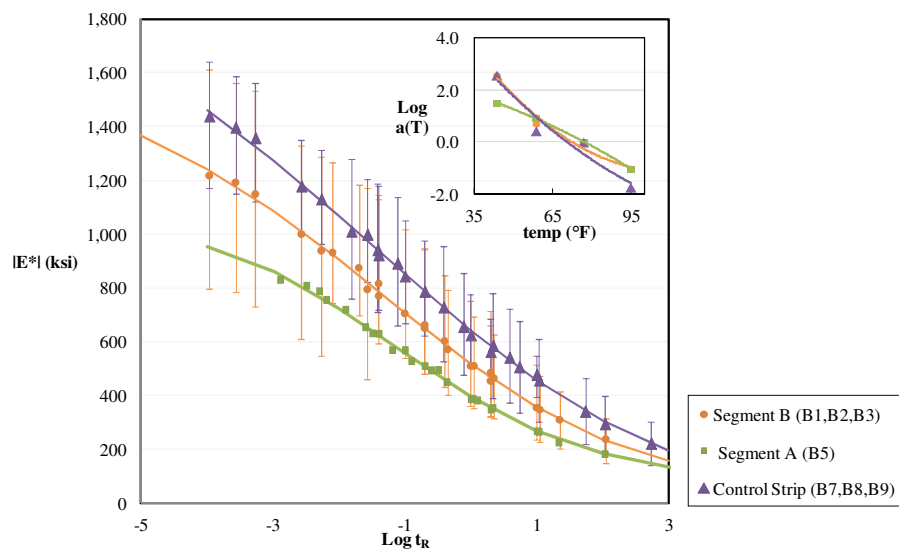


Figure 5.8. Master curves along with their shift factors for FASB-A material from three different test segments at Baltimore-Washington Highway project, at zero confining pressure. Error bars show the maximum, and minimum $|E^*|$ for a given temperature and loading rate time

It is also clear from Figure 5.7 that the DM for field cores (specimens F and B) show more variability than for the laboratory specimens (I specimens; the error bars for I specimens plot very small in Figure 5.7). However, the dynamic moduli measured from laboratory specimens of FASB-H mix are much lower than those of field specimens of FASB-A mix. It is believed that the primary reason for the low dynamic moduli for the I specimens is inadequate compaction in the laboratory. The secondary reason is related to mixture differences; the indirect tensile strength (ITS) for the FASB-H mix was lower than that of FASB-A mix (see Chapter 4).

It is believed that the dynamic moduli for the I specimens with a more field-representative compaction and curing would be higher than the values in Figure 5.6. A correlation was found between dynamic moduli from the laboratory specimens and indirect tension resilient moduli from field cores of the same mixture obtained from the I-81 Highway (VA) reconstruction project (personal communication with Mr. Alex Apeagyei, VDOT). The data are presented in Table 5.2. A study by Xiao (2009) showed that indirect resilient modulus (M_r) has the best correlation with DM ($|E^*|$) at a 5 Hz loading frequency. The average ratio of $M_r/|E^*|$ was 2.4. Dynamic moduli from the laboratory specimens after correction by this factor are plotted as “corrected I” on Figure 5.9. As can be seen, the corrected I curve plots relatively closer to FASB-A curve (B cores) but slightly lower. This observation is expected given that the ITS for FASB-H was lower than FASB-A mixture. A study done by Kim et al. (2009) on FASB mixtures with 100% RAP aggregate (similar to FASB-H mixture) compacted by gyratory compactor also suggested $|E^*|$ values in the range of the “corrected I” master curve. The DM test results from Kim et al. (2009) are explained in Chapter 3. This suggests that the modified Proctor compaction procedure (AASHTO T-180) used for granular materials is not appropriate for FASB compaction; the gyratory compactor is better representative of field compaction conditions.

Table 5.2. Comparison between laboratory DM ($|E^*|$) at 5 Hz and field core indirect tension resilient modulus (M_r) for FASB-H (I Specimens)

T (°F)	M_r (ksi)	$\log a(T)$	$\log t_R$	$ E^* $ @ 5Hz	$M_r/ E^* $
39.2	1064	1.8933	-2.5923	411	2.59
68	534	0.4631	-1.1621	276	1.93
100.4	270	-1.7408	1.0418	94	2.87

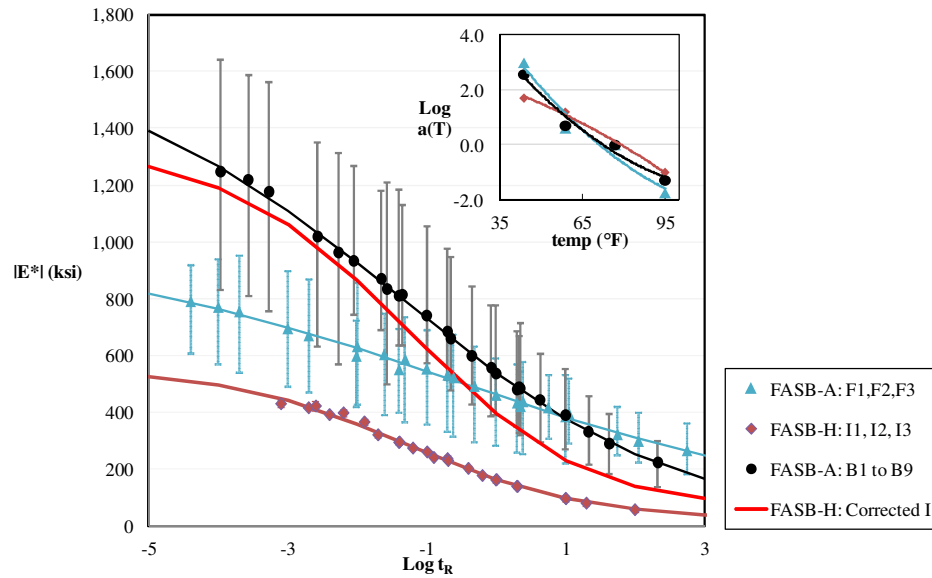


Figure 5.9. Master curves along with their shift factors for all the field and laboratory specimens of FASB-A and FASB-H mixtures and corrected FASB-H mixture

Figure 5.10 shows the master curves along with their temperature shift factors for all FASB-A cores combined together (B1 to B9 and F1 to F3). FASB-H data is not shown on this graph to exclude data with different experimental conditions. Error bars show the maximum and minimum measured DM and the shaded area shows mean DM \pm one standard deviation.

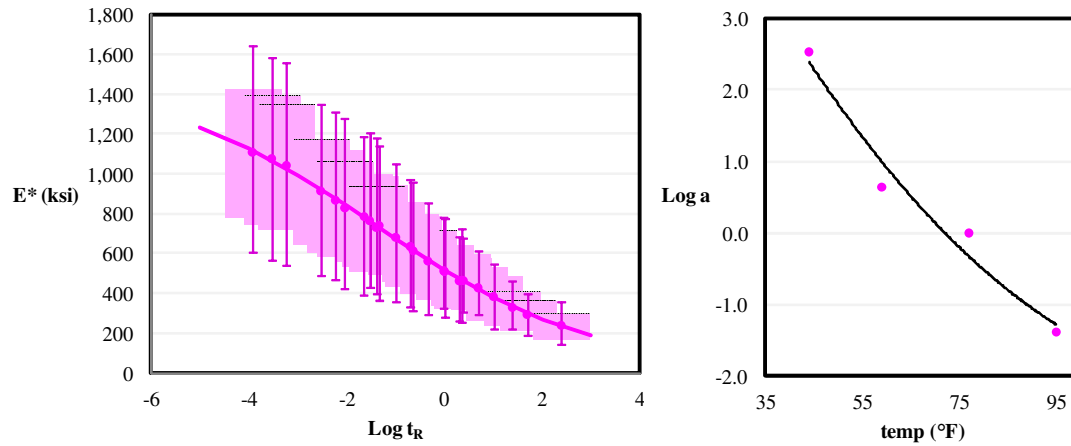


Figure 5.10. Master curves for all FASB-A specimens. For a given temperature and loading rate, error bars show the maximum and minimum $|E^*|$, and the shaded area shows \pm one standard deviation

Table 5.3 shows the average phase angle for FASB mixtures at different temperatures and loading frequencies. The phase angle increased as the temperature and loading time increased. FASB phase angle was compared to a typical HMA (data from Clyne *et al.* (2004)) and is illustrated in Figure 5.11. Generally, FASB exhibited lower phase angles as compared to HMA. This is due to the fact that FASB contains less amount of new binder than any HMA and therefore, less viscoelastic.

Table 5.3. Average Phase angle for FASB mixtures

Temp (°F)	Frequency (Hz)	Phase Angle (δ°)	Temp (°F)	Frequency (Hz)	Phase Angle (δ°)
44	25	12.4	77	25	17.9
44	10	13.2	77	10	19.3
44	5	13.8	77	5	20.6
44	1	15.2	77	1	22.7
44	0.5	16.1	77	0.5	23.3
44	0.1	17.7	77	0.1	24.7
59	25	14.5	95	25	18.6
59	10	16.3	95	10	20.6
59	5	17.3	95	5	21.5
59	1	18.6	95	1	22.8
59	0.5	19.4	95	0.5	23.2
59	0.1	21.0	95	0.1	23.7

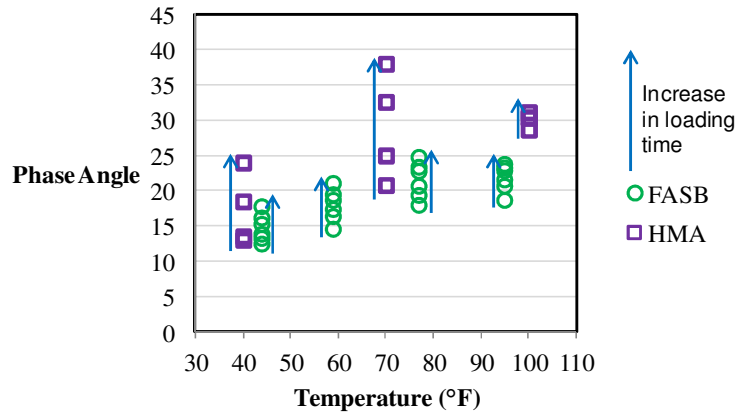


Figure 5.11. Comparison of phase angle of FASB and HMA

Table 5.4 summarizes the parameters of sigmoidal function for master curve (λ , α , γ , β), temperature shift factors ($a(T_i)$), as well as coefficients in the quadratic temperature shift factor formulation $\log(a(T))=a*T^2+bT+c$ for all the mixtures. Chapter 3 explains the master curve formulation in detail. Σe^2 shows the sum of the errors assessing the goodness of fit.

Table 5.4. Regression coefficient for master curve and its temperature shift factors for different mixtures

	FASB-H (I1, I2, I3)	FASB-A (B and F cores)	FASB-A (B1 to B9)	FASB-A (F1,F2,F3)
Σe^2	2.347E-03	7.498E-04	7.856E-04	2.236E-03
λ	1.3689	1.6544	1.3972	1.2345
α	1.3818	1.5287	1.8405	1.8667
γ	0.6820	0.3885	0.3936	0.2324
β	-0.4623	-0.8094	-0.9771	-1.1644
$a(T_1)$ 44°F	46.67	339.29	339.29	339.43
$a(T_2)$ 59°F	15.50	4.37	4.41	3.90
$a(T_3)$ 77°F	1	1	1	1
$a(T_4)$ 95°F	0.10	0.04	0.05	0.03
$\log a(T_1)$	1.67	2.53	2.53	2.53
$\log a(T_2)$	1.19	0.64	0.64	0.59
$\log a(T_3)$	0	0	0	0
$\log a(T_4)$	-1.00	-1.38	-1.33	-1.56
a	-0.0003	0.0006	0.0006	0.0005
b	-0.0131	-0.1526	-0.1574	-0.1393
c	2.8620	7.9836	8.1202	7.6059

5.3. RLPD test results

To assess the rutting susceptibility of FASB material RLPD tests were performed on B, F, and I specimens as given in Table 5.1. The test configurations are based on the NCHRP 9-30A (2011) recommendations for HMA and are summarized in Table 5.5 for the individual specimens.

Table 5.5. Test variables for RLPD test

Specimen	Average test temperature, T (°F)	Confining stress, σ_c (psi)	Deviatoric stress, σ_d (psi)
B1	110	10	70
B2	109	10	70
B3	107	10	70
B5	114	10	70
B7	107	10	70
B8	102	10	70
B9	105	10	70
F1	94	10	70
F2	98	5	70
F3	98	5	70
F4	103	10	70
F5	102	10	70
F6	106	10	70
I3	106	10	70
I4	106	10	70

The axial permanent strain for each specimen is illustrated in Figure 5.12. It is clear that only the I3 and I4 laboratory samples of FASB-H reached the tertiary failure stage. The flow numbers as determined using the Franken Model (Chapter 3) are summarized in Table 5.6. The low flow number and high strains at flow observed in these samples suggest a high susceptibility to rutting. However, comparing these results with RLPD tests performed on field cores of the same mixture from the I-81 project (A. Apeagyei, personal communication) reveals that the laboratory prepared samples significantly underestimate the rutting resistance of FASB-H. This discrepancy between laboratory prepared specimens

and field cores is similar to that observed for stiffness, as discussed earlier in this chapter. The RLPD tests on the field cores were performed at 129.2°F under 10 psi confining pressure and 70 psi deviator stress. Even though the test temperature was higher in the RLPD tests on the field cores, a significantly higher rutting resistance (higher flow number) was observed as compared to the RLPD tests results on the laboratory samples.

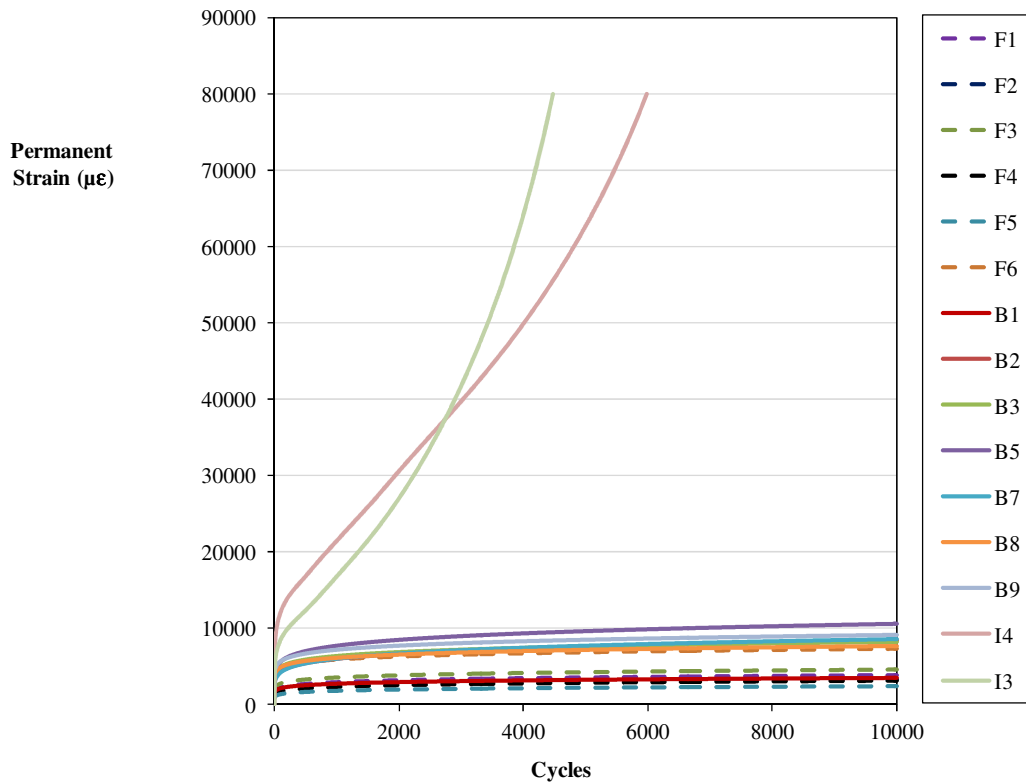


Figure 5.12. Triaxial RLPD test results for B, F, and I specimens

Table 5.6. Flow number and strain at flow for I specimens (Mix FASB-H)

Test sample	Flow number	Strain at flow (µε)
I3	896	16278
I4	1342	24879
Laboratory- Average	1119	20578.5
Field cores- Average	9013	21900

Test results from FASB-A specimens from P. Flanigan and Son demonstration strip site (F cores) and Baltimore-Washington Parkway (B cores) are shown in Figure 5.13. Some findings from the test results are summarized below:

- The FASB-A mixtures did not enter the tertiary stage of permanent deformation, indicating good resistance to rutting.
- Overall, the cores from the P. Flanigan and Sons demonstration strip (F cores) exhibited lower permanent deformations after 10,000 cycles than did the cores from the Baltimore-Washington Parkway (B cores).
- The slope of secondary stage in log-log space (Figure 5.13.b) shows a similar slope for all of the evaluated F and B cores, with the B cores being slightly steeper.
- The intercept of the secondary stage as illustrated in Figure 5.13.b was lower for the F cores. This could be due to the fact that this site was older and was already more densified under truck traffic.
- B5 showed the highest permanent deformation among the FASB-A cores. This could be partly due to its higher test temperature and also because it was obtained from Segment A, where the two 4-inch lifts were placed at different times. Note that this specimen showed the lowest DM as well.
- A limited comparison within F1, F2, and F3 was conducted to explore the effect of confining pressure on permanent deformation. As shown in Figure 5.14, no significant trend was observed.
- Effect of temperature was also compared for cores F1, F2, and F3, which were tested at an average temperature of 95°F, and F4, F5, and F6, which were tested at an average temperature of 104°F (Figure 5.15). F4 to F6 showed slightly higher permanent deformation susceptibility, as expected. This effect might have been more pronounced if temperature control had been tighter. There is only a 4 degree temperature difference between F2/F3 and F5 (Table 5.5).

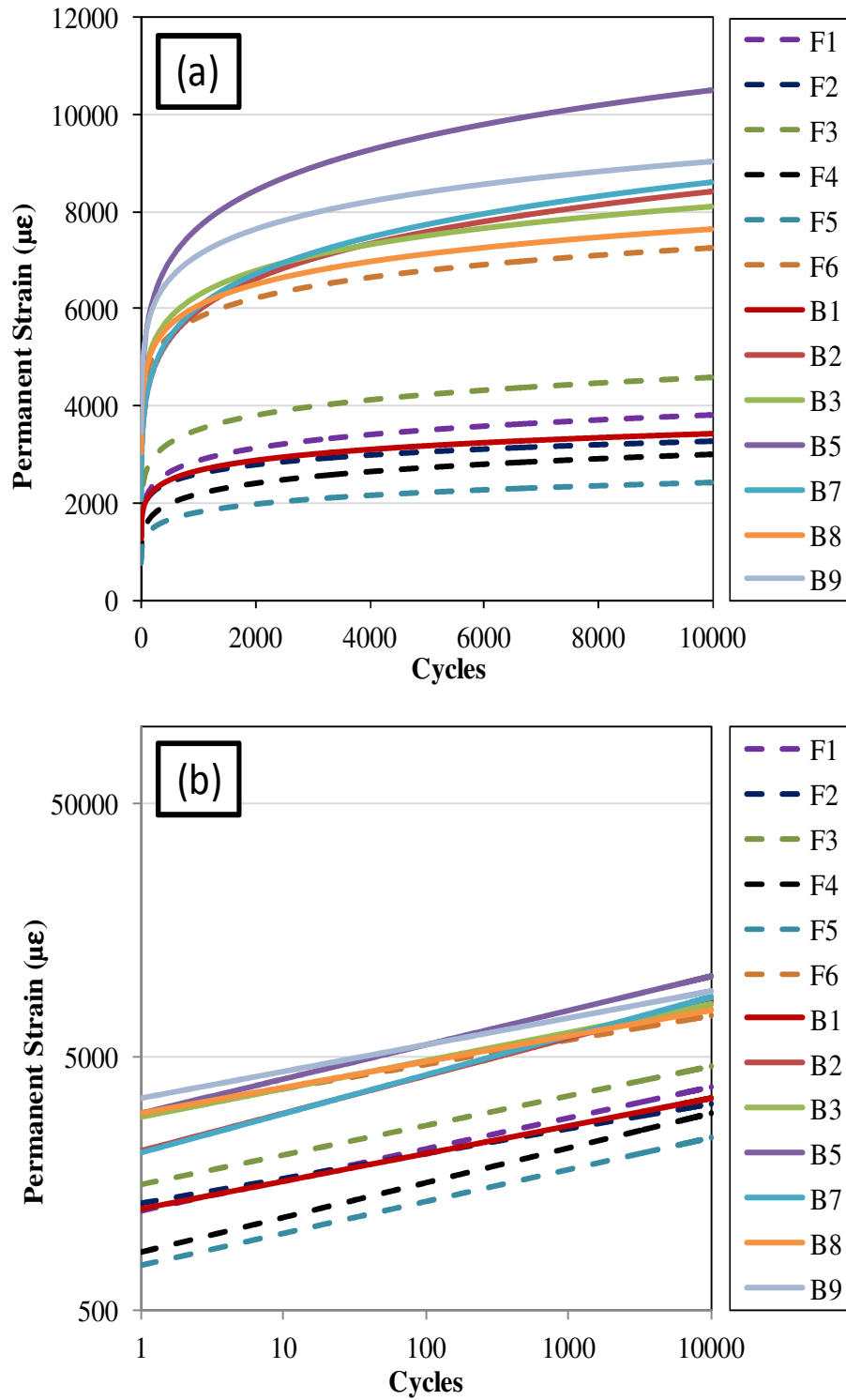


Figure 5.13. (a) Triaxial RLPD test results on FASB-A mixture; (b) Test results in log-log space

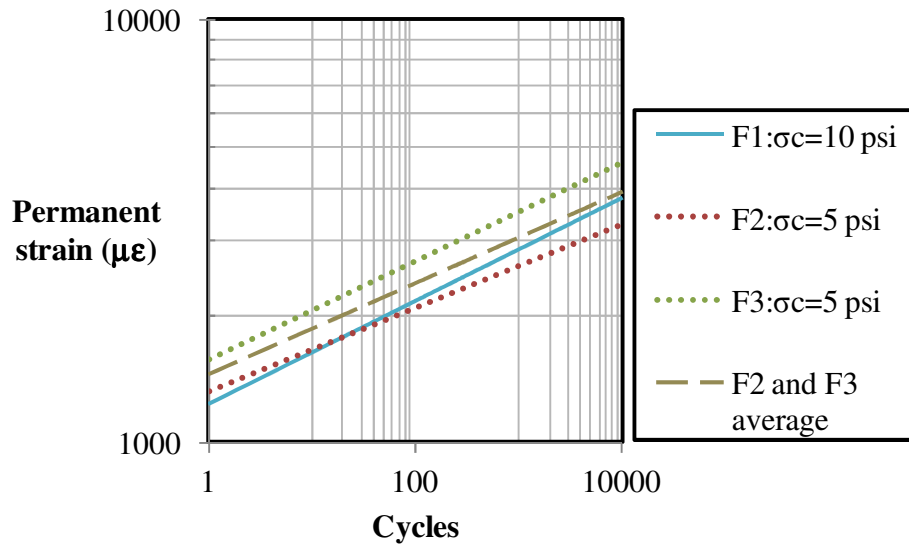


Figure 5.14. Effect of confining pressure on F cores (F1, F2, F3) tested at 95°F

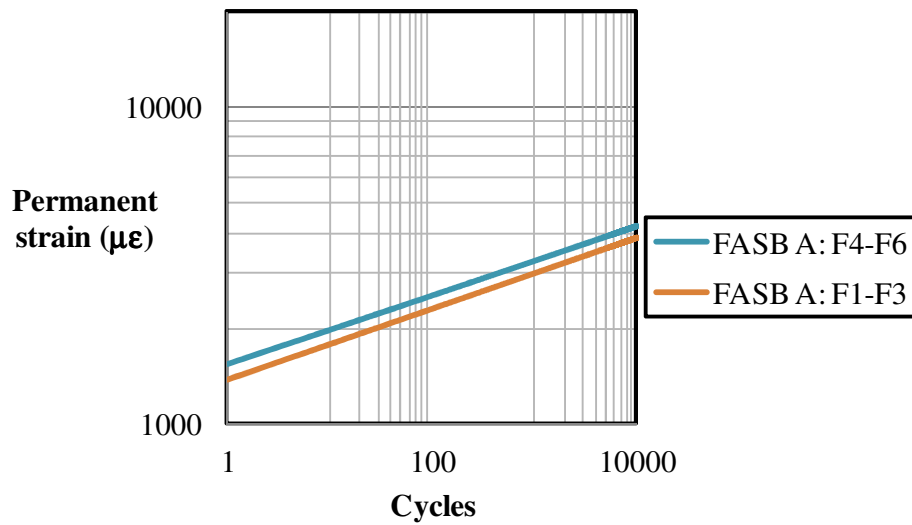


Figure 5.15. Effect of test temperature on RLPD test results. F1-F3 tested at 95°F (average) and F4-F6 were tested at 104°F (average)

Table 5.7 summarizes the regression constants for the power law and Franken models as determined by a non-linear least-squares regression procedure using Microsoft Excel Solver.

Table 5.7. Regression constants for RLPD fitted models

Regression Constants	Fit model	A	B	C	D
B1	Power law ¹	1258.3	0.1094		
B2	Power law	2128.8	0.1492		
B3	Power law	2918.4	0.1111		
B5	Power law	2985.3	0.1365		
B7	Power law	2081.5	0.1539		
B8	Power law	3025.4	0.1006		
B9	Power law	3450.4	0.1044		
F1	Power law	1239.2	0.1219		
F2	Power law	1316.7	0.0986		
F3	Power law	1576.3	0.116		
F4	Power law	854.95	0.1566		
F5	Power law	752.4	0.1267		
F6	Power law	3008.9	0.0954		
I3	Franken ²	422.7	0.7801	309423	-0.00028
I4	Franken	536.4368	0.6884	170183.6	-0.00027

1. Power law model: $\epsilon_p = AN^B$ and N is number of cycles

2. Franken model: $\epsilon_p = AN^B + C(e^{DN} - 1)$

Overall, the permanent deformation resistance of FASB was found satisfactory as compared to HMA. At 104°F and the same loading conditions (10 psi confining pressure and 70 psi deviatoric stress) the typical range of permanent deformation at 10,000 cycles for HMA is 0.7% to 2% (NCHRP 9-30A, 2011) while it varied from 0.2% to 1% for FASB-A field cores (B and F specimens). At 129°F and under the same stress levels, HMA generally reaches the tertiary stage with average permanent strain of 2% at flow (NCHRP 9-30A, 2011). The average permanent strain at flow for FASB-H field cores was also 2%, suggesting a similar rutting resistance as HMA. As an added advantage, FASB as a base course material in high volume pavements experiences lower stress states in the field

than HMA. Given all of this, rutting is not expected to be a concern for FASB mixtures of interest in Maryland.

5.4. Structural layer coefficient for AASHTO design

In the older AASHTO empirical pavement design procedure (AASHTO, 1993), a structural layer coefficient is assigned to each layer in pavement structure in order to assess the relative contribution of the pavement layer as a structural component of the pavement. In this section the structural layer coefficient is estimated from the DM and ITS of the FASB materials.

Figure 5.16 to Figure 5.18 show the charts used to estimate the layer coefficient of the FASB materials. The FASB structural layer coefficient was estimated using the elastic (resilient) modulus (M_r) at 68°F and unsoaked ITS mean values and mean values minus one standard deviation (σ). The indirect resilient modulus of FASB-H was provided by A. Apeagyei, VDOT (personal communication). For FASB-A, the resilient modulus was obtained from DM. Table 5.8 presents the DM obtained at 5Hz loading frequency and 68°F from the constructed master curves (based on Equations 3.5 to 3.7). The coefficients of the master curves and the shift factors for FASB-A are provided in Table 5.4. Only data obtained from field cores were used in this analysis.

Four different approaches were employed for estimating the FASB structural layer coefficient: For method 1 (HMA a_1 relationship), the justification is that the E^* and RLPD behavior of FASB is much like a base asphalt material and thus using a_1 vs. M_r relationship is justified. For method 2 (a_2 for unstabilized base), state that this is a theoretical relationship based on substitution ratio concepts, but that for FASB it is extrapolated beyond the conditions for which it was originally derived. For method 3 (a_2 from bitumen stabilized base), state that this is the recommendation from AASHTO 86 but that there is very little detail provided in the AASHTO 86 appendices describing the theoretical or empirical basis. For method 4, the justification is that this is the most widely commonly-used method in practice today.

1. The AASHTO (1993) relationship for a_1 for dense graded HMA based on resilient modulus M_r (Figure 5.16). This method was used since the $|E^*|$ and RLPD behavior

of FASB is much like a base asphalt material and thus using a_1 versus M_r relationship is justified.

2. The AASHTO (1993) relationship for a_2 for unstabilized granular base layer $a_2 = 0.297\log(M_r) - 0.977$. This is a theoretical relationship based on substitution ratio concepts which adjusts the layer coefficient of a granular base layer with respect to a reference GAB material with a given M_r and layer coefficient to get a same surface deflection under a given loading condition. However, for FASB the layer coefficient extrapolated beyond the conditions for which the formulation was originally derived.
3. The AASHTO (1993) relationship for a_2 for bitumen stabilized granular base layers based on M_r (Figure 5.17). This method is recommended for bituminous stabilized granular material similar to FASB by AASHTO 86 but that there is very little detail provided in the AASHTO 86 design guide appendices describing the theoretical or empirical basis.
4. The Wirtgen (2010) recommendations based on ITS (Figure 5.18). This is the most widely commonly-used method for FASB structural design in practice today.

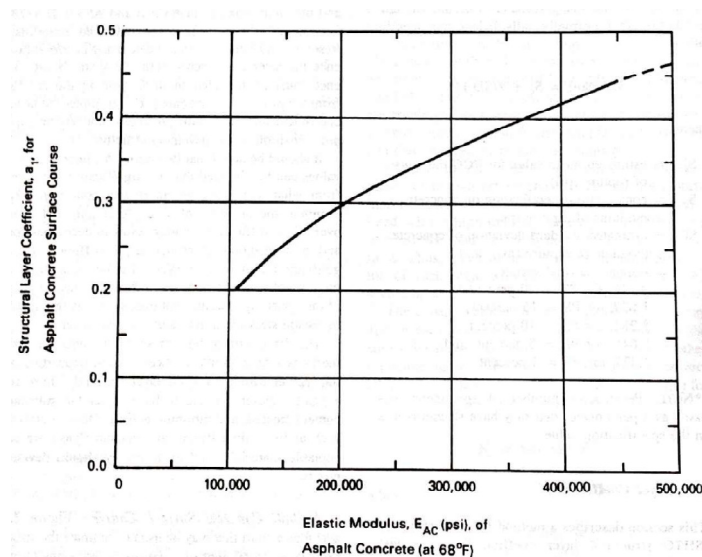


Figure 5.16. Chart for estimating the structural layer coefficient a_1 of dense-graded asphalt concrete based on resilient modulus (AASHTO, 1993)

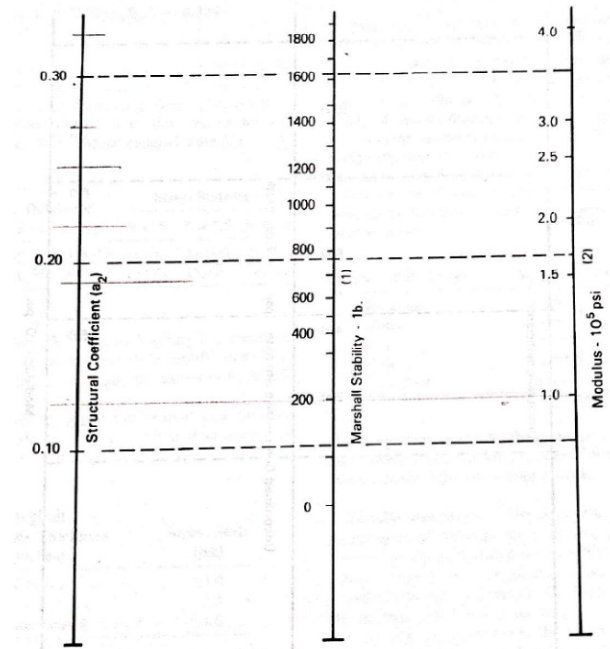


Figure 5.17. Variation in structural layer coefficient a_2 with base strength parameters for bituminous treated bases (AASHTO, 1993)

STRUCTURAL LAYER COEFFICIENT (per inch)		0.18	0.23	0.28	max 0.35
TG2 (2009) CLASSIFICATION		BSM3		BSM2	BSM1
MATERIAL PROPERTIES AFTER STABILISATION					
100mm dia briquettes ITS _{DRY} (kPa)	125		175		225
150mm dia specimens ITS _{EQUIL} (kPa)	95		135		175
150mm Triaxial Cohesion (kPa)	50		100		250
Angle of Friction (°)	25		30		40
MATERIAL CBR VALUE BEFORE STABILISATION (at 100% compaction)					
Materials with CBR < 20% not recommended	20		40		80
ANTICIPATED APPLICATION RATE OF BITUMEN FOR STABILISATION (% by mass)					
		BSM3	BSM2	BSM1	
		2.5 - 4.0	2.3 - 3.0	2.0 - 2.5	

Figure 5.18. Suggested structural layer coefficients for bitumen stabilized materials (Wirtgen, 2010)

A study by Xiao (2009) showed that indirect resilient modulus (M_r) has the best correlation with DM ($|E^*|$) at a 5 Hz loading frequency. To assess the layer coefficients, DM of FASB-A specimens was determined at 68°F and 5Hz loading frequency using the constructed master curves and their temperature shift factors (Table 5.3). The method is explained in Chapter 3. The modulus values \pm one standard deviation ($\pm\sigma$) are tabulated in Table 5.8.

Table 5.8. M_r at 68F and unsoaked ITS for FASB mixtures, Average value $\pm \sigma$

Mixtures	FASB-H (cores)	FASB-A (F and B cores)	FASB-A (F cores)	FASB-A (B cores)
$\log a(68^\circ\text{F})$	-	0.3812	0.4455	0.1914
$\log t_R$ at 5Hz, 68°F	-	-1.0802	-1.1445	-0.8904
M_r at 68°F ($ E^* $ at 5Hz, 68°F) $\pm\sigma$, ksi	534	687 \pm 179	551 \pm 146	711 \pm 161
Unsoaked ITS $\pm\sigma$, psi	53 \pm 3	76 \pm 8		

Table 5.9 summarizes the estimated layer coefficients of the FASB materials using the different methods based on the average M_r and unsoaked ITS values while Table 5.10 provides similar estimates from average M_r and unsoaked ITS minus one standard deviation.

The a_2 values ranged from 0.32 to over 0.44 (the typical layer coefficient of HMA) based on the different methodologies shown in Tables 5.8 and 5.9. Since the long term performance of FASB material in high volume pavement structures in Maryland has not yet been documented, the lower bound value of 0.32 is considered a reasonable and conservative structural layer coefficient to assign to FASB mixtures of interest in Maryland.

Table 5.9. Estimated layer coefficients based on average M_r and average unsoaked ITS

Mixtures	FASB-H (cores)	FASB-A (F and B cores)	FASB-A (F cores)	FASB-A (B cores)
M_r at 68°F ($ E^* $ at 5Hz, 68°F), ksi	534	687	551	711
Unsoaked ITS, psi	53	76		
Methodology	Structural Layer Coefficient			
Based on asphalt layer method ¹	0.44 (0.47) ⁵	0.44 (0.51)	0.44 (0.47)	0.44 (0.52)
Based on granular base method ²	0.45	0.48	0.45	0.48
Based on Bituminous treated base method ³	0.36	0.39	0.36	0.40
Based on ITS method for FASB ⁴	0.35 (0.36)	0.35 (0.42)		

1. Figure 5.16 based on M_r .
2. $a_2 = 0.249 \cdot \log_{10} E$ (psi) - 0.977 for unstabilized base layers..
3. Figure 5.17 based on M_r
4. Figure 5.18 based on unsoaked ITS
5. Numbers in parenthesis show the layer coefficients extrapolated beyond the range of the charts.

Table 5.10. Estimated layer coefficients based on average M_r - σ and average unsoaked ITS - σ derived from different methods

Mixtures	FASB-H (cores)	FASB-A (F and B cores)	FASB-A (F cores)	FASB-A (B cores)
M_r at 68°F ($ E^* $ at 5Hz, 68°F) - σ , ksi	-	509	405	551
Unsoaked ITS- σ , psi	50	68		
Methodology	Structural Layer Coefficient			
Based on asphalt layer method ¹	-	0.44 (0.46) ⁵	0.42	0.44 (0.47)
Based on granular base method ²	-	0.44	0.42	0.45
Based on Bituminous treated base method ³	-	0.35	0.32	0.36
Based on ITS method for FASB ⁴	0.35	0.35 (0.40)		

1. Figure 5.16 based on M_r .
2. $a_2 = 0.249 \cdot \log_{10} E$ (psi) - 0.977 for unstabilized base layers
3. Figure 5.17 based on M_r
4. Figure 5.18 based on unsoaked ITS
5. Numbers in parentheses show the layer coefficients extrapolated beyond the range of the charts.

The a_2 values ranged from 0.32 to over 0.44 (the typical layer coefficient of HMA) based on the different methodologies shown in Tables 5.8 and 5.9. Since the long term performance of FASB material in high volume pavement structures in Maryland has not yet been documented, the lower bound value of 0.32 is considered a reasonable and conservative structural layer coefficient to assign to FASB mixtures of interest in Maryland.

5.5. Conclusions and recommendations

Triaxial DM tests were performed on field and laboratory specimens of the FASB-A and FASB-H mixtures. It was found that the influence of deviatoric stress and confining pressure is negligible as compared to the effects of loading rate and temperature on the measured stiffness values. At a 77 °F temperature and a 10 Hz loading rate typical for base layer conditions in high volume highway pavements, the mean value of DM for the evaluated mixtures ranged between 250 ksi and 750 ksi. The lower DM limit is substantially greater than the typical 25 ksi design modulus for GAB material and the upper limit of the measured DM is close to the lower bound of HMA at this temperature and loading rate. The effect of improper construction was observed on the measured DM from field cores from Baltimore-Washington Parkway site. Field cores from Segment A where the material was placed in two lifts at different times (4 days apart) exhibited lower DM as compared to Segment B and the control strip where the FASB material was placed on the same day.

Furthermore, considerable variability was observed in the DM test results of the same FASB mixture but from two different sites. Cores from P. Flanigan and Sons demonstration strip (F cores) that were directly exposed to the environment and truck traffic for more than two years had lower dynamic moduli with less loading rate dependency and more confining pressure dependency as compared to cores from Baltimore-Washington Parkway site (B cores) where the FASB layer was cured and covered with HMA and the cores were obtained before opening the site to traffic. The lower viscoelasticity observed in the F cores could be due to foamed asphalt oxidization. The lower DM could be due to distress and minor cracks in these cores. In addition,

placement of the HMA layer may have improved the curing of the underlying FASB for the B cores by applying additional heat and enhancing moisture evaporation.

There was a much larger variability observed in the field cores as compared to the laboratory prepared specimens of FASB-H. On the other hand, the laboratory compacted specimens significantly underestimated the stiffness. This underestimation was verified by comparing the indirect resilient modulus of FASB-H field cores from I-81 Highway project to the DM (5 Hz and 68°F) of laboratory prepared specimens of the same mixture compacted with Proctor hammer according to AASHTO T-180.

Overall, the field cores of FASB-A and FASB-H exhibited similar modulus values with FASB-A being slightly higher.

Triaxial RLPD tests were also performed on the same mixtures. The test stress levels and temperature were selected based on the NCHRP 9-30A (2011) recommendations of 10 psi confining pressure and 70 psi deviatoric stress in order to compare the rutting susceptibility of FASB mixtures to that of a typical HMA. Overall, the permanent deformation resistance of FASB cores from both mixtures was found satisfactory as compared to HMA. This is especially true given that FASB will experience lower stress levels in the field as it is placed deeper in the pavement structure than the HMA layer.

The laboratory prepared specimens underestimated the resistance to permanent deformation. Underestimation of stiffness and resistance to permanent deformation in laboratory prepared samples suggests that the modified Proctor compaction procedure (AASHTO T-180) used for granular materials is not appropriate for FASB compaction; the gyratory compactor is better representative of field compaction conditions.

Finally, resilient modulus and DM test results (5 Hz and 68°F) and unsoaked ITS values were employed to estimate the a_2 structural layer coefficient for use in the AASHTO empirical pavement design method. Estimates were based on both the mean stiffness/strength values and on the mean minus one standard deviation. The estimated values for a_2 ranged from 0.32 to over 0.44. The lower bound value of 0.32 is recommended as a reasonable and conservative value for use in pavement design in Maryland.

CHAPTER 6. Summary and Conclusions

6.1. Mix Design Test Results and Interpretations

Eight different FASB mixtures having different proportions of RAP, RC, and GAB aggregates were designed and evaluated for their indirect tensile strength (ITS) in soaked and unsoaked conditions to evaluate the effects of foaming asphalt content, aggregate proportioning, active additives, mixing moisture content, soaking process, and stockpiling the material. In order to effectively explain how and why each of these components affected the strength of FASB material, a comprehensive understanding of the internal structure of FASB is necessary.

The ITS of FASB material in the unsoaked condition is not only from the foamed asphalt bonds but also from other factors such as matric suction from residual water, cohesive bonds from partially oxidized residual binder in recycled asphalt pavement (RAP) (Fu *et al.*, 2008), cementitious bonds from residual non-hydrated cement in recycled concrete (RC) or newly introduced cement, the weak chemical bonds in the mineral phase of the aggregate (Fu *et al.*, 2008), and the orientations, mechanical properties, and other characteristics of the contacts within the aggregate skeleton. Therefore, the effect of foamed asphalt stabilization is largely masked in the unsoaked condition because of the combined effects of the various bonding elements in the mixture.

When the specimens are soaked, many of these bonds are negatively affected by the induced moisture to various extents. Matric suction from residual water, weak chemical bonds in mineral phase, and adhesion from partially oxidized residual binder in RAP are vulnerable to induced moisture. On the other hand, cementitious bonds and interlocking in aggregate skeleton are only slightly get affected by the induced moisture. Foamed asphalt bonds are in the middle of the range and are moderately sensitive to moisture content (Fu *et al.*, 2008). Under soaked condition, many of these bonds go away depending on the extent of their moisture susceptibility.

Unsoaked and soaked ITS tests on Marshall compacted specimens were performed to examine the effects of different design factors. Key conclusions drawn from the results of this study include the following:

1. There is a low to moderate sensitivity of ITS in both the soaked and unsoaked conditions to foamed asphalt content. The reason is that the effects of these bonds are masked by the other bonding components.
2. Increasing the ratio of RAP/RC tends to decrease unsoaked and soaked ITS. The reason is that RC is a more angular aggregate type and has a stiffer skeleton than that of RAP. In addition, it provides some cementitious bonds which governs the ITS in soaked condition.
3. Increasing the ratio of RAP/GAB tends to decrease the unsoaked ITS while increasing the soaked ITS. The reason is that GAB, similar to RC, is a structurally stronger aggregate and therefore replacing it with RAP will decrease the unsoaked ITS. However, in the soaked condition the effect of matric suctions and cohesion in the mineral phase goes away and the effect of foamed asphalt bonds becomes more apparent. Foamed asphalt bonds stick better to the RAP aggregates because of the partially oxidized binder on the RAP surface.
4. Replacing RC with GAB dramatically decreases the soaked ITS. The reason is that RC provides strong brittle cementitious bonds that do not exist in GAB.
5. Blends with a higher percentage of RC absorb more water when soaked because of the relatively high absorption of the RC, but this does not affect the soaked strength; blends with higher RC/RAP ratio show higher soaked strength.
6. The ITS of FASB mixtures significantly depends on the mother aggregate characteristics and therefore design tests are required for each individual mixture.
7. Adding cement as an active filler increases unsoaked and soaked ITS. It is particularly effective in the mixtures with low tensile strength ratio (TSR).
8. Mixing moisture content (MMC) does not have a significant impact on the ITS of the mixes with low percentages of fines; the tensile strength is mainly affected by the conventional moisture-density behavior of the granular material.

6.2. Performance Test Results and Interpretations

Triaxial dynamic modulus (DM) tests were performed on field and laboratory specimens from FASB-A and FASB-H mixtures, respectively. It was found that the role of deviatoric stress and confining pressure is negligible as compared to the role of loading rate and temperature on the measured stiffness values. At a 77 °F temperature and 10 Hz loading rate typical for base layer conditions in highway pavements, the mean value of DM for the evaluated mixtures varied between 250 ksi and 750 ksi. The lower DM limit is substantially greater than the typical 25 ksi design modulus for GAB material and the upper limit of the measured DM is close to the lower bound of HMA at this temperature and loading rate. The effect of improper construction was observed on the DM measured from field cores from Baltimore-Washington Parkway site. Field cores from Segment A where the material was placed in two lifts at different times (4 days apart) exhibited lower DM values as compared to Segment B and the control strip where the FASB material was placed on the same day.

Furthermore, considerable variability was observed in DM test results of the same FASB mixture but from two different sites. Cores from P. Flanigan and Sons demonstration strip site (F cores) which were directly exposed to environment and truck-traffic for more than two years exhibited lower dynamic moduli with lower loading rate dependency and more confining pressure dependency as compared to cores from Baltimore-Washington Parkway site (B cores) where the FASB layer was cured and covered with HMA and the cores were obtained before opening the site to traffic. The lower viscoelasticity observed in the F cores could be due to foamed asphalt oxidization. The lower DM could be due to distress and minor cracks in these cores caused by truck traffic. In addition, placement of the HMA layer may improve curing of the underlying FASB at the Baltimore-Washington Parkway site by applying additional heat and enhancing moisture evaporation.

There was a large variability observed in field cores as compared to the laboratory made specimens of FASB-H. On the other hand, the laboratory compacted specimens significantly underestimated the stiffness. This underestimation was verified by comparing the indirect resilient modulus of FASB-H field cores from I-81 Highway project to DM (5 Hz and 68°F) of the laboratory prepared specimens of the same mixture compacted with

Proctor hammer according to AASHTO T-180. Field cores of FASB-A and FASB-H exhibited similar modulus values with FASB-A being slightly higher.

Triaxial RLPD tests were also performed on the same mixtures. The test stress levels and temperature were selected according to NCHRP 9-30A (2011) report as 10 psi confining pressure and 70 psi deviatoric stress in order to compare the rutting susceptibility of FASB mixtures to that of a typical HMA. Overall, the permanent deformation resistance of FASB cores from both mixtures was found satisfactory as compared to HMA. This is especially true because FASB will experience lower stress levels in the field as it is placed deeper in the pavement structure as HMA layer.

The laboratory prepared specimens underestimated the resistance to permanent deformation. Underestimation of stiffness and resistance to permanent deformation in laboratory prepared samples suggests that the modified Proctor compaction procedure (AASHTO T-180) used for granular materials is not appropriate for FASB compaction. The gyratory compactor is expected to better simulate field compaction conditions.

The laboratory DM test results (5 Hz and 68°F) from field cores and unsoaked ITS values from mix design specimens were also employed to estimate an appropriate structural layer coefficient value for FASB for use in the AASHTO (1993) empirical pavement design method. Both average and average minus one standard deviation stiffness and strength values were evaluated. Four different approaches were used to estimate the layer coefficient. Overall, the results suggest that a structural layer coefficient of 0.32 is a justifiable and conservative value based on the measured stiffness and strength properties.

Appendix I

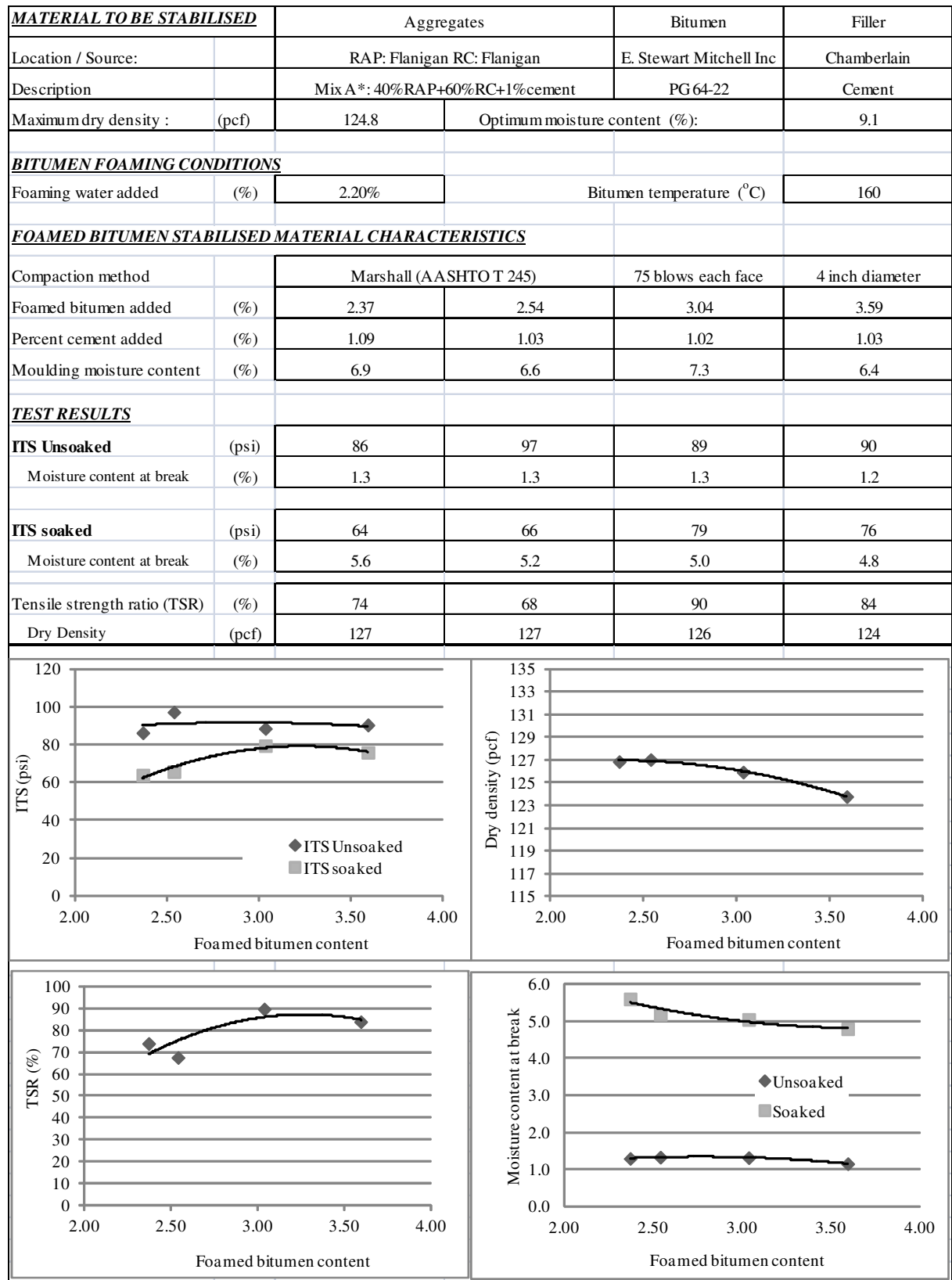
<u>MATERIAL TO BE STABILISED</u>		Aggregates		Bitumen	Filler
Location / Source:		RAP: Flanigan RC: Flanigan		E. Stewart Mitchell Inc	No
Description		Mix A: 40% RAP+ 60% RC+0% cement		PG 64-22	No
Maximum dry density :	(pcf)	124.8	Optimum moisture content (%):		9.1
<u>BITUMEN FOAMING CONDITIONS</u>					
Foaming water added	(%)	2.20%	Bitumen temperature (°C)		160
<u>FOAMED BITUMEN STABILISED MATERIAL CHARACTERISTICS</u>					
Compaction method		Marshall (AASHTO T 245)		75 blows each face	4 inch diameter
Foamed bitumen added	(%)	2.13	2.58	3.04	3.62
Percent cement added	(%)	0.00	0.00	0.00	0.00
Moulding moisture content	(%)	8.4	6.6	7.2	7.9
<u>TEST RESULTS</u>					
ITS Unsoaked	(psi)	86	66	75	75
Moisture content at break	(%)	1.2	0.8	1.2	1.2
ITS soaked	(psi)	64	59	64	70
Moisture content at break	(%)	5.3	4.7	4.9	4.7
Tensile strength ratio (TSR)	(%)	74	88	85	92
Dry Density	(pcf)	126	125	127	126

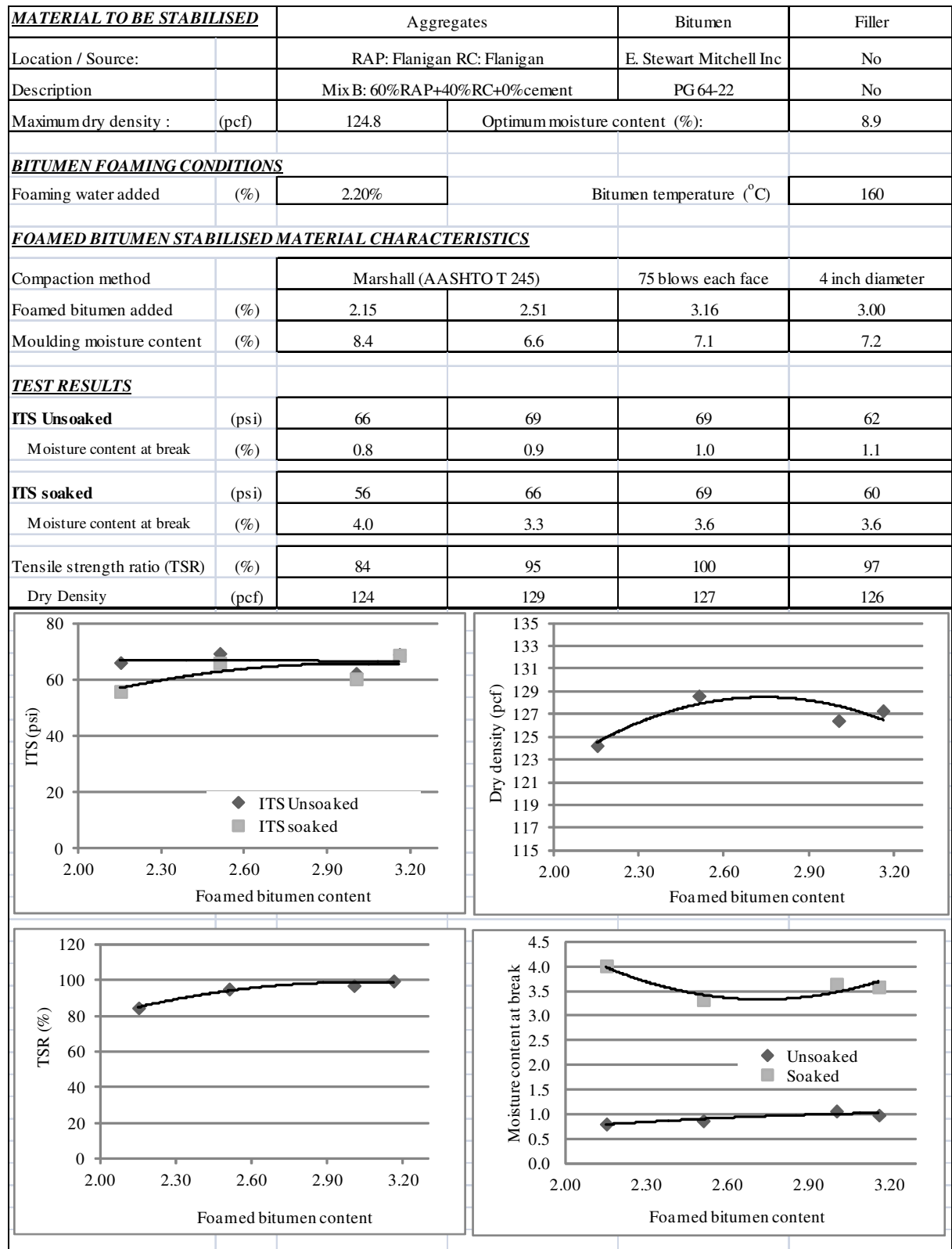
Foamed bitumen content (%)	ITS Unsoaked (psi)	ITS soaked (psi)
2.13	86	64
2.58	66	59
3.04	75	64
3.62	75	70

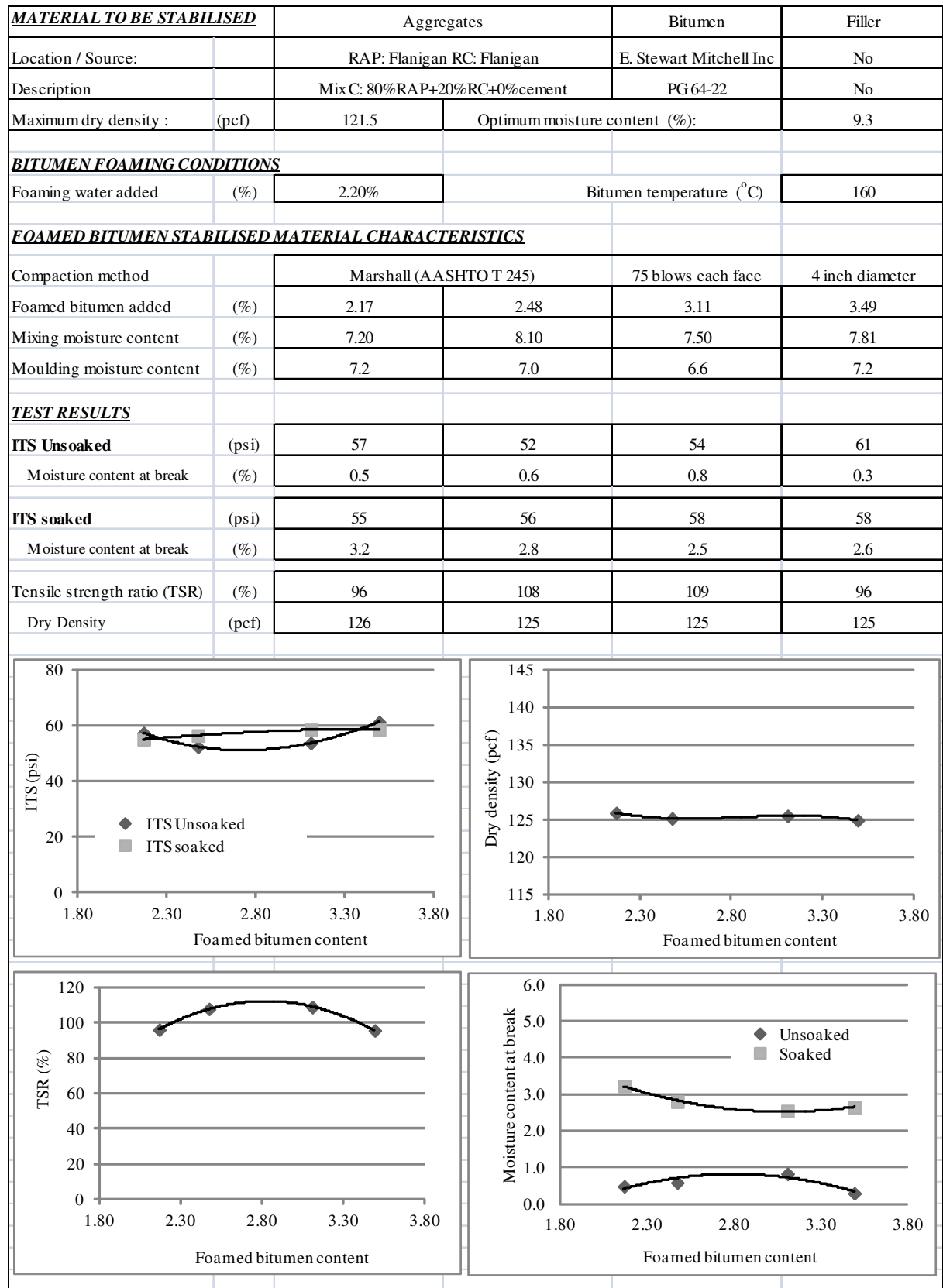
Foamed bitumen content (%)	Dry density (pcf)
2.13	126
2.58	125
3.04	127
3.62	126

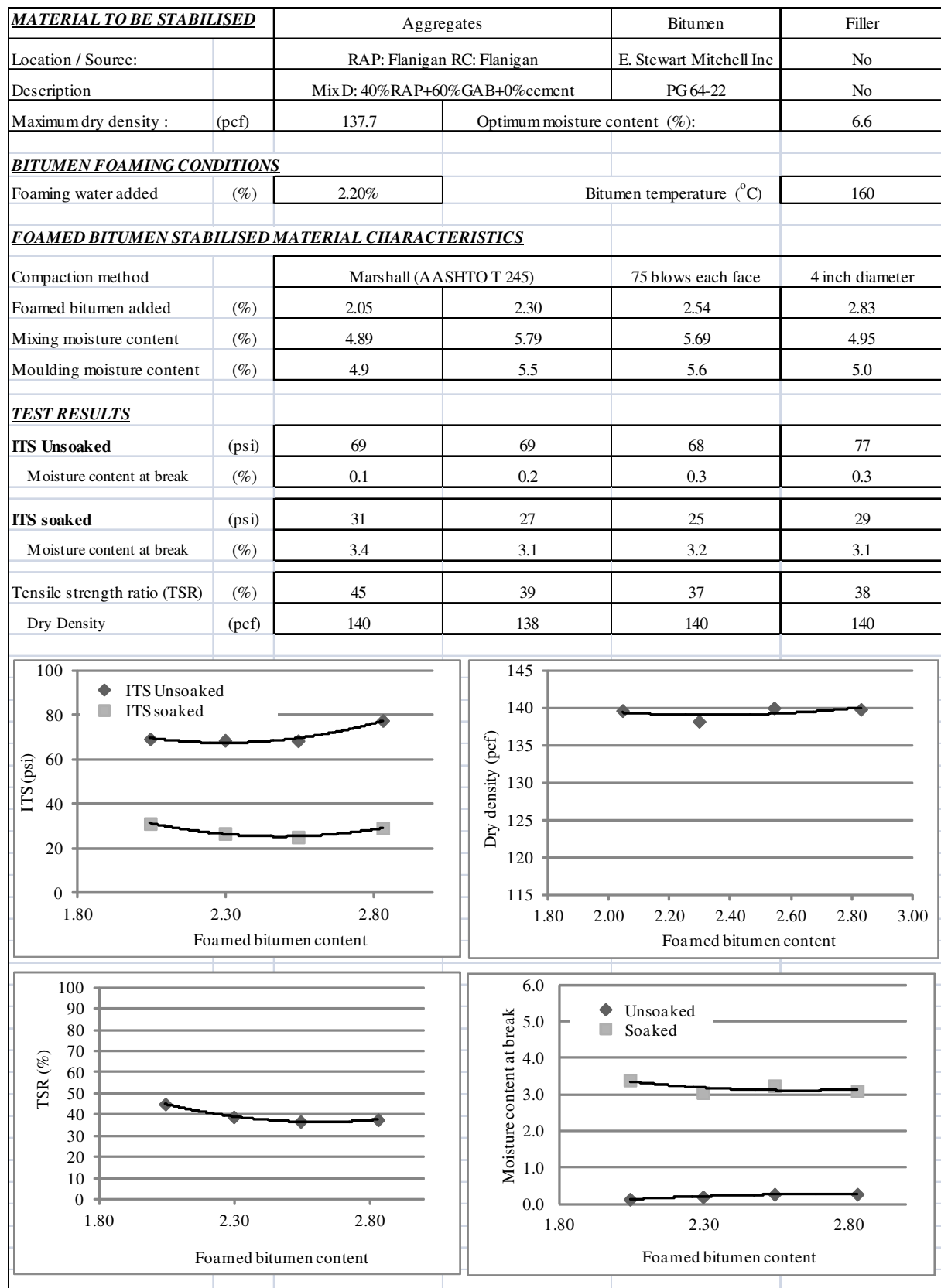
Foamed bitumen content (%)	TSR (%)
2.13	74
2.58	88
3.04	85
3.62	92

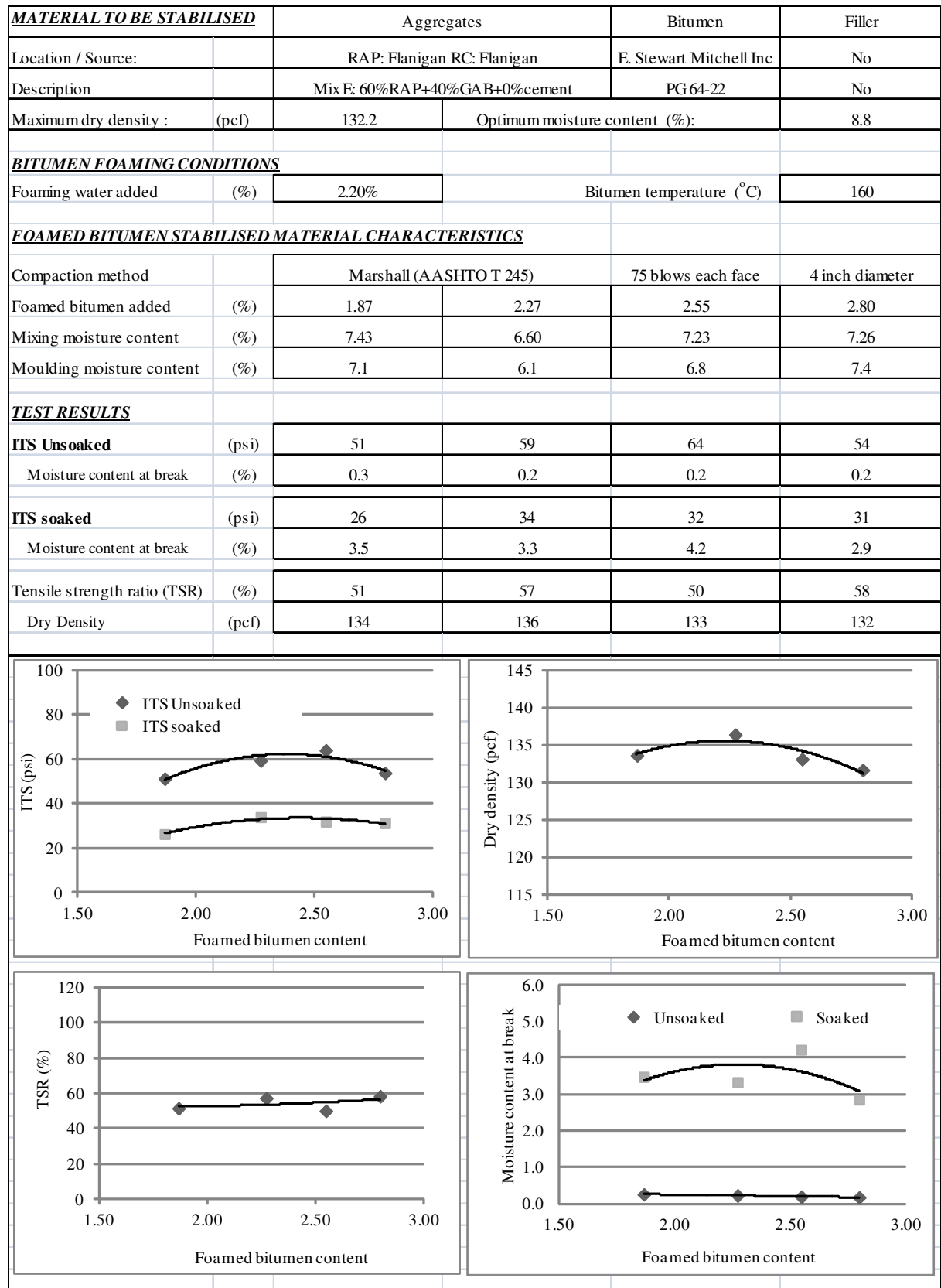
Foamed bitumen content (%)	Unsoaked (%)	Soaked (%)
2.13	1.2	5.3
2.58	0.8	4.7
3.04	1.2	4.9
3.62	1.2	4.7

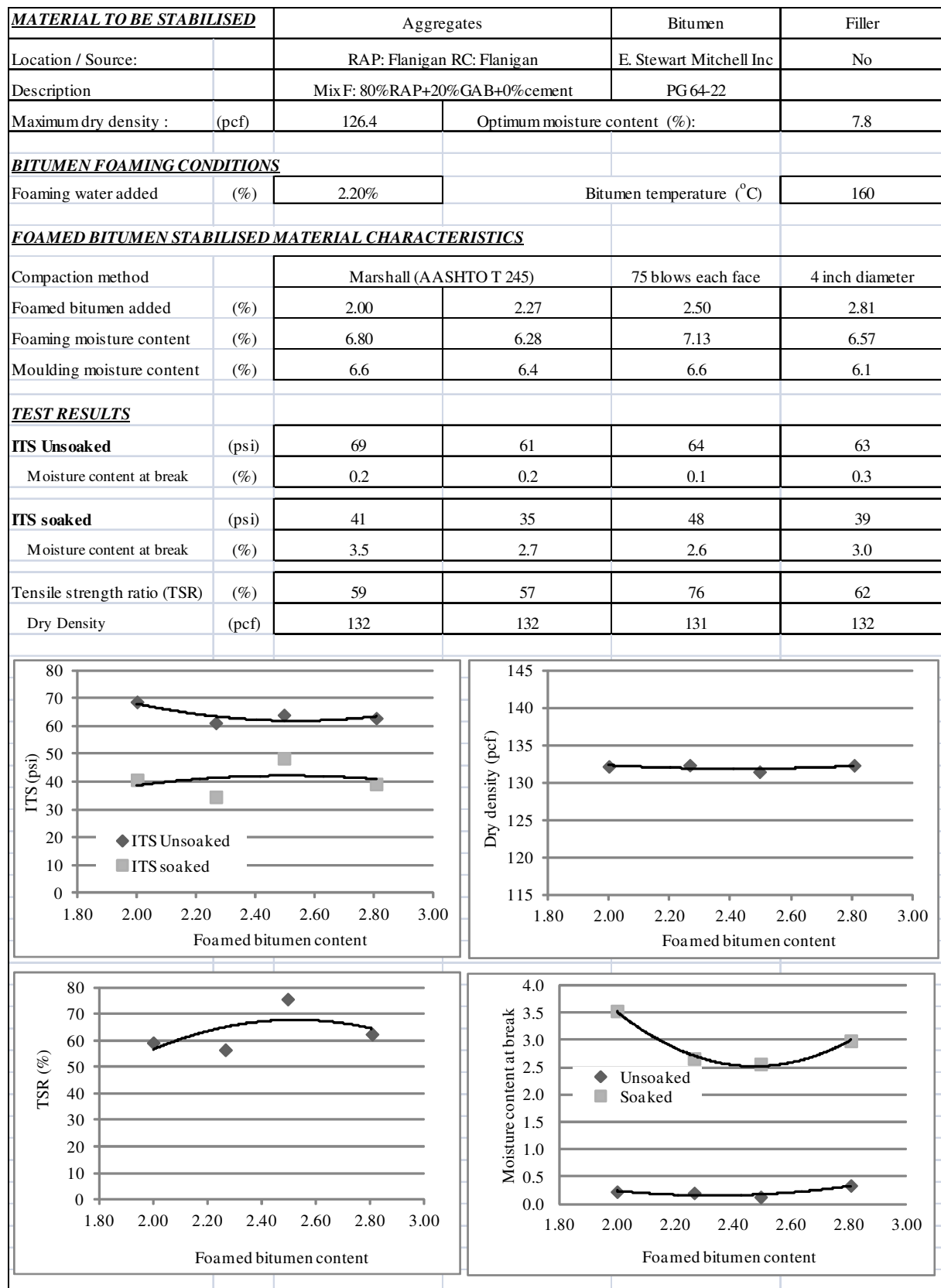












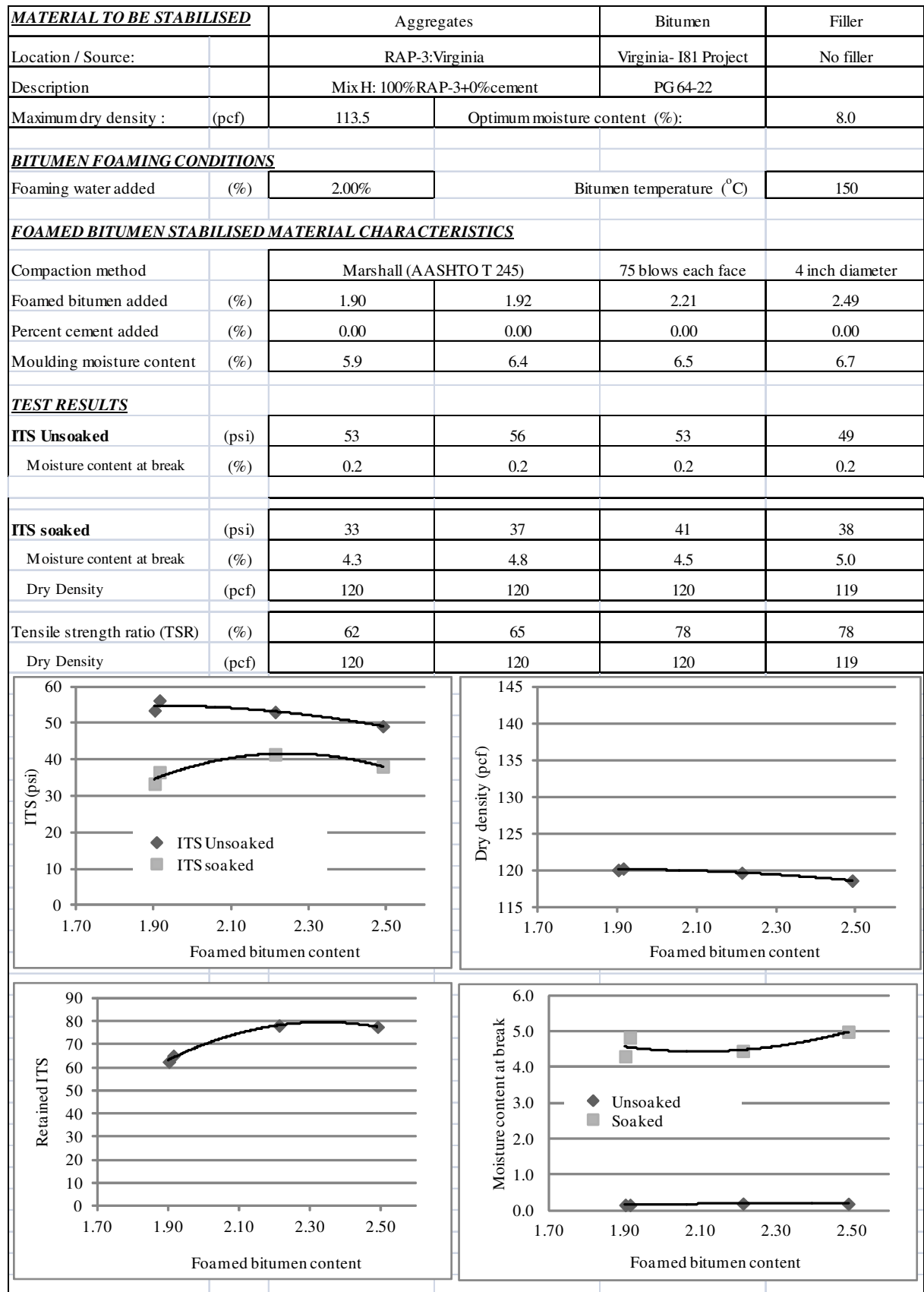
<u>MATERIAL TO BE STABILISED</u>		Aggregates		Bitumen	Filler
Location / Source:		RAP: Chamberlain		NuStar	Chamberlain
Description		Mix G and G*: 100% RAP+ 1% Cement		PG 64-22	Cement
Maximum dry density	(pcf)	131	Optimum moisture content (%)		7.6
<u>BITUMEN FOAMING CONDITIONS</u>					
Foaming water added	(%)	3.00%	Bitumen temperature (°C)		160
<u>FOAMED BITUMEN STABILISED MATERIAL CHARACTERISTICS</u>					
Compaction method		Marshall (AASHTO T 245)		75 blows each face	4 inch diameter
Foamed bitumen added	(%)	2.00	2.30	2.60	2.30
Percent cement added	(%)	1.00	1.00	1.00	0.00
Moulding moisture content	(%)	6.7	6.7	6.7	6.7
<u>TEST RESULTS</u>					
ITS Unsoaked	(psi)	67	62	65	44
Moisture content at break	(%)	1.0	1.4	1.0	0.8
ITS soaked	(psi)	48	61	50	15
Moisture content at break	(%)	4.8	3.3	4.0	3.6
Tesnsile strength ratio (TSR)	(%)	71	98	77	34
Dry Density	(pcf)	132.6	133.4	131.5	133.5

Graph 1: ITS (psi) vs Foamed bitumen content (%). The y-axis ranges from 0 to 100 psi. The x-axis ranges from 1.80 to 2.80. Data series: Unsoaked-1% cement (diamonds), Soaked-1% cement (squares), Unsoaked-0% cement (triangles), Soaked-0% cement (crosses). Unsoaked-1% cement shows a peak around 2.30% bitumen. Soaked-1% cement shows a peak around 2.30% bitumen. Unsoaked-0% cement shows a peak around 2.30% bitumen. Soaked-0% cement shows a sharp drop at 2.30% bitumen.

Graph 2: Dry density (pcf) vs Foamed bitumen content (%). The y-axis ranges from 115 to 145 pcf. The x-axis ranges from 1.80 to 2.80. Data series: 1% cement (diamonds), 0% cement (squares). Both series show a peak around 2.30% bitumen.

Graph 3: TSR (%) vs Foamed bitumen content (%). The y-axis ranges from 0 to 120%. The x-axis ranges from 1.80 to 2.80. Data series: 1% cement (diamonds), 0% cement (squares). Both series show a peak around 2.30% bitumen.

Graph 4: Moisture content at break (%) vs Foamed bitumen content (%). The y-axis ranges from 0.0 to 6.0%. The x-axis ranges from 1.80 to 2.80. Data series: Unsoaked (diamonds), Soaked (squares). Both series show a peak around 2.30% bitumen.



References

- ARRA (2001). *Basic Asphalt Recycling Manual. Asphalt Recycling and Reclaiming Association*, Annapolis, MD.
- Asphalt Academy (2002). The Design and Use of Foamed Bitumen Treated Materials. Interim Technical Guideline (TG2), 2st edition, Pretoria, South Africa.
- Berthelot, C., Marjerison, B., Houston, G., McCaig, J., Warrener, S., and Gorlick, R. (2007). Mechanistic Comparison of Cementitious and Bituminous Stabilized Granular Base Systems. *Transportation Research Board, 86th Annual Conference*, Washington, DC.
- Chen, D.H., Bilyeu, J., Scullion, T., Nazarian, S., and Chiu., C.T. (2006). Failure Investigation of a Foamed-Asphalt Highway Project. *Journal of Infrastructure Systems*, 12(1), pp 33-40.
- Chiu C.T., Lewis A.J.N. (2006). A study on properties of foamed-asphalt-treated mixes. *Journal of Testing and Evaluation*, Vol. 34, No. 1, pp. 5-10.
- Clyne, T. R., et al. (2004). Determination of HMA modulus values for use in mechanistic-empirical pavement design. University of Minnesota, Minneapolis, Minn.
- Collings D., Lindsay R., Shunmugam R. (2004). LTPP exercise on a foamed bitumen treated base -evaluation of almost 10 years of heavy trafficking on MR 504 in Kwazulu-Natal. *Proceedings 8th Conference on Asphalt Pavements for Southern Africa*, pp. 468-499.
- Csanyi, L. H. (1957). Foamed Asphalt in Bituminous Paving Mixtures. *National Research Council*, Washington, D.C.: Highway Research Board Bulletin, pp. 108-122.
- Fredlund, D. G., and Rahardjo, H. (1993). Soil mechanics for unsaturated soils. Wiley, New York.
- Fu, P., and Harvey, J.T. (2007). Temperature Sensitivity of Foamed Asphalt Mix Stiffness: Field and Lab Study. *International Journal of Pavement Engineering*, 8(2), pp. 137–145.
- Fu, P., Jones, D., Harvey, J. T., and Bukhari, S. A. (2008). Dry and Soaked Laboratory Tests for Foamed Asphalt Mixes. *Journal of the Association of Asphalt Paving Technologists*, 71-106.
- Fu, P., Jones, D., Harvey, J.T., and Bukhari, S.A. (2009). Laboratory Testing Methods for Foamed Asphalt Mix Resilient Modulus. *Road Materials and Pavement Design*, 10(1): 187-212.

- Fu, P., Jones, D., and Harvey, J. (2010.a). Micromechanics of the Effects of Mixing Moisture on Foamed Asphalt Mix Properties. *Journal of Materials in Civil Engineering*, ASCE.
- Fu, P., Jones, D., Harvey, J.T., and Halles F.A. (2010.b). Investigation of the Curing Mechanism of Foamed Asphalt Mixes Based on Micromechanics Principles. *Journal of Materials in Civil Engineering*, 22(1), pp. 29-38.
- Fu, P., Jones, D., and Harvey, J.T. (2011). The Effects of Asphalt Binder and Granular Materials Characteristics on Foamed Asphalt Mix Strength. *Construction and Building Materials*, 25(2), pp. 1093-1101.
- Gonzalez, A., Cubrinovski, M., Pidwerbesky, B., Alabaster, D. (2011). Strength and deformational characteristics of foamed bitumen mixes under suboptimal conditions. *J Trans Eng*, 137, pp. 1–10
- Huang, Y. H. (1993). Pavement Analysis and Design. *Pearson Education, Inc., Pearson Prentice Hall Company*, 2nd Edition.
- Jenkins, K.J., Molenaar, A.A.A., de groot, J.L.A., van de Ven, M.F.C. (2000). Developments in uses of foamed bitumen in road pavements. *Heron*, Vol. 45, No. 3, pp. 167-176.
- Jenkins, K.J., Long, F.M., and Ebels, L.J. (2007). Foamed bitumen mixes = Shear performance? *International Journal of Pavement Engineering*, Vol. 8, No. 2, June, pp. 85-98.
- Khweir, K. (2007). Performance of foamed bitumen-stabilised mixtures. *Proceedings of the Institution of Civil Engineers: Transport*, Vol. 160, No. 2, pp. 67-72.
- Khosravifar, S., Goulias, D. G., and Schwartz, C. W. (2012). Laboratory Evaluation of Foamed Asphalt Stabilized Base Materials. *Proceeding, ASCE GeoCongress*, Oakland, CA
- Kim, Y. and Lee, H. (2006). Development of mix design procedure for cold in-place recycling with foamed asphalt. *Journal of Materials in Civil Engineering*, ASCE, Vol. 18, No. 1, pp. 116-124.
- Kim, Y., Lee, H., and Heitzman, M. (2007). Validation of new mix design procedure for cold in-place recycling with foamed asphalt. *Journal of Materials in Civil Engineering*, ASCE, Vol. 19, No. 11, pp. 1000-1010.
- Kim, Y., Lee, H., and Heitzman, M. (2009). Dynamic Modulus and Repeated Load Tests of Cold In-Place Recycling Mixtures Using Foamed Asphalt. *Journal of Materials in Civil Engineering*, Vol. 21, No. 6, June 1, pp. 279–285.

- Lee, D.Y. (1981). Testing marginal aggregates and soils with foamed asphalt. *Proceedings, Association of Asphalt Paving Technologists*, Vol. 50, pp. 211-250.
- Loizos, A., Collings, D., and Jenkins, K. (2004). Rehabilitation of a major Greek highway by recycling/stabilizing with foamed bitumen. *8th Conference on Asphalt Pavements for Southern Africa (CAPSA-04)*, pp. 1199-1206.
- Loizos, A. (2007). In-situ characterization of foamed bitumen treated mixes for heavy-duty pavements. *International Journal of Pavement Engineering*, Vol. 8, No. 2, June, pp. 123-135.
- Long, F. and Theyse, H. (2004). Mechanistic-empirical structural design models for foamed and emulsified bitumen treated materials. *8th Conference on Asphalt Pavements for Southern Africa (CAPSA-04)*, pp. 553-567.
- Long and Ventura (2004). Laboratory testing for the HVS test on the N7. *Confidential Contract Report*, Pretoria, CSIR Transportek, Contract Report CR-2003/56
- Marquis, B., Bradbury, R., Colson, S., Malick, R., Nanagiri, Y., Gould, J., et al. (2003). Design Construction and Early Performance of Foamed Asphalt Full Depth Reclaimed (FDR) Pavement in Maine. *Compendium of Papers CD-Rom of the 82th Annual Meeting of Transportation Research*.
- Mohammad, L.N., Abu-Faraskh, M.Y., Wu, Z., and Abadie, C. (2003). Louisiana Experience with foamed recycled asphalt pavement base materials. *Proceedings, 82nd Annual Meetings of the Transportation Research Board (CD-ROM Paper No. 03-3856)*, Washington, DC, 8 pp.
- Mohammad, L., Abu-Farsakh, M., Wu, Z., and Chris, A. (2003). Louisiana Experience with Foamed Recycled Asphalt Pavement Base Materials. *Transportation Research Record*, pp. 17-24.
- Mohammad, L.N., Herhath, A., Rasoulilian, M., and Zhongjie, Z. (2006). Laboratory evaluation of untreated and treated pavement base materials. *Transportation Research Record 1967*, Transportation Research Board, National Research Council, Washington, DC, pp. 78-88.
- Muthen, K. M. (1999). Foamed Asphalt Mixes, Mix Design Procedure. Report CR-98/077. CSIR Transportek, Pretoria, South Africa.
- Nataatmadja, A. (2001). Some Characteristics of Foamed Bitumen Mixes. *Transportation Research Record: Journal of the Transportation Research Board*, pp. 120-125.
- Nataatmadja, A. (2002). Foamed bitumen mix: soil or asphalt. *9th International Conference on Asphalt Pavements*, pp. 14–21.

Nunn, M. and Thom, N. (2002). Foamix: Pilot Scale Trials and Design Considerations. *Viridis Report VRI*, Transport Research Laboratory, United Kingdom.

Papagiannakis, A. T., Masad, E. A. (2007). Pavement Design and Materials. *John Wiley and Sons, Inc.*, Hoboken, New Jersey.

Ramanujam, J., and Jones, J. (2007). Characterization of Foamed-Bitumen Stabilization. *International Journal of Pavement Engineering*, pp. 111-122.

Romanoschi, S. A., Hossain, M., Gisi, A., and Heitzman, M. (2004). Accelerated pavement testing evaluation of the structural contribution of full-depth reclamation material stabilized with foamed asphalt. *Transportation Research Record 1896*, Transportation Research Board, National Research Council, Washington, DC, pp. 199-207.

Ruckel, P. J., Acott, S. M., and Bowering, R. H. (1983). Foamed-Asphalt Paving Mixtures: Preparation of Design Mixes and Treatment of Test Specimens. *Transportation Research Record*, pp. 88-95.

Saleh, M. F. (2004). New Zealand Experience with Foam Bitumen Stabilisation. *Transportation research record*, pp. 40-49.

Saleh, M. F. (2006). Effect of aggregate gradation, type of mineral fillers, bitumen grade and source on the mechanical properties of foamed bitumen stabilized mixes. *85 th Annual Meeting of Transportation Research Board*.

Schimmoller, V.E., Holtz, K., Eighmy, T.T., Wiles, C., Smith, M., Malasheskie, G., Rohrbach, G.J., Schaftlein, S., Helms, G., Campbell, R.D., Van Deusen, C.H., Ford, B., Almborg, J.A. (2000). Recycled Materials in European Highway Environments: Uses, Technologies, and Policies. *Report FHWA-PL-00-025, Office of International Programs, Federal Highway Administration, U.S. Department of Transportation*, Washington, DC.

SECTION 50X (2009). Foamed Asphalt Stabilized Base Courses, Provisional Specifications. *Maryland State Highway Administration*, MD.

Twagira M.E., Jenkins K.J., Ebels L.J. (2006). Characterization of fatigue performance of selected cold bituminous mixes. *Proceedings of the 10th International Conference on Asphalt Pavements*, Quebec City, Canada.

Von Quintus, H. L., Mallea, J., Bonaquist, R., Schwartz, C. W., Carvalho, R. L. (2011). Calibration of Rutting Models for HMA Structural and Mixture Design. *National Cooperative Highway Research Program (NCHRP 9-30A)*, Washington, DC.

Wirtgen (2004). Wirtgen Cold Recycling Manual (2nd Ed.). *Wirtgen GmbH*, Windhagen, Germany.

Wirtgen. (2008). Suitability Test Procedures of Foam bitumen Using Wirtgen WLB 10 S. *Wirtgen GmbH*, Windhagen, Germany.

Wirtgen (2010). Wirtgen Cold Recycling Manual (3nd Ed.). *Wirtgen GmbH*, Windhagen, Germany.

Xiao, Y. (2009). Evaluation of Engineering Properties of Hot Mix Asphalt Concrete for the Mechanistic-Empirical Pavement Design, *PhD dissertation*, The Florida State University.